8-2-2003

Influence of Aluminum Ion on the Anaerobic Treatment of a Poultry Slaughterhouse Wastewater

Julio Alberto Martinez

INFLUENCE OF ALUMINUM ION ON THE ANAEROBIC TREATMENT OF A POULTRY SLAUGHTERHOUSE WASTEWATER

By

Julio Alberto Martinez

A Thesis
Submitted to the Faculty of
Mississippi State University
in Partial Fulfillment of the Requirements
for the Degree of Master of Science
in Chemical Engineering
in the Dave C. Swalm School of Chemical Engineering

Mississippi State, Mississippi

August 2003

INFLUENCE OF ALUMINUM ION ON THE ANAEROBIC TREATMENT

OF A POULTRY SLAUGHTERHOUSE WASTEWATER

By

Julio Alberto Martinez

Approved:

Donald O. Hill Professor Emeritus of Chemical Engineering (Major Professor)	Hossein Toghiani Associate Professor of Chemical Engineering (Committee Member)
Clifford E. George Professor of Chemical Engineering (Committee Member)	Irvin A. Jefcoat Professor of Chemical Engineering (Committee Member)
Mark E. Zappi Professor of Chemical Engineering and Graduate Coordinator of the Dave C. Swalm School of Chemical Engineering	A. Wayne Bennett Dean of the College of Engineering

Name: Julio Alberto Martinez

Date of Degree: August 2, 2003

Institution: Mississippi State University

Major Field: Chemical Engineering

Major Professor: Dr. Donald O. Hill

Title of Study: INFLUENCE OF ALUMINUM ION ON THE ANAEROBIC TREATMENT OF A POULTRY SLAUGHTERHOUSE WASTEWATER.

Pages in Study: 127

Candidate for Degree of Master of Science

The influence of Al^{3+} on the anaerobic treatment of a poultry slaughterhouse wastewater was studied in this work. The soluble *COD* (*SCOD*), volatile acid (*VA*) concentrations, and methane yield values were measured and compared for zero, 15, and 40 ppm Al^{3+} runs. Methane yields of 55.4, 144.2, and 215.4 ml CH_4/g. *COD* for zero, 15, and 40 ppm Al^{3+} concentrations, respectively, were observed. Furthermore, *SCOD* and *VAs* were not detectable in the reactor that was seeded with 40 ppm Al^{3+}. It was concluded that inhibitory effects of long chain fatty acids (*LCFAs*) on aceticlastic methanogens were reduced by aluminum ion. This conclusion was also corroborated by a new mathematical model for estimating the Monod parameters developed in this work. The main characteristic of this new model is that estimated parameters must satisfy some restrictions, which provides consistency for the estimated parameters.

DEDICATION

I dedicate this thesis to my lovely wife, Sandra V. Bennun Serrano, and my beautiful son, Nathaniel, for being an important part of my life and for their support throughout this endeavor. Their patience and love have been the source of inspiration to accomplish this goal. I would also like to dedicate this thesis to my mother, Frida Gillig, and my father, Julio R. Martinez, who dedicated their entire life to make this precious goal become true. I extend this dedication to my mother-in-law, Luisa Serrano, who will remain in my memory forever.

ACKNOWLEDGEMENTS

I would like to thank my major adviser, Dr. Donald O. Hill, for his support, guidance, and contributions to this thesis. The freedom of work and thoughts that I had during this research will be appreciated always. I would like to express my gratitude to Dr. Hossein Toghiani for his invaluable assistance and training on analytical equipment. To Dr. Clifford E. George, Dr. Irvin A. Jefcoat, Dr. Hossein Toghiani, and Dr. Mark E. Zappi, I extend my gratitude for their time, efforts, and contributions to improving the quality and scientific insight of this thesis. Special thanks is extended to Dr. William T. French, Dr. Mark E. Zappi, and Dr. Mark Bricka for providing access to some of the analytical equipment employed throughout this research, and to Prasanth Buchireddy for performing the aluminum analyses.

I would like to thank Dr. Rebecca K. Toghiani for my nomination to the Barrier Fellowship. I extend my gratitude to the Dave C. Swalm School of Chemical Engineering and to the Barrier Scholarships for the financial support of this research.

TABLE OF CONTENTS

APPENDIX Page

LIST OF TABLES

TABLE Page

LIST OF FIGURES

FIGURE Page

FIGURE Page

CHAPTER I

INTRODUCTION

Proteins from animal sources have been recognized as an important constituent of today's diet. In order to satisfy the requirements for animal proteins in this relatively fast growing society, it is necessary to incorporate into the diet, animals that have a fast growing period such as pigs and chickens. Statistics show that the consumption of pork in the United States was relatively constant at 70 pounds/person from 1970 to 1999, and chicken consumption increased from 45 to 95 pounds/person during the same period (Mississippi Department of Agriculture and Commerce). The poultry industry has become one of the largest industries in Mississippi. In 2001, Mississippi ranked fourth in the entire nation as a broiler producer state (The Clarion Ledger). The revenues that this industry generated in Mississippi for 2001 were about $1.54 billion for poultry and egg farm production, an increase of about 12% from 2000 production (The Clarion Ledger).

As any fast growing industry, the amount of waste to treat also increased. For environmental engineers, one of the branches related to the poultry industry that receives more attention is the poultry slaughter branch since this industry produces large amounts of wastewater with high fat, grease, and protein content. It has been an objective of the poultry industry in Mississippi to reduce non-production related costs. For example, a medium sized chicken slaughterhouse (260,000 birds/day) expends $50,000/month treating its wastewater with a conventional aerobic process.

Anaerobic wastewater treatment has become an important wastewater treatment technology, because it produces less sludge than the aerobic process, eliminates venting of greenhouse gases, and produces methane that is used as an energy source. Moreover, it diminishes the survival of many pathogenic organisms (Ghosh et al., 1975). However, anaerobic wastewater treatment by itself is, most of the time, considered as a pretreatment process that is usually located upstream of an aerobic process. This is in part due to the failure of the anaerobic treatment unit when operating conditions change even for a short period of time.

Nowadays, efforts in improving the performance of anaerobic wastewater treatment units at field operations have been focused mainly on control systems and supporting materials. On the other hand, at the bench scale, improvements are focused on understanding interrelations between acidogenic and methanogenic microorganisms, which are the two primary groups that govern any anaerobic process. As a consequence, understanding those interrelations would provide more tools for a better performance of anaerobic processes.

Anaerobic lagoons have been difficult to design and are often described as just a hole in the ground. However, because some anaerobic lagoons achieve 50 to 60 % removal and others achieve well above 95% removal, there is renewed interest. This is due to the additional aeration cost of aerobic processes as well as to relieve older plants that are receiving higher than design loadings. One of the difficulties with anaerobic lagoons is they defy mathematical calculations. That is due to the fact that one cannot state that they are plug flow, complete mixed, or another flow regime that could be

addressed mathematically. Engineers working on anaerobic lagoons are left with a collection of workshop papers that are now 35 years old or their personal experience. Anaerobic lagoons installed in the last 10 years have been designed to be 15 to 18 feet deep (deeper if possible), loaded organically at a nominal 15 pounds per 100 cubic feet, and with a retention time of 5 to 10 days. Typically, there is a conflict between loading and retention time, which must be balanced to suit the designer. Historically, there has been only one tool to measure the performance of an anaerobic lagoon and that is the % removal of organics, which ranges from 50 to more than 95 % plus.

It has been observed in the field that the addition of Al^{3+} to the influent of an anaerobic lagoon treating poultry slaughterhouse wastewater exceptionally improves the % removal of organic. This research has as its main objective the study of possible processes that are involved during the addition of Al^{3+} to the anaerobic treatment of poultry slaughterhouse wastewater. Although the purpose of adding Al^{3+} to the anaerobic lagoon mentioned before is to remove material from its influent, this research is focused on studying other possible processes involved in the increased lagoon performance. It has been hypothesized that this increase, due to the addition of Al^{3+}, would be associated with physicochemical or microbial influence of Al^{3+}. Furthermore, the combination of these factors is likely to be responsible for the field observation.

Besides the study of the influence of Al^{3+} in anaerobic wastewater treatment processes, a bio-kinetic study is performed with the purpose of revealing any increase in degradation rate. The sigmoidal responses for substrate depletion and microbial growth due to microbial activity in a batch reactor have been represented by several equations.

Among them, the Christensen-McCarty (CM) equation (Christensen and McCarty, 1975) is preferred by environmental engineers, because of its simplicity and good correlation between experimental and calculated data. Although this equation is preferred, it cannot be employed for a batch reactor when microbial endogenous decay is taken into account (Rittmann and McCarty, 2000). However, this reactor configuration is preferred for biodegradation rate studies because it does not require long experimental runs and employs relatively small amounts of substrate. Presently, the known integrated Monod equation, employed for batch reactor studies, is obtained from the CM equation in which the endogenous decay term is neglected. Thus, estimated Monod kinetic parameters are biased by error that is independent of the experimental error (Robinson and Tiedje, 1983). A major concern for this research is the influence of endogenous decay over the estimated Monod kinetic parameters, because it is well known that microbial endogenous decay is important for anaerobic systems. Therefore, an approach that minimizes the error in these estimates will be developed and employed in this research.

CHAPTER II

LITERATURE REVIEW

Anaerobic Degradation of Wastewater

Introduction

The anaerobic degradation process is essentially a two-stage process in which two groups of microorganisms (acids and methane formers) coexist in order to transform wastewater into biomass and biogas. It has been realized that the physiological and nutritional requirements of these two groups are different (Pohland and Ghosh, 1971), so a better understanding of these requirements should improve the quality of the final effluent. In Figure 2.1, a schematic representation for the anaerobic degradation of wastewater is shown. It can be appreciated that the main final products for the acidogenic-fermentation step are low molecular weight monocarboxilic acids, such as acetic and propionic as well as H_2, and CO_2. These compounds are further biodegraded in the methanogenic step to CH_4 and CO_2, which are the ultimate mineralization products.

Presently, three different fermentation types for the acidogenic step are known (Ren et al., 1997). One is called butyric-type fermentation that is characterized by the production of butyric and acetic acid plus, CO_2 and H_2. Another is the propionic-type that produces mainly propionic and acetic acids with no significant gas production. The third is called ethanol-type which yields as fermentation products ethanol, acetic acid, H_2, and CO_2. Experimentally, it has been concluded that acidogenic degradation of organic

wastewater is carried out through the propionic-type fermentation (Ren et al., 1997).

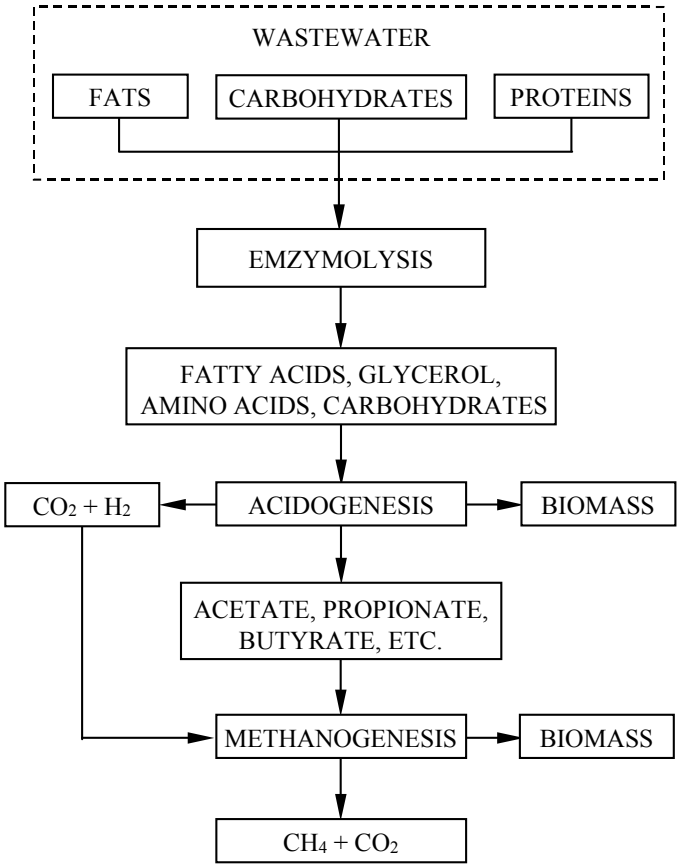

Figure 2.1. General scheme for anaerobic degradation.
(adapted from Zoetemeyer et al., 1982).

Thermodynamic Considerations

It is well known that biological processes often have a large variety of chemical reactions occurring at the same time. This situation makes their study a difficult task, but the thermodynamic approach for the study of these processes has been very helpful in providing some explanation for a process that is not completely understood. For a given chemical reaction, it can be spontaneous only if the relation, $\Sigma \Delta G'_f$(products) – $\Sigma \Delta G'_f$

(reactants), is less than zero. Also, it is known that the Gibbs function, G, of any compound is only dependent on the state and conditions at which this substance is considered. Therefore, by only evaluating the Gibbs function for final degradation products and starting substrates, one can have an idea of feasibility for a given biodegradation process. In this work, the approach proposed by Thauer et al. (1977) is employed for the estimation of the change in Gibbs free energy. Thauer and his team proposed that, under normal microbial physiological conditions, the $\Delta G^{0'}$ which is the Gibbs free energy at standard conditions and pH = 7, rather than pH = 0, should be employed instead of ΔG^{0}. $\Delta G^{0'}$ for a given reaction is affected by Equation 2.1, when the reaction conditions differ from the standard state conditions. These conditions are a concentration of 1 M for substances in solution, 1atm for gases, and pH = 7. For the following reaction, one has.

$$a\,A + b\,B \rightleftharpoons c\,C + d\,D \tag{2.1}$$

$$\Delta G' = \Delta G^{0'} + R\,T\,\ln\frac{C^{c}\,D^{d}}{A^{a}\,B^{b}}$$

in which A, B, C, and D are the molar concentrations of substrates and products respectively, R is the universal gas constant, and T is the absolute temperature of the media.

Table 2.1 contains some of the experimentally observed metabolic products from the anaerobic degradation of pure substrates, but most of the substrates listed in this table are found in many wastewater streams. As shown in this table, $\Delta G^{0'}$ for the acetogenesis of propionate is highly unfavorable. However, methogenesis of propionate was observed

at bench-scale by the combined action of three species of bacteria in which the overall $\Delta G^{0'}$ is less than zero (Smith and McCarty, 1989). Thus, thermodynamic considerations for biological systems should be supported by experimental observations in order to avoid erroneous conclusions.

Table 2.1. $\Delta G^{0'}$ of experimentally observed metabolic products from anaerobic degradation of pure substrates.

Substrate	Products	$\Delta G^{0'}$ (KJ/mol) [2]
	Acidogenesis	
Volatile acids		
Propionate + 3 H_2O	Acetate + HCO_3^- + H^+ + 3 H_2	+ 76.1
Butyrate + 2 H_2O	2 Acetate + H^+ + 2 H_2	+ 48.1
Valerate + 2 H_2O	Acetate + Propionate + H^+ + 2 H_2	+ 25.1
Alcohol		
Ethanol + H_2O	Acetate + H^+ + 2 H_2	+ 9.6
Glycerol + 2 H_2O	Acetate + HCO_3^- + 2 H^+ + 3H_2	– 73.2
Amino acids		
2 Glycine + 4 H_2O	Acetate + HCO_3^- + H^+ + 2 NH_4^+ + 2 H_2	– 51.5
Alanine + 3 H_2O	Acetate + HCO_3^- + H^+ + NH_4^+ + 2 H_2	+ 7.5
Fatty acids		
Palmitate + 14 H_2O	8 Acetate + 7 H^+ + 14H_2	+ 345.6
Stearate + 16 H_2O	9 Acetate + 8 H^+ + 16 H_2	+ 496.5
[1] Oleate + 16 H_2O	9 Acetate + 8 H^+ + 15 H_2	+ 390.9
[1] Linolate + 16 H_2O	9 Acetate + 8 H^+ + 14 H_2	+ 312.3
Carbohydrates		
Glucose + 4 H_2O	2 Acetate + 2 HCO_3^- + 4 H^+ + 4 H_2	– 206.3
Glucose + 5 H_2O	Propionate + 3 HCO_3^- + 4 H^+ + 5 H_2	– 177.9
Glucose + 2 H_2O	Butyrate + 2 HCO_3^- + 3 H^+ + 2 H_2	– 253.8
Ribose	Acetate + pyruvate + 2 H^+ + H_2	– 166.5
	Methanogenesis	
Acetate + H_2O	CH_4 + HCO_3^-	– 31.0
H_2 + ½ CO_2	½ CH_4 + H_2O	– 65.4
Propionate + H^+ + ½ H_2O	7¼ CH_4 + 5¼ CO_2	– 62.2
Ethanol	3½ CH_4 + ½ CO_2	– 91.6

[1] These metabolic pathways were proposed by Lalman and Bagley (2001).
[2] Thermodynamic values obtained from Thauer et al. (1977) and Lalman and Bagley (2000)

The production of H_2 in most of the reactions shown in Table 2.1 for the acidogenic step indicates that, at certain H_2 partial pressure, P_{H_2}, any of the reactions could progress in one or another direction. For example, the build up of propionate in anaerobic wastewater treatment units has been associated with an increase in P_{H_2}. Smith and McCarty (1986) estimated that acidogenesis of propionate can be carried out when P_{H_2} is confined between 10^{-4} and 10^{-6} atm. However, Ren et al. (1997) observed that the production of H_2 in acidogenesis was not related to the production of propionic acid when they studied the biochemical processes related to the anaerobic acidogenesis of glucose. Their findings are not consistent with the $\Delta G^{0'}$ values in Table 2.1. The use of H_2 for hydrogenotrophic methanogenic microorganisms (microorganisms that generate CH_4 from H_2 and CO_2) ensures an H_2 concentration at a sufficiently low level that the oxidation of propionate can occur.

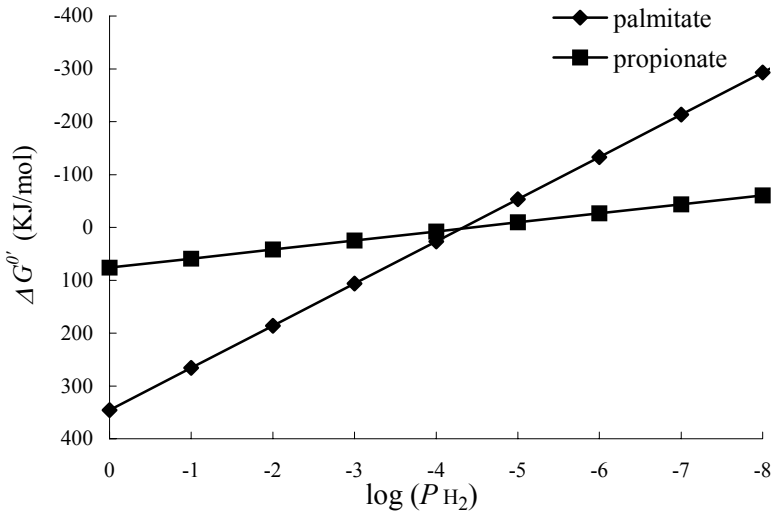

Figure 2.2. Influence of P_{H_2} in the acidogenic degradation of palmitate and propionate.

Figure 2.2 provides a good example of the influence of P_{H_2} over $\Delta G^{0'}$ as a function of P_{H_2}. It is observed that the degradation of palmitate, a common fatty acid, is possible at P_{H_2} smaller than 10^{-4} atm. The relatively large slope of the palmitate curve implies that the P_{H_2} plays a very important role in the degradation of palmitate, so it is important to reduce the hydrogen partial pressure in the system as much as possible. Also evident from Figure 2.2 is that palmitate is more susceptible to acidogenic degradation than propionate when changes in P_{H_2} occur. Therefore, the build up of long chain fatty acids concentrations may be an early indicator of reactor failure than propionate concentration. Details of the calculation for Figure 2.2 are presented in appendix B.

Degradation of Oils and Fats

Oil and fats are chemically composed of glycerol and high-molecular-weight organic acids called fatty acids, or *LCFAs*. Generally, *LCFAs* contain an even number of carbon atoms and they can be saturated or unsaturated with at least one carbon-carbon double bond. Fatty acids are expressed by the number of carbon atoms and the number of double bonds in it. For example, the linoleic acid (an 18 carbons with two double bonds) is denoted as C18:2. Linoleic (C18:2), oleic (C18:1), stearic (C18:0), and palmitic (C16:0) acids represent the most common fatty acids found in wastewaters (Lalman and Bagley, 2000; Viswanathan et al., 1962).

Biodegradation of oil and fat first requires the action of extracellular enzymes called lipases that break down oil and fats into glycerol and fatty acids. Then fatty acids

and glycerol are transported into the cell for further biodegradation. There is no thermodynamic limitation for the biodegradation of glycerol into acetic acid. However, the biodegradation of fatty acids is not favorable at standard conditions. As shown in Table 2.1, the degradation of fatty acids is strongly influenced by P_{H_2}. Thus hydrogenotrophic methanogenic microorganisms play an important role during fatty acids acidogenesis in order to keep H_2 at low enough concentrations to make it possible for the degradation to occur.

Fatty acids are degraded through a mechanism called β-oxidation (Jeris and McCarty, 1965; Weng and Jeris, 1976). During β-oxidation, a given fatty acid is degraded into acetate, H^+, and a fatty acid of n-2 carbons providing 4 e^- that are carried from the cell by *FADH* and *NADH* to the electron acceptor which is H^+. A basic representation for the two half reactions involved during β-oxidation is given in Figure 2.3.

$$CH_3(CH_2)_nCOOH + 2\ H_2O \longrightarrow CH_3(CH_2)_{n-2}COOH + CH_3COOH + 4\ e^- + 4\ H^+$$

$$4\ e^- + 4\ H^+ \longrightarrow 2\ H_2$$

Figure 2.3. Schematic representation for β oxidation of fatty acids. (adapted from Lalman and Bagley, 2000).

Inhibitory Effect of Fatty Acids

It has been experimentally observed that fatty acids possess inhibitory effects on anaerobic degradation of wastewater. The anaerobic process is basically made of two consortia of microorganisms that are interrelated, so the presence of inhibitory effects on

either of these two groups affects the overall performance of the process. Hanaki and his team (Hanaki et al., 1981) reported inhibition on the acetogenic stage due to the excessive presence of fatty acids by studying the effects of a fatty acid mixture over sludge acclimated with whole milk. They found that the addition of such a mixture in a range between 250 –2000 mg/l (as oleate) produced microbial inhibition since an increase in the lag period for cumulative methane production was observed when it was compared to 0 mg/L *LCFAs* control sample. They also showed the inhibitory effect of fatty acids by measuring the concentration of adenosine 5-triphosphate, *ATP*, in the mixed liquor. *ATP* drastically decreased after the addition of the fatty acid mixture and it did not recover to the original level after fatty acids were degraded. Furthermore, they concluded that *LCFAs* also had inhibitory effects over aceticlastic methanogenic microorganisms, but inhibition was not detectable for H_2–consuming bacteria since there was not a build up of H_2 in the biogas.

Several studies have shown the inhibitory effects of *LCFAs* on methanogenic bacteria. Gram-positive microorganisms have been reported to be negatively affected by *LCFAs* (Kabara et al., 1977; Nieman, 1954). Furthermore, methanogens have been classified as gram-positive microorganisms by Zeikus (1977). Therefore, *LCFAs* should inhibit the growth of methanogenic microorganisms. Koster and Cramer (1987) showed a 50% reduction of the methanogenic activity from acetate degradation at a concentration of >10 mM for caprylic (C8:0), 5.9 mM for capric (C10:0), 4.3 mM for lauric (C12:0), 4.8 mM for myristic (C14:0), and 4.35 mM for oleic (C18:1) acids. Also, they reported that inhibition was increased by a mixture of fatty acids, which is probably the case for a

real wastewater since it does not contain only a single but several fatty acids. Lalman and Bagley (2000) also reported inhibitory effects of linoleic acid (C18:2) on aceticlastic methanogenic microorganisms at a concentration of 30 mg/l or greater for culture acclimated with glucose. They reported a year later (Lalman and Bagley, 2001) that oleic acid (C18:1) at concentrations above 30 mg/l inhibited aceticlastic methanogenic microorganisms, but stearic acid (C18:0) did not present an inhibitory effect. Inhibitory effects of hydrogenotrophic methanogens due to fatty acids have been reported by Lalman and Bagley (2002). They compared hydrogen consumption rates in reaction medias containing linoleic, oleic, stearic, and a mixture of these three *LCFAs*. They concluded that hydrogenotrophic methanogenic microorganisms were slightly affected by stearic acid, but an increase in inhibition was observed for the C18 unsaturated fatty acids. Synergic interaction among fatty acids was not observed during their experiments.

Interaction of Wastewater Constituents with Al^{3+}

Aluminum salts have been used as a coagulant for decades in environmental applications to remove material in auxiliary wastewater treatment units. Generally, this chemical sludge as well as the sludge discarded from the biological unit are mixed and anaerobically digested in order to stabilize them. This is one of the conditions that must be met before final deposition in, for example, a landfill. However, a reduction in the stabilization rate, when chemically produced sludge was digested, has been reported (Gossett et al., 1978; Hsu, 1973). After four months of field observations, Gossett and coworkers (Gossett et al., 1978) observed a drastic reduction in methane production from a municipal anaerobic digester when this digester was fed with sludge coagulated with

alum ($Al_2(SO_4)_3 \cdot 18H_2O$). This field observation generated significant concerns since the residence time for sludge stabilization would need to be extended in order to counteract the effects due to the presence of chemically coagulated sludge. In order to establish if this reduction was associated with the coagulant addition rather than any variation in composition of sludge-fed, Gossett et al. (1978) performed a series of experiments at the bench scale with chemically coagulated sludge from wastewater samples collected at one time. Also, they established a control sample sludge from the same wastewater but settled by gravitational forces. In order to determine if chemical coagulation was detrimental to the anaerobic digestion, Gossett and coworkers defined a set of measurable variables that showed the performance of the digestion process which are listed in Table 2.2. It is observed from these variables that the presence of sludge coagulated by alum did have an adverse effect on the anaerobic digestion of sludge. In addition, Hsu (1973) observed that the gas generation rate was decreased during anaerobic digestion of sludge containing a concentration of Al^{3+} larger than 100 mg/L.

Table 2.2. Performance of anaerobic degradation of chemical coagulated sludge as function of alum concentration employed for coagulation.

Variables	Control	200 mg/l	250 mg/l	325 mg/l	400 mg/l
Gas production (ml/mg VSS)	674	600	532	546	553
Methane production (ml/g COD fed)	295	271	239	254	268
% COD reduction	62	57	51	52	50

An earlier research by Rudolfs et al. (1932) showed that the influence of matter coagulated from wastewater by sodium aluminate ($Na_2Al_2O_4$) was not detrimental to the sludge-digestion process. However, coagulation performed by alum using the same experimental conditions decreased the rate of sludge digestion. They also showed that the amount of biogas produced during the digestion of aluminate-coagulated sludge was the highest from a set of samples containing other coagulants. Furthermore, they experimentally determined that sludge produced by the addition of $Na_2Al_2O_4$ required the least stabilization time. Rudolfs and his team attributed this behavior to an adverse effect on the microbial population in the digester due to metallic-counter ions of each coagulant employed during their experimental research. They observed that during the digestion of sludge produced by the addition of $Na_2Al_2O_4$ at 5, 10, and 20 ppm, the concentration of microorganisms present in the media was not affected. However for sludge generated by addition of $FeCl_3$ at the same concentration levels, a drastic reduction of microbial populations was observed. Hsu (1973) also concluded that microbial inhibition was responsible for a decrease in digestion rate, and he specifically attributed this situation to adverse effects of Al^{3+} ion on acetogenic microorganisms.

Gossett et al. (1978), Dentel and Gossett (1982), and Dentel (1984) explained the reduction on the anaerobic digestion rate for chemically coagulated sludge based in chemical and/or physical interactions between Al^{3+} and wastewater constituents. Gossett et al. (1978) associated this reduction with some kind of barrier or "caged" effect for microbial enzymatic processes produced by the interaction of aluminum-organic compounds. Some years later, Dentel and Gossett (1982) followed the same trend

proposed by Gossett and further showed that the strength of chemical bonding between Al^{3+} and organic compounds was in part responsible for the change in sludge digestion rate. Dentel and Gossett (1982) experimentally observed that sludge produced by the addition of alum to butyric acid and D-glucose solutions had no effect on sludge digestion rate, but the addition of alum to a palmitic acid solution, which makes strong bonds with Al^{3+}, decreased its digestibility. The influence, as a function of particle diameter on sludge digestion rate, has been also studied by Dentel and Gossett (1982) and Dentel (1984). They reported that the aluminum ion showed more interaction with a particle of smaller diameter, and concluded that a decrease in diameter increased the amount of "active sites" for aluminum to bind at the surface of a particle. In addition, Yu et al. (2001) studied the enhancement of sludge granulation due to the presence of $AlCl_3$ in upflow anaerobic sludge reactors (*UASB*) receiving a synthetic influent composed of glucose, meat extract, and bacteriological peptone. They reported that the required time to reach good granule size was reduced by 1/3 due to the addition of 300 mg/l of Al^{3+} to the influent, but at steady state operation values for methane content in the biogas, biogas yield, and *COD* reduction proved to be the same as those observed with an *UASB* reactor that received no Al^{3+}.

Sulfate Influence on the Methane Yield

In order to avoid any interference in methane production due to the presence of SO_4^{2-}, this research employed $AlCl_3$ instead of alum since SO_4^{2-} is known to reduce the amount of methane yield. The competition of sulfate reducing bacteria and methane producing bacteria for organic substrates has been studied for many years. Figure 2.4

shows the metabolic pathway for the reduction of sulfate and the production of methane from acetate acting as electron donor in both cases. It is observed that sulfate reduction is more thermodynamically favorable than methane production, so under normal circumstances, SO_4^{2-} reduction should overcome the methane production.

$$CH_3COO^- + SO_4^{2-} \longrightarrow HS^- + 2\,HCO_3^- \qquad \Delta G^{0'} = -71 \text{ KJ/mol}$$

$$CH_3COO^- + H_2O \longrightarrow CH_4 + HCO_3^- \qquad \Delta G^{0'} = -31 \text{ KJ/mol}$$

Figure 2.4. Degradation of acetate by methanogenic and sulfate reducer microorganisms.

The reduction of SO_4^{2-} yields S^{2-}, which is an inhibitory compound for methane producers as well for sulfate reducers. The inhibitory effects of S^{2-} were extensively studied by McCartney and Oleszkiewicz (1993) and Choi and Rim (1991). McCartney and Oleszkiewicz observed that sulfate reduction process most affected acetotrophic methane producing bacteria. Furthermore, Choi and Rim observed that for a ratio COD/SO_4^{2-} of 0.4, only sulfate degraders survived during the anaerobic degradation of seafood waste.

Although during the present research the source of Al^{3+} was not alum, sulfate was added to the reactor media by incorporating the nutrients listed in Table 4.2. During the experimental runs, 400 mg/L of $MgSO_4 \cdot 7H_2O$ and 300 mg/L of $Na_2S \cdot 9H2O$ were added, which could theoretically yield a maximum of 92 mg/L of S^{2-}. This relatively low S^{2-} concentration did not show any inhibitory effect in any of the runs. Furthermore, the ratio $SCOD(\text{fed})/SO_4^{2-}$ was always larger than 4.9, which ensured the predominance of

methane producers over sulfate reducers, so an appreciable yields of methane should be expected during each of these runs.

Estimation of Bio-kinetic Parameters

Introduction

Estimation of biodegradation kinetic parameters for a complex wastewater is an area in which environmental engineers have not found a procedure that is agreed upon by the entire scientific community due to a large number of different and simultaneous degradation processes. Bio-kinetic parameters for the anaerobic degradation of poultry slaughterhouse wastewaters have been represented by two models, proposed by Batstone et al. (1997) and Salminen et al. (2000). Even though these two models are conceptually different, they share common assumptions, including first order kinetics for enzymatic degradation of macromolecules and Monod kinetic for the degradation of low molecular weight substances. Batstone et al. (1997) and Salminen et al. (2000) proposed to determine the Monod parameters by a numerical solution of the Monod equation. However, it is not clear in their approaches if the Monod parameters satisfy some constraints. In this thesis, the theory behind the Monod equation will be studied in depth, and a new approach for estimating the Monod kinetic parameters will be proposed. This new approach will provide parameters that must satisfy experimental constraints that are obvious, but which most methods in current use do not utilize.

Modeling of microbial growth within a batch bioreactor was proposed by Monod (1949). However, it has been recognized that the Monod equation, Equation 2.2, is only

applicable for the exponential growth phase, because it does not contemplate the loss of active biomass due to endogenous decay.

$$\frac{1}{X_a}\frac{dX_a}{dt} = \mu_{\max}\frac{S}{K+S} \tag{2.2}$$

where:

μ_{max} = Maximum specific growth rate (time^{-1}).

X_a = Active matter concentration (mg active biomass/liter).

S = Substrate concentration (mg/liter).

K = Half saturation constant (mg substrate/liter).

t = Time.

Several equations have been proposed after Monod that incorporates endogenous decay. Among them, the Christensen and McCarty (CM) equation (1975) is employed in this study because of its simplicity. Conceptually, the CM equation, Equation 2.3, arises when the endogenous-decay coefficient is incorporated into the Monod equation.

$$\frac{dXa}{dt} = -y\frac{dS}{dt} - b\,X_a \tag{2.3}$$

$$\frac{dS}{dt} = -\frac{\mu_{\max}}{y}\frac{S}{K+S}X_a \tag{2.4}$$

where:

y = yield (mg active biomass generated/mg substrate).

b = Endogenous decay coefficient (time^{-1}).

Equation 2.3 has historical precedents (Van Uden, 1967; Lawrence et al., 1970), but it was Christensen and McCarty who incorporated the concept of active and inert biomass. They assumed that the observable biomass is composed of active biomass, which is associated with microbial processes, and inert biomass, which are the remains from the death of microbes that cannot be degraded by other microorganisms. Mathematically, the generation of inert biomass is formulated as:

$$\frac{dX_i}{dt} = (1 - f_d)\, b\, X_a \tag{2.5}$$

where:

f_d = Bacterial degradable fraction.

X_i = Inert matter concentration (mg inert biomass/liter).

A batch bioreactor is preferred for estimating Monod kinetic parameters due to economy and time limiting factors. Therefore, this type of reactor will be employed for the estimation of Monod kinetic parameters for the biodegradation of poultry slaughterhouse wastewater. Due to the mathematical relation between X_a and S in the mass balances for a batch bioreactor, analytical solution is not possible. Historically, it was assumed that the endogenous decay was a negligible microbial process in order to simplify the model. This assumption makes it possible to integrate these mass balances, so the known integrated Monod equation is obtained (Equation 2.6). In essence, this assumption makes the CM equation equal to the Monod equation.

$$t = \frac{y}{\mu_{\max}} \left\{ \left(\frac{K}{X_a^0 + y\, S^0} + \frac{1}{y} \right) Ln\left(X_a^0 + y\left(S^0 - S\right)\right) - \left(\frac{K}{X_a^0 + y\, S^0} \right) Ln\left(\frac{S\, X_a^0}{S^0} \right) - \frac{1}{y}\, Ln\left(X_a^0 \right) \right\} \quad (2.6)$$

where:

X_a^0 = Initial active matter concentration (mg active biomass/liter).

S^0 = Initial substrate concentration (mg/liter).

Known Parameter Estimation Methodologies

The estimation of bio-kinetic parameters for a particular degradation process has direct technical and economical implications, because these parameters are the key for estimating the necessary size of a wastewater treatment unit and the final effluent concentration to satisfy environmental regulations. Currently, there are no widely accepted methodologies for estimating the Monod kinetic parameters. However, most of the available parameter estimation approaches employ the integrated Monod equation to determine Monod parameters that provide the best fit to experimental data. In this study, two of these methodologies are presented and discussed with the purpose of providing a point of comparison between the known methodologies and the one proposed in this work.

Robinson and Tiedje Methodology

This is perhaps one of the best-known methodologies for estimating Monod kinetic parameters. Robinson and Tiedje (1983) proposed a methodology that employs a Gaussian nonlinear regression approach for the estimation of K, y, and μ_{max} from S versus t data by applying the integrated Monod equation (Equation 2.6). The nonlinear

regression procedure requires the input of good initial estimates for the parameters to be regressed in order to force the convergence of the studied function to a local point that minimized sum of the square of residuals. It is probable the function could converge to other local minimums. Robinson and Tiedje proposed the following relations, Equations 2.7 and 2.8, which result from mathematical manipulations of the Monod equation in which dt, dS, and dX_a are considered equal to Δt, ΔS, and ΔX_{obs}, respectively, and X_a is assumed to be equal to the observable biomass concentration (X_{obs}).

$$-\frac{\Delta t\, X_{obs}}{\Delta S} = \frac{K\, y}{\mu_{\max}}\frac{1}{S} + \frac{y}{\mu_{\max}} \tag{2.7}$$

$$-\frac{\Delta t\, X_{obs}}{\Delta X_{obs}} = \frac{K}{\mu_{\max}}\frac{1}{S} + \frac{1}{\mu_{\max}} \tag{2.8}$$

Robinson and Tiedje mentioned in their study that erroneous Monod kinetic parameters may be obtained when the integrated Monod equation is employed for experimental data sets in which endogenous decay effects are important. However, they did not evaluate the magnitude of these deviations. The Figure 2.5 provides a schematic representation of the steps involved in the estimation of Monod parameters using Robinson and Tiedje methodology.

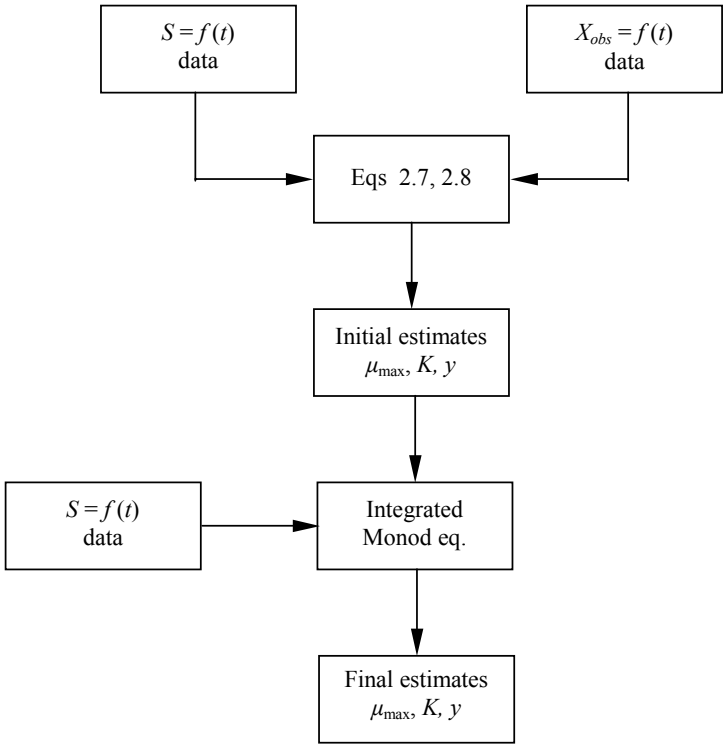

Figure 2.5. Steps involved in the estimation of Monod parameters using Robinson and Tiedje methodology.

Ong Methodology

This methodology employs the integrated Monod equation in a very ingenious way proposed by Ong (1993). Ong manipulated the integrated Monod equation in order to make it a linear function of experimental data (Equation 2.9). Then, he proposed a methodology based on the least-squares procedure for the linearized integrated Monod equation. Therefore, his approach avoids the problem of obtaining good initial values for the parameters to be evaluated. However, the linearization of nonlinear equations for parameter estimation purposes has been criticized because it violates some statistical assumptions Goovaerts et al. (2001).

$$\frac{1}{t}\ln\left(\frac{S}{S^0}\right) = b\left(\frac{\ln\left[1+a\left(S^0-S\right)\right]}{t}\right) - c \qquad (2.9)$$

where:

$a = y / X^0_{obs}$

$b = 1 + \left(X^0_{obs} + y\, S^0\right) / \left(y\, K\right)$

$c = \mu_{\max}\left(X^0_{obs} + y\, S^0\right) / \left(y\, K\right)$

The slope of Equation 2.9, *b*, and its intercept, *c*, are obtained by a linear regression of $(1/t)\ln(S/S^0)$ versus $(1/t)\ln[1+ a\ (S^0-S)]$. However, the value of *a* is not known a priori because *y* is one of the Monod parameters to be estimated during this process. Ong's methodology calculates the value of *a* by a trial and error process in which the objective function is to obtain the best correlation coefficient from the linear regression of experimental data using Equation 2.9. Once the optimum value of *a* is determine, the values of *b* and *c* are calculated. Ong showed, in his study for simulated experimental data, that Equation 2.9 predicts Monod kinetic parameters with a small margin of error even when endogenous decay is included in the data, but the maximum value he tested for endogenous-decay was 5% of μ_{max}. The major drawback of Equation 2.9 is the fact that it cannot contemplate experimental data at $t = 0$ because at this point Equation 2.9 yields the value of *0/0*. Figure 2.6 shows a schematic representation of Ong methodology.

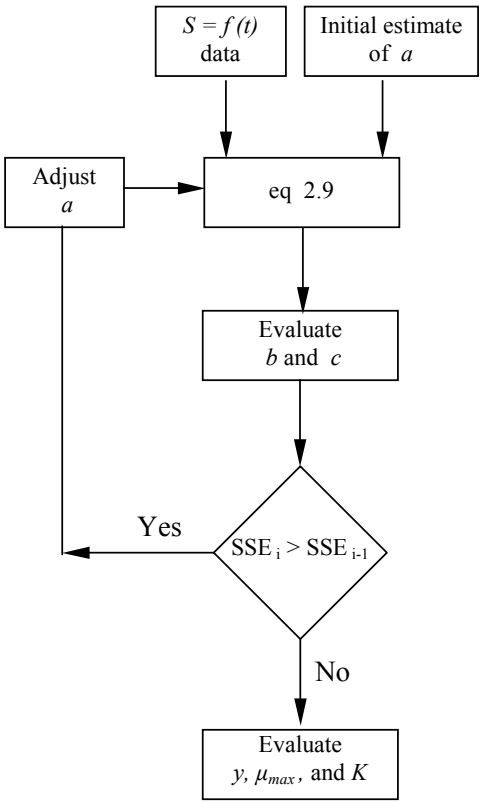

Figure 2.6. Steps involved in the estimation of Monod parameters using Ong methodology.

CHAPTER III

PROPOSED PARAMETER ESTIMATION METHODOLOGY

Introduction

Monod kinetic parameters have historically been estimated by several methods. Among these the Robinson and Tiedje methodology has been most widely used. Regression of experimental data using the integrated Monod equation ignores the endogenous decay coefficient, *b*. For a system where microbial endogenous decay is important, estimated bio-kinetic parameters are subject to bias that is independent from experimental error. Even though this situation is well known, there has not been any attempt to improve estimation procedures for the Monod kinetic parameters.

In this study, it was hypothesized that the incorporation of biomass generation data during the estimation of Monod kinetic parameters would basically include the endogenous decay effect in the estimated parameters because it is from the observable biomass data that the endogenous process is quantified. The first step is to obtain an integrated CM equation that includes all terms. Once this equation is obtained, it will be necessary to establish a new methodology for the estimation of Monod kinetic parameters because of the inclusion of *b* in the formulation.

Equations 2.3, 2.4, and 2.5 represent X_a, S, and X_i mass balances in a batch bioreactor. Upon integration of Equation 2.3, an equation that represents X_a after substrate depletion and loss of active biomass due to endogenous decay is obtained.

$$X_a = X_a^0 + y\left(S^0 - S\right) - b\int_0^t X_a\, dt \tag{3.1}$$

Presently, the integral term in Equation 3.1 is neglected, and the resulting expression is substituted in Equation 2.4, from which the known integrated Monod equation is obtained.

Proposed Approach

In this study, a different approach for solving Equation 3.1 is proposed, in which microbial endogenous decay is not neglected. Mathematical manipulation of Equation 2.4 provides an expression that can be substituted for the integral term of Equation 3.1:

$$-\int_0^t X_a dt = \int_{S^0}^{S} \frac{y}{\mu_{\max}}\left(1 + \frac{K}{S}\right) ds$$

$$\Rightarrow -\int_0^t X_a dt = \frac{y}{\mu_{\max}}\left(\left[S - S^0\right] + K\ln\left(\frac{S}{S^0}\right)\right) \tag{3.2}$$

Therefore, an exact expression for $X_a = f(S)$ is obtained by the substitution of Equation 3.2 into Equation 3.1:

$$X_a = X_a^0 + \gamma\left(S^0 - S\right) + \beta\ln\left(\frac{S}{S^0}\right) \tag{3.3}$$

where:

$$\gamma = y\left(1 - \frac{b}{\mu_{\max}}\right)$$

$$\beta = \frac{y\, b\, K}{\mu_{\max}}$$

The unique relation among X_a, the Monod kinetic parameters, and S (expressed by Equation 3.3) makes it possible to obtain an integrated form of Equation 2.3 that is valid for any stage of microbial growth. However, analytical integration of this equation is not possible due to the functionality of X_a. Thus, an approximate equation is proposed in this work. Upon substitution of Equation 3.3 into Equation 2.3, an expression is obtained in which the only term that cannot be integrated is dS/X_a. Therefore, it is assumed that X_a can be represented by a second degree Taylor polynomial expanded about S^0 for the integration of the dS/X_a term**.** By doing so, the proposed equation takes the form:

$$t = \frac{1}{b}\left[\frac{y}{\xi}\left(ln(A) - ln(B)\right) - ln\left(\frac{X_a}{X_a^0}\right)\right] \tag{3.4}$$

where:

$$A = 1 + \frac{-\beta/\left(S^0\right)^2\left(S^0 - S\right)}{\gamma - \beta/S^0 - \xi}$$

$$B = 1 + \frac{-\beta/\left(S^0\right)^2\left(S^0 - S\right)}{\gamma - \beta/S^0 + \xi}$$

$$\xi = \sqrt{\left(\gamma - \frac{\beta}{S^0}\right)^2 + 2\,\beta\frac{X_a^0}{\left(S^0\right)^2}}$$

Although Equation 3.4 is applicable to any stage of microbial growth, it is not useful in this form for most environmental applications because the parameters γ, β, X_a^0 cannot be estimated from Equation 3.3. This is because X_a cannot be measured by common analytical methods. Therefore, Equation 3.4 must be expressed in term of measurable quantities. As is known, the observable biomass, X_{OB}, is the sum of X_a and

X_i, so an expression that relates the Monod kinetic parameters to X_{OB} and S can be obtained through an appropriate combination of Equations 2.3, 2.4, and 2.5. Through this approach, Equation 3.5 is obtained, which provides a mathematical relation among observable biomass generation, substrate depletion, and the Monod kinetic parameters.

$$X_{obs} = X_{obs}^{0} + C\left(S^{0} - S\right) + D\ln\left(\frac{S}{S^{0}}\right) \tag{3.5}$$

where:

$$C = \gamma\, f_d + y\left(1 - f_d\right)$$

$$D = f_d\, \beta$$

The substitution of C and D into Equation 3.4 yields an equation, Equation 3.6, which is only a function of y, μ_{max}, and X_a^{0}. In this last step, the inclusion of observable biomass data is accomplished. The process of estimating Monod kinetic parameters can now be carried out using the experimental data.

$$t = \frac{f_d\, y}{\mu_{\max}\left(y - C\right)}\left[\frac{y}{\xi'}\left(\ln\left(A'\right) - \ln\left(B'\right)\right) - \ln\left(\frac{X_a}{X_a^{0}}\right)\right] \tag{3.6}$$

where:

$$A' = 1 - \frac{D}{f_d}\frac{\left(S^{0} - S\right)}{S^{0^2}}\frac{1}{\left[\frac{C}{f_d} + y\left(1 - \frac{1}{f_d}\right) - \frac{D}{f_d\, S^{0}}\right] - \xi'}$$

$$B' = 1 - \frac{D}{f_d}\frac{\left(S^{0} - S\right)}{S^{0^2}}\frac{1}{\left[\frac{C}{f_d} + y\left(1 - \frac{1}{f_d}\right) - \frac{D}{f_d\, S^{0}}\right] + \xi'}$$

$$\xi' = \sqrt{\left(\frac{C}{f_d} + y\left(1 - \frac{1}{f_d}\right) - \frac{D}{f_d\, S^{0}}\right)^{2} + 2\frac{D}{f_d}\frac{X_a^{0}}{\left(S^{0}\right)^{2}}}$$

Presently, the Monod parameters estimated using most of the available methodologies are not subject to any type of constraints. Sometimes, it is mentioned that estimated y should be smaller than its thermodynamic value, but this constraints is not used during Monod parameter estimation. In contrast, the methodology proposed in the current research provides constraints that the estimated Monod parameters must satisfy during the estimation process. These constraints are supported by the formulations that have been obtained. The constraints are the following:

- Estimated y is forced to be larger than C.
- Calculated b is smaller than the estimated μ_{max}.
- Calculated K is only a function of y, C, and D values.

One limitation of Equation 3.6 is its functionality with respect to X_a^0, which is a non-measurable value. This limitation is also observed for the known integrated form of the Monod equation. For the later equation, X_a^0 is assumed equal to other measurable quantities such as initial volatile suspended solids, VSS^0, and initial total suspended solids, TSS^0, etc. However, these quantities include a certain amount of inert mass, which is not capable of degrading substrate. Therefore, this assumption introduces error in the estimated parameters that is independent of the experimental error.

Several solutions have been proposed to overcome this limitation (Kesaven and Law, 1998; Nihtilä and Virkkunen, 1977; Orzechowski, 1994). For example, the approach taken by both Kesaven's group and Nihtilä's group deals with the CM equation, and evaluates the Monod kinetic parameters, X_a^0, and S^0 that provide the best fit to

experimental data through nonlinear parameter regression. One limitation of these approaches is that the estimated X_a^0 can be larger than the initial biomass. On the other hand, Orzechowski's approach is based on a modified Monod equation, which is a function of *VSS*. Orzechowski contemplated the difference between X_a and *VSS* by approximating the later as the power of a number, which is experimentally obtained and ranges from 0 to 1. However, his experimental data revealed that the power was equal to zero. In other words, Orzechowski's expression reduced to the unmodified Monod equation.

Sensitivity analysis was performed on Equation 3.6 in order to provide a solution for the X_a^0 dilemma. Due to the complexity of Equation 3.6, numerical differentiation was carried out for the sensitivity analysis with an increment of 0.01% for X_a^0, y, and μ_{max}. For the first order substrate degradation rate region as well as the zero order region (Figures 3.1 C, and 3.1 A), nonlinear regression analysis cannot provide unique values for μ_{max} and y because their derivatives with respect to S are multiples of one another. For the mixed order region (Figure 3.1 B), unique values for μ_{max} and y are expected. These conclusions are the same as those obtained by Robinson and Tiedje (1983) for the known integrated Monod equation. Although Equation 3.6 is conceptually complete compared to the known integrated Monod equation, both equations perform the same on these three regions for μ_{max} and y estimation. However, they have a distinct difference. While X_a^0 is considered as a non-estimable parameter for the known Monod integrated equation, X_a^0 is estimated from Equation 3.6 in the method proposed in this work.

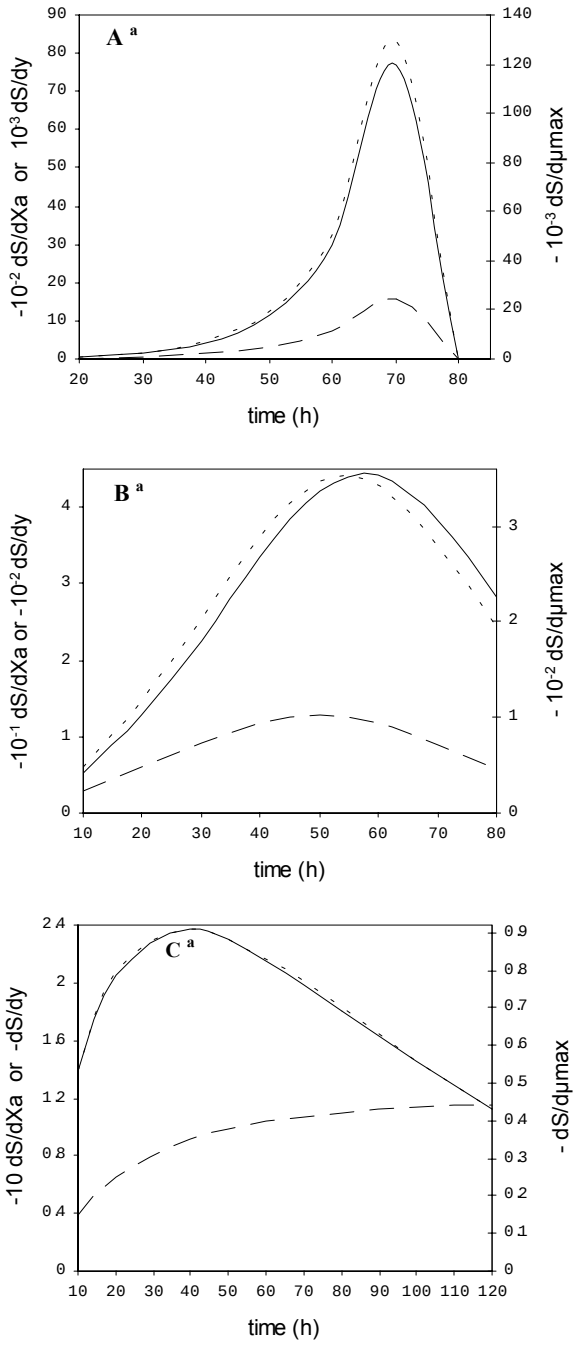

[a] Parameters $\mu_{max} = 0.1\ h^{-1}$, $y = 0.2$, $b = 0.02\ h^{-1}$, $f_d = 0.8$, $K = 50$ mg/l, and $X_a^0 = 1.5$ mg/l. (- - -) dS/dy, (—) $dS/d\mu_{max}$, and (— —) dS/dX_a^0. $S^0 = 5000$ mg/l for A. $S^0 = 50$ mg/l for B. $S^0 = 0.5$ mg/l for C.

Figure 3.1. Sensitivity analysis study.

Furthermore, it is observed in Figure 3.1 that unique values for X_a^0 are expected for each region. Therefore, the X_a^0 dilemma seems to be resolved since X_a^0 can be estimated from the proposed formulations. However, the only restriction on the estimated X_a^0 is that it is mathematically defined smaller than X_{OB}^0. This condition may not be satisfied during the parameter estimation process.

The following steps describe evaluation of the Monod kinetic parameters using the proposed methodology.

1. Estimation of C and D: By multiple regression of $(X_{OB} - X_{OB}^0)$ versus S data, C and D are obtained from Equation 3.5;
2. Initial estimates for Equation 3.6: As it was stated before, the substitution of numerical values of C and D into Equation 3.6 yields an expression in which the estimable parameters are y, μ_{max} and X_a^0. However, these parameters are evaluated by nonlinear regression, so initial estimates for y, μ_{max}, and X_a^0 must be provided. These initial estimates are obtained by the following steps:

- Initial estimate for y: It is assumed that $b/\mu_{max} = 0.12$, which is the mean value of b/μ_{max} for 19 different kinds of biodegradation systems published by Pavlostathis and Giraldo-Gomez (1991). By assuming this as the initial value for b/μ_{max}, Equation 3.7 provides an initial estimate for y.

$$y = \frac{C}{1 - f_d\,(0.12)} \tag{3.7}$$

- Initial estimate for μ_{max}: It is assumed in Equation 2.3 that $X_a = X_{OB}$, $S >> K$, and $b/\mu_{max} = 0.12$. The resulting expression is then integrated, and an equation is obtained from which μ_{max} can be estimated by linear regression of X_{OB} versus t data is obtained. It is observed that the obtained linear expression represents well data for the growing microbial phase.

$$\frac{1}{0.88}\ln\left(\frac{X_{OB}}{X_{OB}^{0}}\right) = \mu_{\max}\ t \tag{3.8}$$

- Initial estimate for X_a^0: The value of X_{OB}^0 is proposed as the initial estimate of X_a^0.

3. Estimation of K and b: Once the final estimates for y and μ_{max} are obtained, values for K and b are calculated:

$$K = \frac{D}{y - C} \tag{3.9}$$

$$b = \frac{\mu_{\max}}{f_d}\left(1 - \frac{C}{y}\right) \tag{3.10}$$

Modeling

The proposed methodology is tested by numerical simulation. Ten simulated data sets obtained from the numerical integration of Equations 2.3, 2.4, and 2.5 with the application of Runge-Kutta-Fehlberg algorithm (Burden and Faires, 1989) are used as an example that attempts to illustrate the performance of the proposed methodology. To the simulated data points (so called error free data), heteroscedastic errors of known magnitude were randomly introduced. In all cases, a coefficient of variation of 1% for S

and 2% for *VSS* data was randomly introduced to generate pseudo-experimental data. Homoscedastic error was not considered in this work, because the homoscedasticity assumption (error of constant variance) may generate unrealistic pseudo-experimental data (Goovaerts et al., 2001). Nonlinear regression analysis using the Levenberg-Marquardt algorithm (Marquardt, 1963) was applied to the pseudo-experimental data to obtain y, $\mu_{max,}$ K, b, and X_a^0.

In Table 3.1, final estimated parameters for the pseudo-experimental data at two different X_a^0/VSS^0 ratios are shown. In both cases, the obtained error for the mean values of estimated Monod kinetic parameters is less than 2%. However, a deviation of 14% is observed for the mean value of the estimated X_a^0/VSS^0 ratios. The proposed parameter estimation procedure, as well as the equations that are involved, provide good estimates and are not influenced by a change in X_a^0/X_{OB}^0 ratio.

Experimental Data

The proposed methodology demonstrated reasonable performance for parameter estimation from the pseudo-experimental data. In the last example, pseudo-experimental data were used as an approach for the evaluation of the proposed methodology since true parameters were already known. On the other hand, biodegradation rate parameters are not known in most environmental studies because they are estimated from actual experimental data. In this situation, the proposed methodology can only provide a point of comparison with parameters available in the literature.

The Monod kinetic parameters for phenol biodegradation by activated sludge were obtained by Okaygun (1991). Okaygun estimated these parameters by nonlinear

Table 3.1. Estimated Monod kinetic parameters by the proposed methodology [a].

	Final estimates (error free X_a^0/VSS^0=0.5)					Final estimates (error free X_a^0/VSS^0=0.75)				
Simulation case #	μ_{max}	K	y	b	X_a^0/VSS^0	μ_{max}	K	y	b	X_a^0/VSS^0
1	0.0989	51.64	0.197	0.0195	0.525	0.0971	50.8	0.194	0.0193	0.834
2	0.112	57.52	0.206	0.0218	0.336	0.0964	47.75	0.202	0.0212	0.897
3	0.0902	48.29	0.192	0.017	0.689	0.104	55.46	0.198	0.0185	0.582
4	0.0941	47.39	0.199	0.0199	0.632	0.100	51.19	0.2	0.0194	0.709
5	0.0929	45.91	0.201	0.0202	0.675	0.101	49.9	0.206	0.0212	0.718
Mean	0.0976	50.15	0.199	0.0197	0.571	0.0997	51.02	0.2	0.0199	0.748

[a] Original Monod kinetic parameters: μ_{max} = 0.1 h^{-1}, y = 0.2mg $VSS_a/mg\ S$, b = 0.02 h^{-1}, K = 50mg/L, f_d = 0.8, Initial conditions: S^0= 500mg/L, VSS^0= 2mg/L.

regression of the known integrated Monod equation. Table 3.2 includes parameters estimated by Okaygun as well as those estimated using the proposed methodology with the same set of experimental data. The difference between the parameters for these two methods is remarkable. However, the correlation of Okaygun's experimental data by Equations 3.5 and 3.6 turned out to be good for the biomass starved for 10.5 hr (Figures 3.2 and 3.3). Furthermore, the same good performance was observed for the biomass starved for 112.5 hr. Two main contributions could produce these differences among Monod kinetic parameters. One is that the integrated Monod equation considers a linear relation between the substrate consumed and biomass yielded, which is not valid for the employed set of experimental data (Figure 3.3). The other is the fact that, after starving the activated sludge for 10.5 and 112.5 hours, a certain amount of inert biomass should be generated, so it is not appropriate to assume $X_a^0 = TSS^0$.

Table 3.2. Monod kinetic parameters for phenol biodegradation.

Parameters	Okaygun [a]	Present study [d]		Okaygun [b]	Present study [d]
μ_{max} (h^{-1})	0.079	0.929		0.085	5.45
K (mg/L)	7.8	26.9		32.6	10.2
y (mg TSS_a/mg S)	0.717	2.44		0.742	3.58
b (h^{-1})	0.0028	0.75		0.0028	5.23
X_a^0 (mg/L)	1480	379		1520	94
f_d	—	0.8[c]		—	0.8[c]

[a] Biomass starved for 10.5 hours, S^0 = 653.5 mg/L, TSS^0 = 1480 mg/L.
[b] Biomass starved for 112.5 hours, S^0 = 578 mg/L, TSS^0 = 1520 mg/L.
[c] Assumed f_d.
[d] C = 0.863 mg *TSS/mg S* , D = 42.4 mg *TSS/L* for 10.5hr ; C = 0.836 mg *TSS/mg S* , D = 28.1 mg *TSS/L* for 112.5 hr of starvation period.

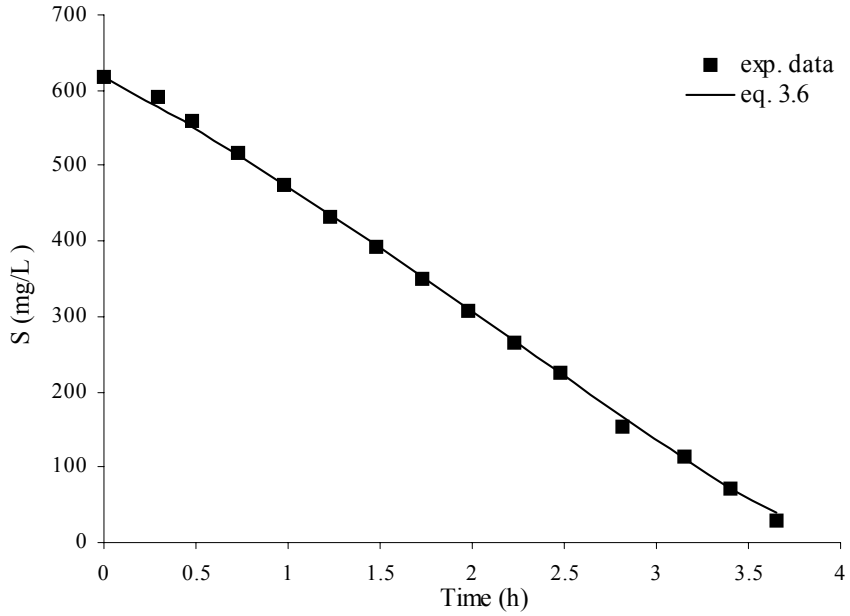

Figure 3.2. Phenol depletion curve for sludge starved during 10.5 hr. Experimental data from Okaygun (1991).

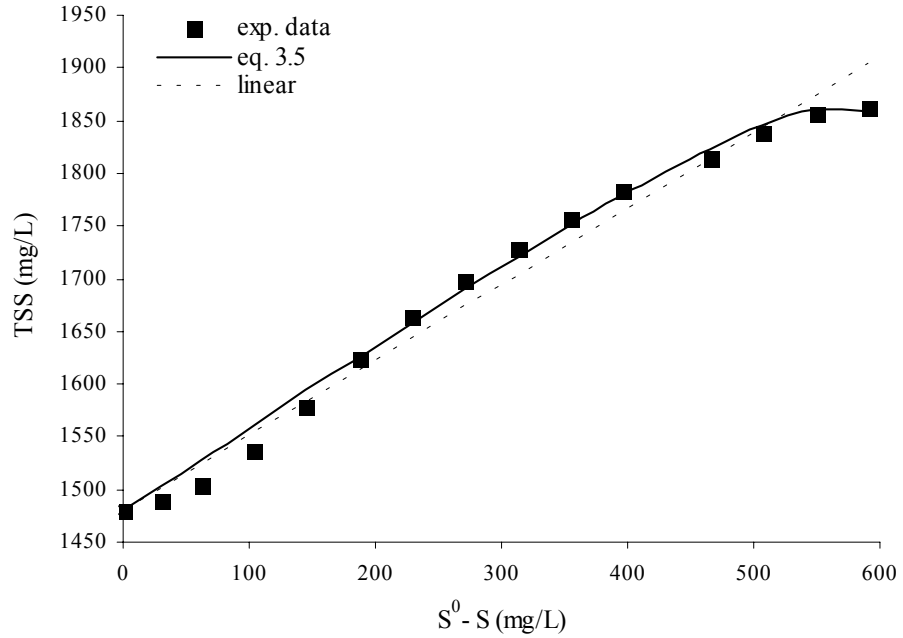

Figure 3.3. Biomass yield from phenol degradation. Sludge starved for 10.5 hr. Experimental data from Okaygun (1991).

Table 3.2 shows results that corroborate, to some extent, the performance of the proposed methodology. One is the fact that the longer the sludge is without substrate, the smaller is the ratio X_a^0/TSS^0, so the proposed methodology satisfies this basic concept. The other is that the culture history influences the biokinetic parameters (Grady et al., 1996). Therefore, estimated Monod parameters should be different for the two cases shown in Table 3.2 since they differ by more than 100 hours of starvation period.

Estimation of y, μ_{max}, K, b, and X_a^0 for the growth of *Trichoderma viride* on glucose was also performed in this study. Experimental data for this particular biodegradation process are provided in Nihtilä and Virkkunen (1977). Estimated Monod kinetic parameters by the proposed methodology are compared in Table 3.3 versus those available in the literature (Kesavan and Law, 1998; Nihtilä and Virkkunen, 1977).

In Table 3.3, it is evident that the obtained X_a^0 as well as S^0 values for Kesaven and Nihtilä's methodologies are larger than TSS^0 and S^0. This is because Kesaven and Nihtilä's methodologies employ a numerical solution of the Monod equation, which has no constraints, so this type of meaningless outcome is expected. On the other hand, the proposed methodology keeps S^0 as an unmodified and non-estimable value. During this process, X_a^0 is also estimated, and the possibility of obtaining a suspected value may exist. However, the fact that Equation 3.5 contemplates that $X_a^0 \leq X_{OB}^0$ makes this situation very unlikely and only dependent on data dispersion. The correlation of Nihtilä and Virkkunen's experimental data by Equations 3.5 and 3.6 are represented in Figures 3.4 and 3.5.

Table 3.3. Comparison of Monod kinetic parameters obtained under 3 different approaches [a].

Parameters	Kesavan [b]	Nihtilä	Present study [d]
μ_{max} (day^{-1})	4.56	2.51	5.69
K (mg/L)	3729	9340	11461
y (mg TSS_a /mg S)	2	0.468	0.961
b (day^{-1})	6.47	0.203	1.68
S^0 (mg/L)	26400	26110	24500
X_a^0 (mg/L)	460	467	206
X_i^0 (mg/L)	—	—	194
f_d	—	—	0.8[c]

[a] S^0 = 24500 mg/L, TSS^0 = 400 mg/L
[b] Kesavan's solution did not converge.
[c] Assumed f_d.
[d] C = 0.734mg $TSS/mg\ S$, D = 2610mg TSS/L

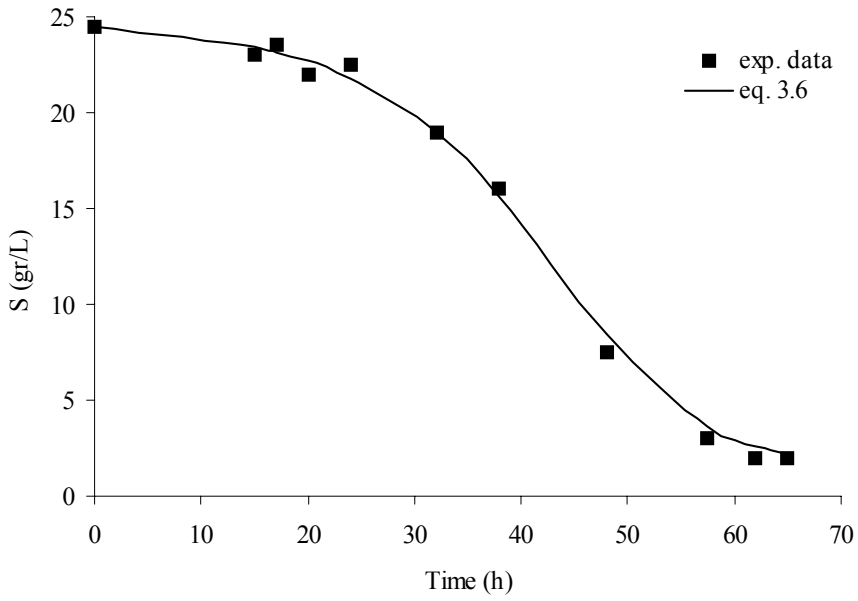

Figure 3.4. S depletion curve for the growth of *T. viride* on glucose. Experimental data from Nihtilä and Virkkunen (1977).

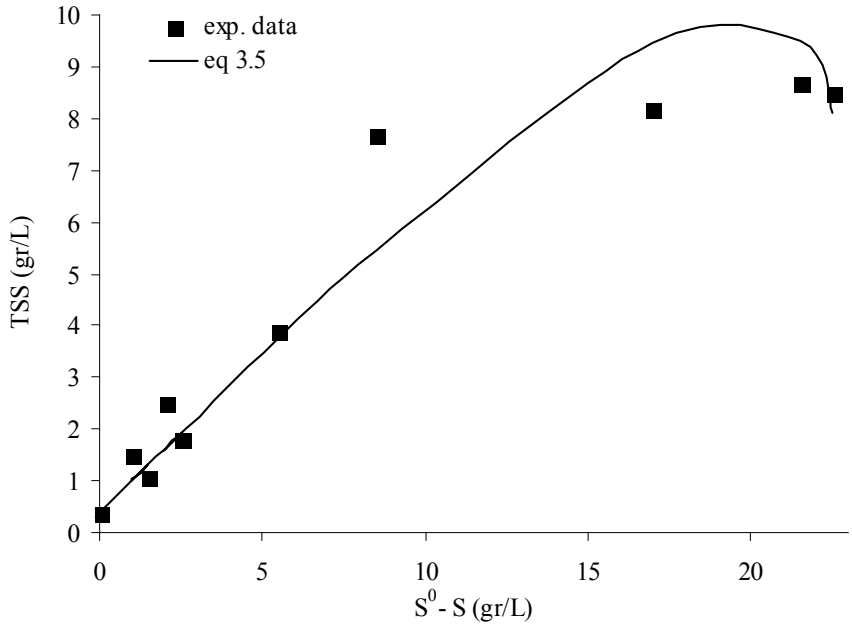

Figure 3.5. *TSS* versus (S^0-*S*) data for the growth of *T. viride* on glucose. Experimental data from Nihtilä and Virkkunen (1977).

CHAPTER IV

EXPERIMENTAL PROCEDURES AND METHODS

In this chapter, experimental methods and procedures employed during the course of this research are described. This chapter is divided into the following sections:

- Wastewater Conditioning.
- Batch Run Operation.
- CSTR Run Operation.
- Analytical Methods.

Wastewater Conditioning

Raw wastewaters from poultry slaughterhouse facilities were the material of study. This wastewater is mainly composed of blood, fat, and water from washing and cleaning processes. Due to the presence of materials such as feathers, chunks of fat, and sometimes pieces of bones that are usually present in this wastewater, a screening process was performed to remove them prior to anaerobic digestion studies.

All containers with raw wastewater were screened and then mixed in a big container. This step eliminated any variation in composition due to the wastewater collection process. The resulting liquid of this operation called "pretreated wastewater" was kept in a refrigerator at 2 °C to avoid any microbial action during the course of this research. Approximately one liter of pretreated wastewater was sent for characterization

to Scales Biological Laboratory in Brandon, Mississippi. Table 4.1 provides the list of the analyses that were performed by the private laboratory and the analytical techniques employed. In order to satisfy microbial requirements for micronutrients, necessary quantities were added to the pretreated wastewater in order to keep micronutrient concentrations at the levels defined in Table 4.2. $AlCl_3$ was also added to the pretreated wastewater in order to provide AL^{3+} concentration in the mixed liquor of 15 and 40 ppm. for each case studied.

Table 4.1. Wastewater characterization parameters.

Parameter	Method [a]
5 days *CBOD*	507
Long Term *CBOD*	507
COD	508 A
TSS	209 C
Oil & Grease, total	503 A
Ammonia Nitrogen, total	417 D
TKN, total	420 A

[a] Standard method for the examination of water and wastewater, 16 th edition, 1985.

Batch Run Operation

Start-up of Biodegradation Process

A bioreactor, model Bioflo 3000® manufacture by New Brunswick Scientific CO., was used in this research for carrying out the biodegradability study of poultry slaughterhouse wastewater under anaerobic conditions. This bioreactor is equipped with

a 15-liter-glass vessel, 5 variable-speed peristaltic pumps, pH and dissolved oxygen probes, variable speed agitation system, automatic temperature control, and a side panel for control and monitoring. Also, this equipment is equipped with a computerized online monitoring system that records operating conditions in the bioreactor.

Table 4.2. Concentration of nutrients in reactor media [a].

Compound	mg/L	Compound	mg/L
$CoCl_2 \cdot 6H_2O$	10	$NaWO_4 \cdot 2H_2O$	0.5
KI	10	Na_2SeO_3	0.5
$(NaPO_3)_6$	10	NH_4Cl	400
$MnCl_2 \cdot 4H_2O$	0.5	$MgSO_4 \cdot 7H_2O$	400
NH_4VO_3	0.5	$FeCl_2 \cdot 4H_2O$	40
$CuCl_2 \cdot 2H_2O$	0.5	$Na_2S \cdot 9H2O$	300
$ZnCl_2$	0.5	$(NH_4)_2HPO_4$	80
$AlCl_3 \cdot 6H_2O$	0.5	KCl	400
$NaMoO_4 \cdot 2H_2O$	0.5	$CaCl_2 \cdot 2H_2O$	50
H_3BO_3	0.5	Cysteine	10
$NiCl_2 \cdot 6H_2O$	0.5		

[a] nutrients recipe suggested by Speece (1996).

Table 4.3. Bioreactor operation conditions.

Temperature	30 °C
Mixer speed	100 RPM
pH	7
DO	0 mg/L

One hundred fifty milliliters of nutrient solution and 50 ml of anaerobic sludge from a municipal anaerobic sludge digester located in Vicksburg, Mississippi, were added to 5 liters of pretreated wastewater in the bioreactor. The resulting liquor was warmed to 30 °C, then purged with N_2 gas while the bioreactor mixer speed was set equal to 500 RPM. When the bioreactor *DO* probe read 0 mg O_2/L in the mixing liquor, the purging process continued for 1/2 hour more to ensure that any oxygen remaining in the liquid media, connection tubes, silicon sampling tube, and reactor headspace was expelled. Completion of this step established the beginning of the sludge acclimation process since this sludge was not previously exposed to poultry slaughterhouse wastewater. The operating conditions for the bioreactor are shown in Table 4.3.

Gas and Liquid Sampling Procedures

The biogas generated during the biodegradation process was collected from the reactor-head space through silicon tubing (1/4" diameter) connected to one of the ports located on the bioreactor lid. The other end of this silicon tubing was introduced into a 1-liter cylinder, which was placed upside down in a container (Figure 4.1). Both container and cylinder were full of water to provide a barrier to prevent atmospheric oxygen from entering the bioreactor. The yield of biogas was recorded as often as needed.

The sampled biogas for composition analyses was obtained from a 1/8-inch silicon tube attached to another port located on the bioreactor lid. This silicon tube was also connected to one of the peristaltic pumps provided with the reactor.

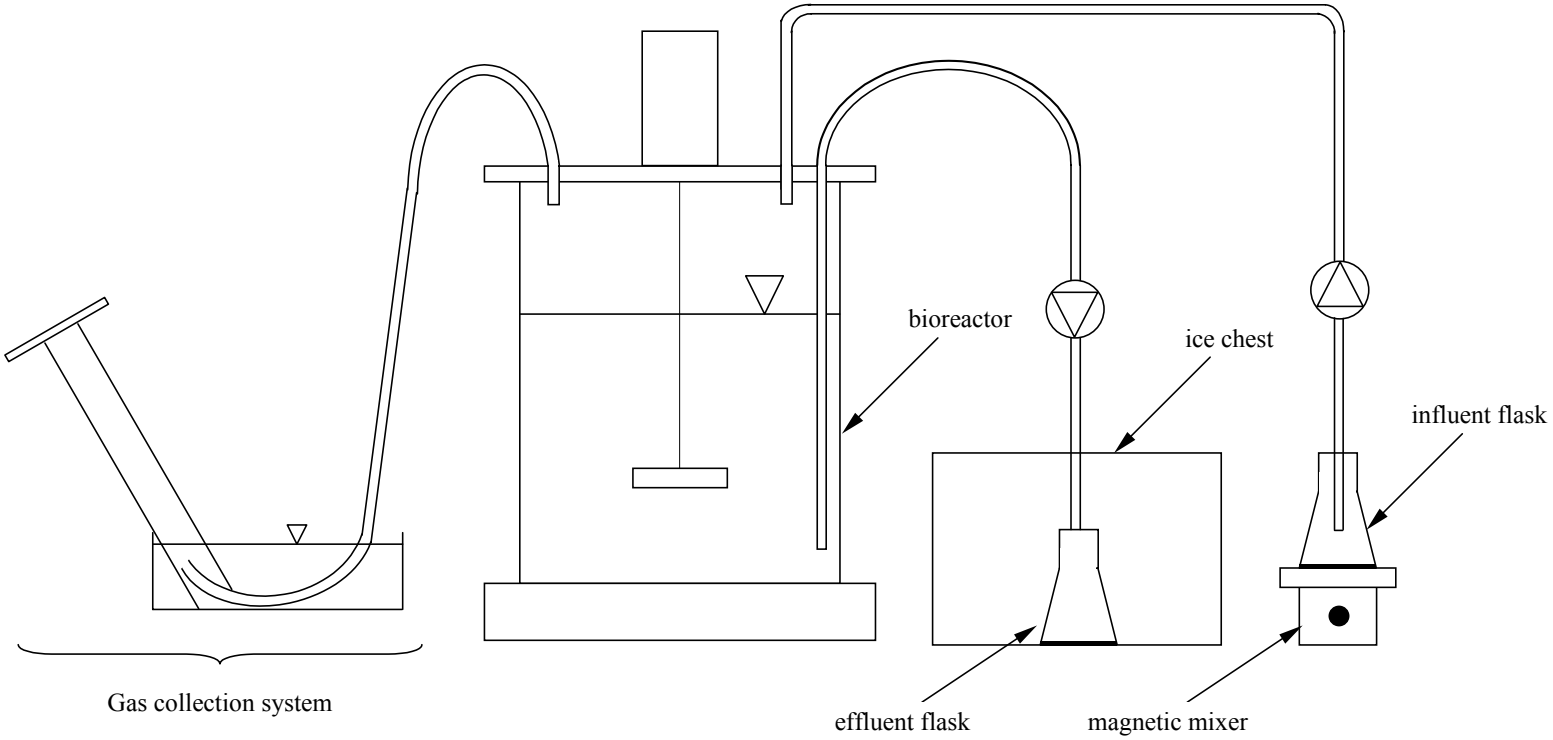

Figure 4.1. Schematic representation of reaction system and its components.

Twenty milliliters of biogas were sampled from the reactor headspace and pumped into a 50 ml glass bottle full of water, supersaturated with salt. This salty water was previously boiled and acidified with 5 drops of concentrated formic acid to remove any dissolved gas.

Approximately every two days, 100 ml of mixed liquor were withdrawn for analysis. The mixed liquor sample was divided into two sub samples. Fifty milliliters was reserved for volatile suspended solids, *VSS*, and total suspended solids, *TSS*, analyses. The remaining 50 ml sample was analyzed for chemical oxygen demand, *COD*, and volatile acids, *VA*. For every collected sample, pH was measured with an external pH-meter to track any change in pH. Although the bioreactor was equipped with an automatic pH control system, its operation was not possible due to sulfur contamination on the membrane of the pH probe within a few days after each experimental run had began.

CSTR Run Operation

Wastewater Reposition

Approximately 20 days after the point at which the anaerobic sludge was acclimated to degraded poultry wastewater, the bioreactor was switched from Batch mode to CSTR. In order to mimic field conditions, reactor sludge retention time, SRT, was set equal to 8 days. Two peristaltic pumps provided constant inlet and outlet volumetric flow rates to meet the needs of this research. Every day at the same time, fresh pretreated wastewater was added to the Erlenmeyer flask from where the

wastewater was pumped into the reactor (Figure 4.1). This fresh wastewater was purged with N_2 gas for 1/2 hour. When this process was completed, the Erlenmeyer flask was sealed and the inlet pump turned on. While the wastewater was pumped into the reactor, a magnetic mixer mixed the influent to the reactor to avoid allowing particulate material to settle in the Erlenmeyer flask.

Gas and Liquid Sampling Procedures

Gas sampling procedures for the biogas yield as well as biogas for composition analyses were the same as those described in the section "batch run operation" at the beginning of the chapter. However, the liquid sampling procedure was different. Due to the characteristics of CSTR operation, effluent from the reactor was collected daily in an Erlenmeyer flask. In order to avoid any microbial activity, this flask was kept inside an ice chest, which was full of frozen pads. During the time when the pretreated wastewater was prepared for pumping into the bioreactor, the flask that contained effluent from the bioreactor was emptied into a sampling container. A 300 ml sample was withdrawn from the total volume and kept for later analyses. The rest was discharged. From the 300 ml sample, 150 ml were used for *TSS, VSS, COD*, and *VA* analyses. The remaining 150ml was reserved for aluminum ion concentration determination.

Analytical Methods

Total Suspended and Volatile Suspended Solids

Measurements for *TSS* and *VSS* contained in the mixed liquor were performed by

following standard method 2540-D for *TSS* and 2540-E for *VSS*. Duplicates analyses for *TSS* and *VSS* were done on the collected sample for this purpose. Two microfibre filters (Whatman® 934-AH) were washed, ashed at 550 °C, and weighted as indicated in standard methods 2540-D and 2540-E. A 10 ml sample of mixed liquor was filtered through each one of the filters under vacuum. Then, the retained solids were treated as described in standard method 2540-D, and the *TSS* value for sample and duplicate were obtained. The standard method 2540-E technique was performed on the remains of the *TSS* test in filters.

Chemical Oxygen Demand

In this research, the substrate concentration available for microbial degradation was estimated by measuring the soluble chemical oxygen demand, *SCOD*. Six culture tubes were filled with collected sample and centrifuged at 3500 rpm for 15 minutes. After centrifugation, the upper layer of liquid from those culture tubes was filtered through a 0.45μm syringe filter and reserved for later analyses.

The *SCOD* was measured by titrimetric method, and triplicates were run for each collected sample in order to estimate variance for *SCOD* values. Although a standardized method for estimating *COD* by dichromate digestion (standard method 5222-E) is available, a similar technique was employed instead. A kit sold by Hach Company was used because of its simplicity. Three 0.2 ml portions of reserved filtered sample were added to 3 high range plus vials and digested at 150 ˚C for 2 hours. This method also requires the analysis of a blank. In this case, blank analyses were performed in duplicate

and the mean value was considered the true blank value. Due to a decrease in the concentration of titrant, Ferrous Ammonium Sulfate or *FAS*, as time progressed, duplicates analyses were performed to the *FAS* solution at the beginning of each analysis lot. The mean value was considered as the true *FAS* value. The following equation was employed to calculate the *SCOD*.

$$SCOD = (A - B)\frac{20000}{C} \tag{4.1}$$

where:

A = ml used in titration of blank

B = ml used in titration of sample

C = ml used in the normalization of *FAS* solution

Volatile Acid Measurement

The volatile acid content in the collected sample was measured by gas chromatography (*GC*). A Hewlett Packard gas chromatograph model 5890 series II equipped with flame ionization detector, *FID*, and capillary column Agilent® model HP-FFAP N° 19091 F112 (bonded and modified cross-linked polyethylene glycol, 25 m x 0.32 m x 0.5 µm) was employed during the course of this research. The *GC* settings for the *VA* analyses were:

- Temperature of inlet: 180 °C
- Temperature of FID: 260 °C

- Oven program: Start at 100 °C for 1 minute, then increase 10 °C/min until 200 °C and keep this temperature for another 10 minutes. The time required for the entire cycle was about 21 minutes.
- Gas carrier and flow: He at 50 ml/min.
- Injection volume: 0.4 μl
- Split mode: Beginning with purged valve on, and 0.2 minutes after injection valve off.

Due to the ionic character of *VA*, which is not suitable for *GC* analyses, samples were acidified with H_3PO_4 prior to injection. For the studied system, the most ionized *VA* of interest was acetic acid, AcH. Therefore, a relation of Ac^-/AcH less than 0.01 prior to sample injection was considered adequate in order to estimate the necessary concentration of H_3PO_4. With a *pKa* value of 4.75 for acetic acid, a concentration 0.03M of H_3PO_4 in the injected sample ensured the proposed Ac^-/AcH relation.

For calibration purposes, it was decided to use an internal standard method, because this method is not influenced by any change in injected volume and/or detector response. These two factors were a big concern for *VA* concentration analyses. The primary limitation of this calibration method is the identification of a chemical compound that can be used as an internal standard, because it must satisfy the following characteristics:

- It must have good peak resolution from other peaks in the sample.
- Its retention time must be very close to the peaks of interest.

- It must have a similar chemical structure to other substances in the sample.
- It must not be present in the original sample.

It was found, after use of several chemicals, that cyclopentanol at a concentration level of 50 ppm in the injected sample would meet these criteria. In addition, four different concentration levels of *VA* were necessary for establishing the calibration table. For this purpose, it was acquired as a standard from Alltech® (catalog number FA-MIX-03) which contains a mixture of *VA* from C-1 to C-5 at 1% (v/v) each in water. From this standard, 4 different levels of *VA* (0.1%, 0.03%, 0.012%, and 0.0048% v/v) were prepared. To each *VA* solution, cyclopentanol and H_3PO_4 were added to obtain *GC* calibration solutions that contained 50 ppm and 0.03 M, respectively.

The collected samples for *VA* analyses were prepared as follows. In a 10 ml graduate cylinder, 0.5 ml of 1000 ppm cyclopentanol and 0.3 ml of 1 M H_3PO_4 acid solutions were added. Then, it was filled to 10 ml of final solution with the remains of the centrifuged and filtered liquid sample (discussed in the Chemical Oxygen Demand section of this chapter). After proper mixing, this solution was ready to be analyzed in the *GC*.

pH.

A Denver Instrument Company pH-meter, model 215, was employed to measure the pH of sampled mixed liquor. Three calibration point buffers (4, 7, and 12) were employed in this research. Due to the presence of H_2S in the sample, the pH-meter electrode was regularly cleaned with weak hydrochloric acid solution and recalibrated.

Aluminum Concentration.

The concentration of aluminum in collected samples was determined during this research in order to determine which portion of the added aluminum flocculated and/or precipitated material from the mixed liquor. For this purpose, a 150 ml of sampled mixed liquor was divided into two 75 ml samples. One of the 75 ml samples was centrifuged for 15 minutes at 3500 RPM and then filtered through a 0.45 μm syringe filter. The obtained clear liquid was reserved for evaluating the concentration of dissolved aluminum. The remaining 75 ml was entirely used for measuring the aluminum concentration in the reactor media. Prior to aluminum analyses, both samples were digested by microwave assisted acid digestion (EPA method 3015A). Then, their aluminum contents were measured in a Perkin-Elmer OPTIMA 4300®, which is an Inductively Coupled Plasma Atomic Emissions Spectroscopy, or ICP-AES equipment. The ICP-AES operating conditions were the following:

- Wavelength: 396.153 nm.
- Plasma: 15 L/min of Argon at 100 psi.
- Nebulizer: Unbaffled cyclonic spray chamber.
- Plasma viewing configuration: Axial mode

Biogas Composition

Gas chromatography was employed to measure volumetric percentages of CH_4, CO_2, and H_2 in the biogas generated during the biodegradation process. Biogas samples prepared according to "gas sampling procedure section for Batch and CSTR mode" were

injected into a Hewlett Packard gas chromatograph model 6890 equipped with thermal conductivity detector, *TCD*, and two packed columns (Supelco® 80/100 Porapak-Q, 6' x 1/8" stainless steel; Supelco® 45/60 molsieve-5A, 10' x 1/8" stainless steel). The *GC* conditions were established as:

- Temperature of inlet: 200 °C
- *TCD* operation: temperature = 250 °C, makeup gas = He, makeup flow = 5 ml/min, negative polarity = off.
- Oven program: Start at 100 °C for 3 minutes, then increase 25 °C/min until 150 °C keep this temperature for another 25 minutes.
- Gas carrier and flow: He at 21 ml/min.
- Injection volume: 100 μl, manual injection.

CHAPTER V

EXPERIMENTAL RESULTS

Introduction

In an attempt to understand an industrial wastewater and its treatment, a treatability study is often performed. When problems occur and expected treatment does not occur, a treatability study is mandatory. Aerobic processes have been studied in detail over the last 50 years and have been the subject of a multitude of books and journals. Historically, treatability studies were thought of in terms of aerobic processes, not anaerobic processes. When this study began, there was little in the literature concerning anaerobic treatability with mixed culture.

This thesis seeks to better understand anaerobic fermentation and processes that face those attempting treatment of poultry slaughterhouse wastewaters. Numerous anaerobic lagoons are currently employed in the state at meat processing facilities. Three facilities were selected for this work in which two were out of state. The names of the companies will not be used in order to maintain confidentially.

Three consultants were utilized by one of the companies to provide information concerning their problematic lagoons. Significant discussion centered on nutrient and micronutrients, and organic acids from acetic to the *LCFAs*. Nutrients and micronutrients recommended by Dr. Speece were used throughout (Table 4.2).

Characterization

Wastewaters have been understood in terms of their organic content, inorganic content, nutrient, and micronutrients. Most often, organics are described in terms of biochemical oxygen demand (*BOD*) and chemical oxygen demand (*COD*). Sometimes, they are described in terms of total organic carbon (*TOC*). Many times, there is a clear understanding of the *BOD* and the *COD* and how they are used in design. Inorganics are thought of as nutrients and micronutrients, principally nitrogen and phosphorus. Micronutrients include a host of metals that include iron, manganese, cobalt, potassium, nickel, and others.

Table 5.1 presents the analytical results of the sample collected from each of three different poultry facilities. Each sample was assigned an identification code and the source of that sample is also included in Table 5.1. Two items should be pointed out relative to the table. *BOD*s are preceded by C indicating they are carbonaceous *BOD*s as opposed to total *BOD*s. Another way of saying the same thing is that nitrification was inhibited. Due to confusion caused by the *BOD* test, *CBOD* is becoming more widely used.

It can be seen in Table 5.1 that poultry slaughterhouse wastewaters share some common characteristics.

- A relation of ammonia–N to *TKN* of approximately 0.5 or larger, which is normal since a larger portion of this wastewater is proteins and blood.
- Relatively high *TKN* concentration.

- Relatively high oil and grease concentrations compared to most municipal wastewaters.

These three characteristics indicate that these wastewaters are not easily degradable under anaerobic conditions since ammonia and fatty acids are known for their inhibitory effects over the anaerobic microorganisms.

Table 5.1. Characterization of poultry slaughterhouse wastewater.

	Wastewater ID		
Parameters	FBF I	FBF II	MC
CBOD (mg/L)	3720		2440
$CBOD_5$ (mg/L)	2700	2505	1655
COD (mg/L)	3819	4767	3627
TSS (mg/L)	1710	1600	550
Oil & Grease (mg/L)	1456	928	1686
Ammonia–N (mg/L)	15.4	344.4	61.6
TKN (mg/L)	19.6	467.6	140
Source of waste	turkey	turkey	chicken

A second item in the characterization of a wastewater is to determine its extent of decay. It was expected that a high percentage of the wastewater would be biodegradable because of the type of waste. These data were analyzed by Scales Biological Laboratory in Brandon, Mississippi, inhibited every 10 days, over a 31 day period. It is interesting to compare the *COD* and the ultimate *BOD*. FBF I showed appreciable biodegradability,

because the ratio *BOD*/*COD* ration was 0.97. However, MC appears not to be as degradable since its ratio *BOD*/*COD* ratio was 0.67.

This research investigates the possible mechanisms that influence the anaerobic degradation of poultry slaughterhouse wastewater due to the addition of Al^{3+}. In attempting to understand and provide a certain degree of comparison over the performance of the aluminum case study, three runs with no aluminum added to the influent, other than that contained in the nutrient recipe, were performed during the course of this research. Wastewaters from FBF I, FBF II, and MC were employed for this purpose. Then, aluminum was added to the wastewater from MC in order to observe the difference, if any, on the performance of anaerobic digestion in comparison with the no aluminum MC run.

Batch Experimental Data for MC Wastewater at 15 ppm Al^{3+}

In order to obtain reproducible experimental data and to not arrive at erroneous conclusions about the influence of aluminum, the acclimation of anaerobic sludge was considered essential since microbes in the sludge should be able to degrade this particular wastewater without limitation. During the course of this research, sludge from an anaerobic municipal sludge digester was the source of anaerobic microorganisms, and was exposed to the wastewater in order to adapt it to the new substrate. Figure 5.1 shows experimental data for *SCOD* and acetic acid concentration recorded during the batch run operation mode. One hundred forty four hours after the beginning of the biodegradation process, the *SCOD* exhibited a maximum value in the reactor media. However, at 288

hours, it was observed that the build up of acetic acid in the system had stopped. At this point, it seems that two distinctive processes occurred. It was previously explained in Chapter 2 that an anaerobic sludge is basically composed of acidogenic and methanogenic microorganisms that are interrelated to each other, with each degrading a specific type of substrate (Figure 2.1). This sludge can be considered completely acclimated only after these two consortia of microbes are adapted to the poultry slaughterhouse wastewater. Since the *SCOD* reduction occurred after 144 hours of batch run, one can assume that acidogens had adapted to the wastewater at that point. However, acclimation of the methanogens appears after 288 hours of experimental run due to the reduction in acetic acid concentration observed from that point. It was explained previously that the presence of long chain fatty acids in wastewater has an inhibitory effect over the activity of methanogens, so acclimation of methanogens to this wastewater can be considered the limiting step. Therefore, it is assumed that the consortia of microorganisms in the degradation media were fully acclimated after 288 hours of experimental run. The concentrations of monocarboxylic organic acids from C_3 to C_5 were also measured in this research and their respective concentrations are shown in Figures 5.2, 5.3, and 5.4. Soon after the beginning of the batch run, the concentration of propionic acid slightly increased, but following this increase, a decrease of about 85% took place in only 96 hours. After that point, the propionic acid concentration stayed constant through the entire batch run. It also was observed that concentrations of C_4 and C_5 organic acids were constant during most of the batch run mode and only showed a decrease near the end of the run. The fact that propionic acid was consumed in a

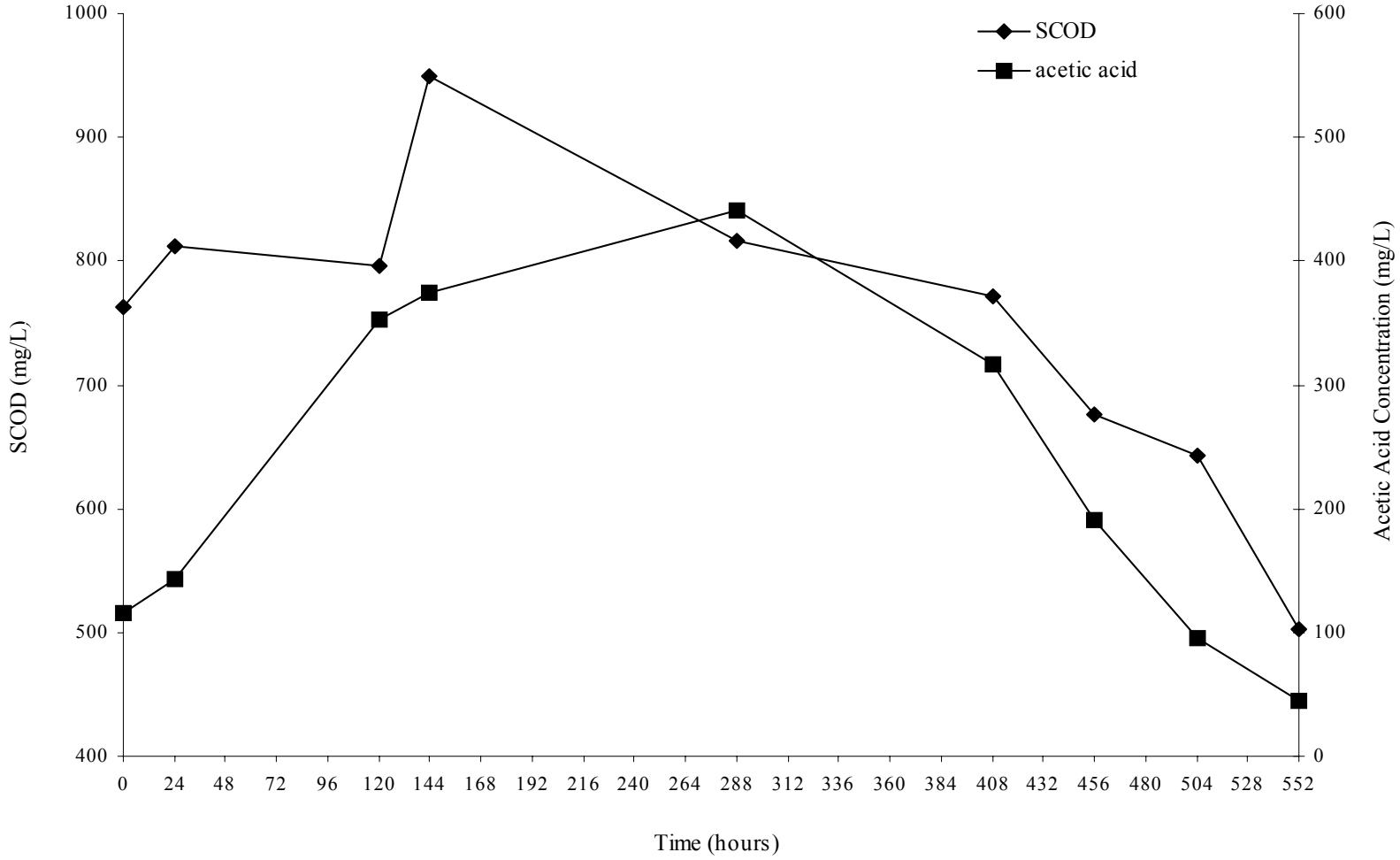

Figure 5.1. SCOD and acetic acid concentration for MC Batch run at 15 ppm of Al^{3+}.

relatively short period of time is an indication that propionoclastic microorganisms were not affected by the new wastewater.

The plateaus observed in Figures 5.2, 5.3, and 5.4 can be explained based on the degradation pathways along which the wastewater constituents were degraded. A large portion of poultry slaughterhouse wastewater is composed of *LCFAs*. As is known, *LCFA* are degraded by acidogenic microorganisms through *β*-oxidation pathways forming acetic acid, so the production of C_3 to C_5 organic acids is expected to be low in this wastewater. However, the acetic, as well as C_3 to C_5 organic acids, are produced by other constituents in the wastewater such as proteins and hydrocarbons. Conceptually, the generation of any substances in a batch reactor should translate into the accumulation of these substances in the reactor media unless they are degraded at the same or larger rate than they are produced. One can assume that the plateaus for C_3 to C_5 organic acid concentrations are due to an equilibrium between the rate of production and consumption being established. This is another clear indication of non-inhibitory effects of *LCFAs* over acidogenic microorganisms.

CSTR Experimental Data for MC Wastewater at 15 and 40 ppm Al^{3+}

Eleven days after the point at which the sludge showed signs of acclimation, the operation mode was switched to CSTR. At this point, slaughterhouse poultry wastewater was pumped into the reactor at a constant flow rate. Due to the addition of fresh wastewater into the reactor, increase in the concentration of *SCOD* and low molecular weight organic acids were observed. These increase were the consequence of microbes being washed out of the reactor media by the effluent. The addition of fresh *LCFA* with

the influent contributed to this process since it had inhibitory effects over methanogenic microorganisms.

One characteristic of the CSTR is that it operated at steady state, which means there was no change in parameters with respect to time. In order to determine when the system reached steady state, there are some commonly used criteria. One criterion that receives general acceptance among environmental engineers is based on the period of time required for a given CSTR to reach steady state (Smith and McCarty, 1989; Bull et al., 1984). It is generally accepted that the length of this period is equal to three times the operational sludge retention time or three SRT. However, the needed start up period criteria was combined in this research with the establishment of the steady states values of measurable variables with respect to time.

After 14 days of experimental run, *SCOD*, butyric, isobutyric, and acetic acid concentrations oscillated around constant values (Figure 5.5, 5.6, 5.8, and 5.9). Propionic acid showed its steady state plateau after 16 days (Figure 5.7). However, valeric and isovaleric acids showed an unsteady plateau between days 14 and 16 of the experimental run (Figure 5.10 and 5.11) during which the concentration of valeric acid was not detectable. On day 18, the concentration of valeric acid increased until it reached another plateau, but isovaleric acid concentration decreased and stayed constant after 22 days. This sudden change could be produced by a given metabolic process that on day 18 found the necessary conditions for its activation (eg., $\Delta G < 0$). It was reported by Wang et al., (1999) that reciprocal isomerization of butyric acid and isobutyric acid occurs by

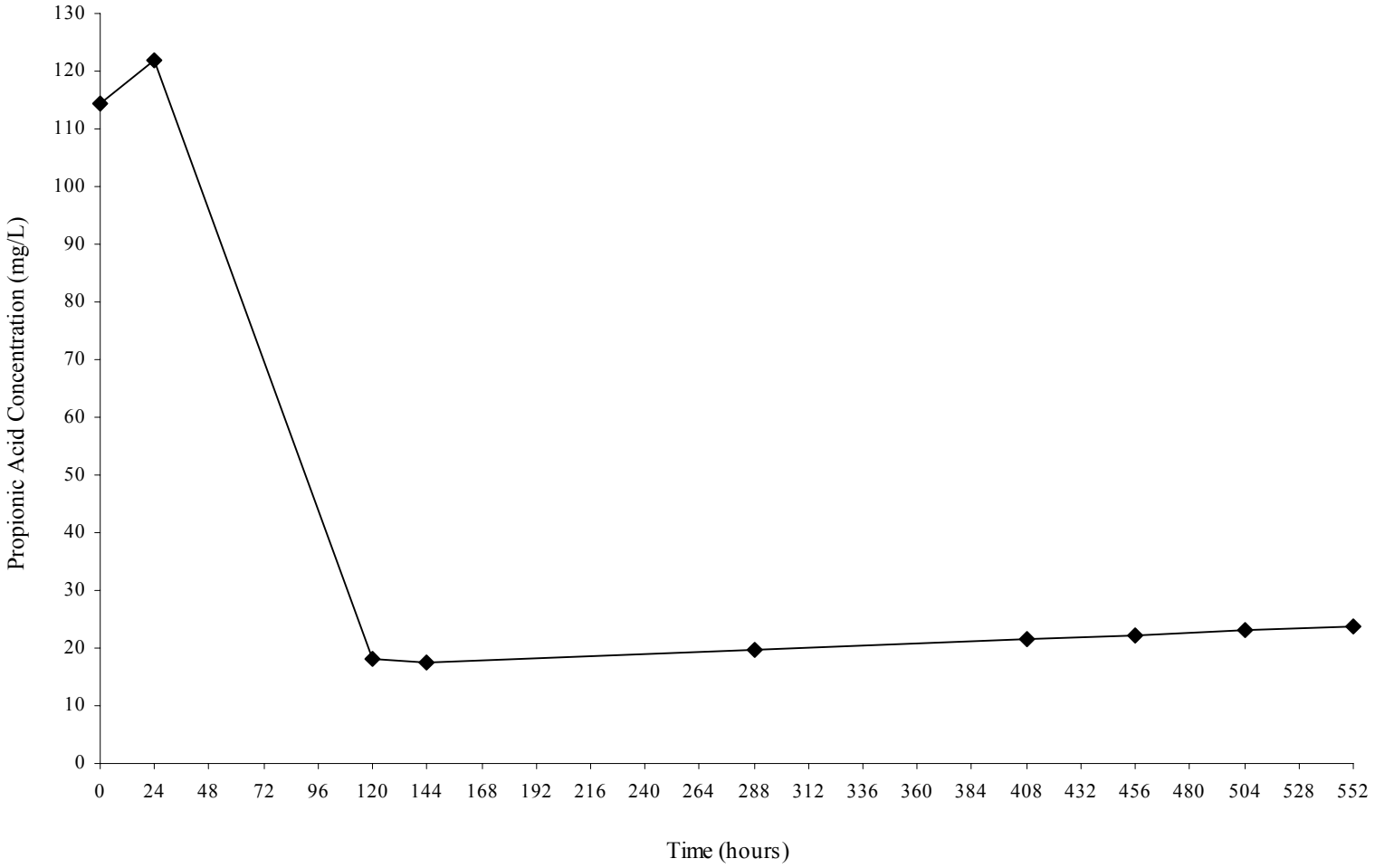

Figure 5.2. Propionic acid concentration for MC Batch run at 15 ppm of Al^{3+}.

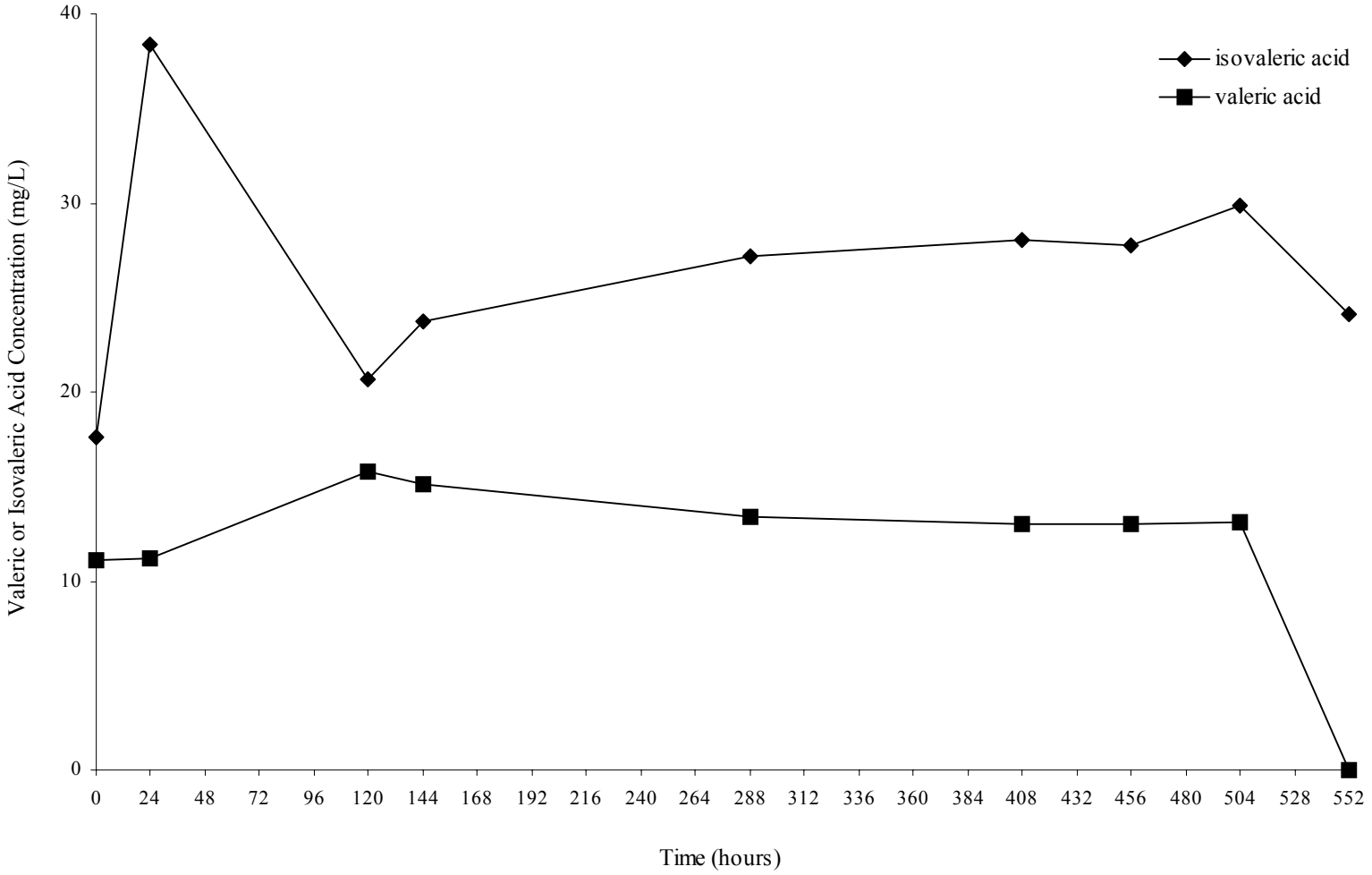

Figure 5.3. Valeric and isovaleric acid concentrations for MC Batch run at 15 ppm of Al^{3+}

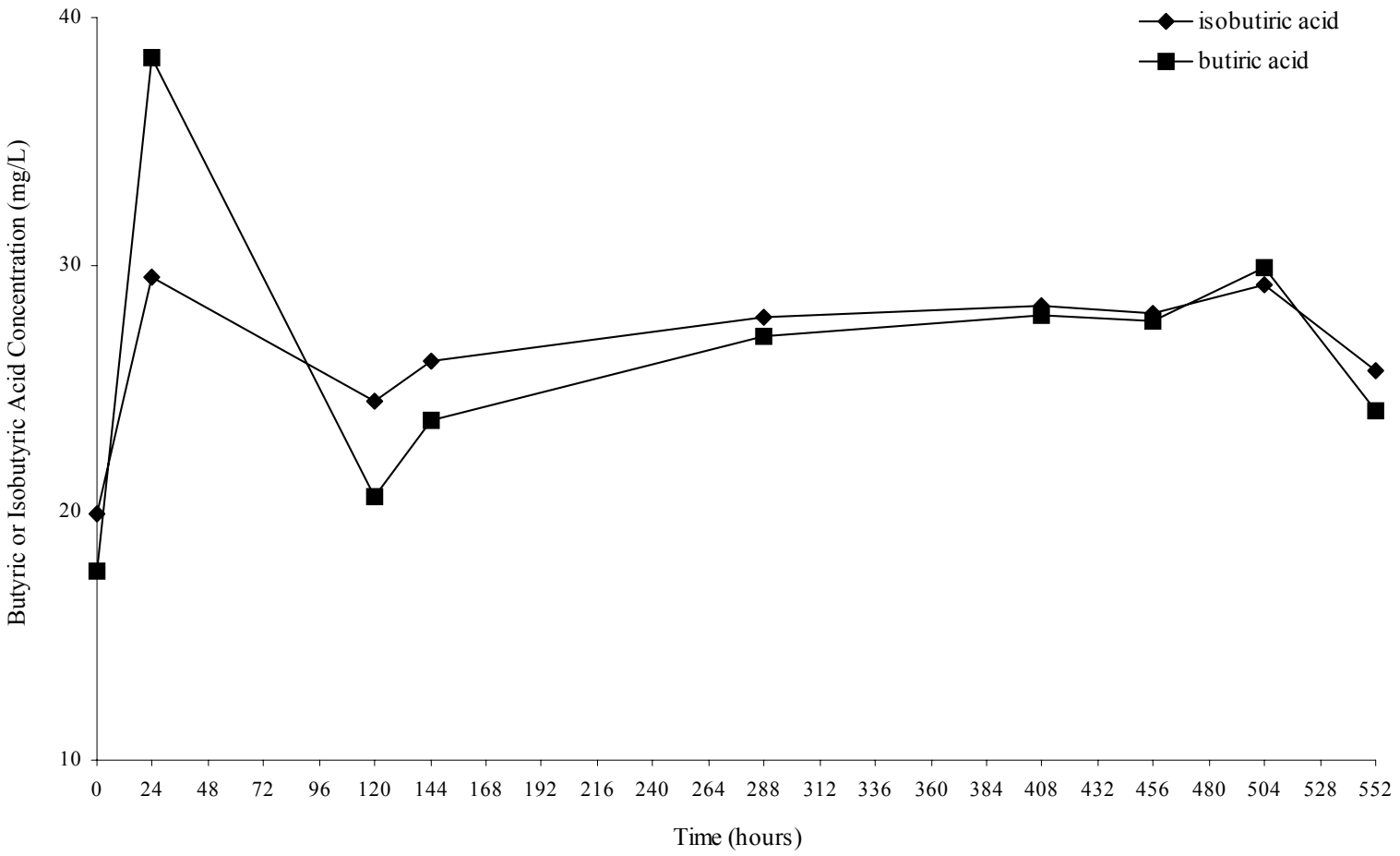

Figure 5.4. Butyric and isobutyric acid concentrations for MC Batch run at 15 ppm of Al^{3+}.

acidogenic microorganisms. However, they did not observe the same behavior for valeric and isovaleric acids. Therefore, the change of valeric and isovaleric acid concentrations is not well understood at this point and may not be related to a reciprocal isomerization process.

By simple observation of Figures 5.5 to 5.9, it can be assumed that the CSTR operating with 15 ppm of Al^{3+} in its influent reached steady state between days 18 and 22. A statistical criterion was adopted in order to establish exactly when steady state was achieved. As is known, experimental data are normally reported as the mean and standard deviation of values for a given collection of data points. For simplicity, this mean value is assumed equal to the true mean value of the sample. However, from a statistical point of view, the true mean is not the calculated mean, rather it is located inside the extremes of an interval defined with statistical tools. Since the true mean is located inside an interval, 2 different calculated mean values for 2 different data samples may or may not be statistically different. This depends upon whether the intervals mentioned before for these samples are, or are not, overlapped. This concept provides a useful tool to establish when the true steady state is reached in the system because the calculated mean values should not be statistically different. Generally, this kind of problem is studied by a procedure called analysis of variances or *ANOVA*. For this purpose, the SAS® software was employed during the course of this research. Details of the *ANOVA* procedure are given in Freund and Wilson (1997). One requirement of this test is to define a level of confidence. Williams et al. (1986), Hsu (1973), and Azbar et al. (2001) solved a similar statistical problem by using in their analyses a 95%

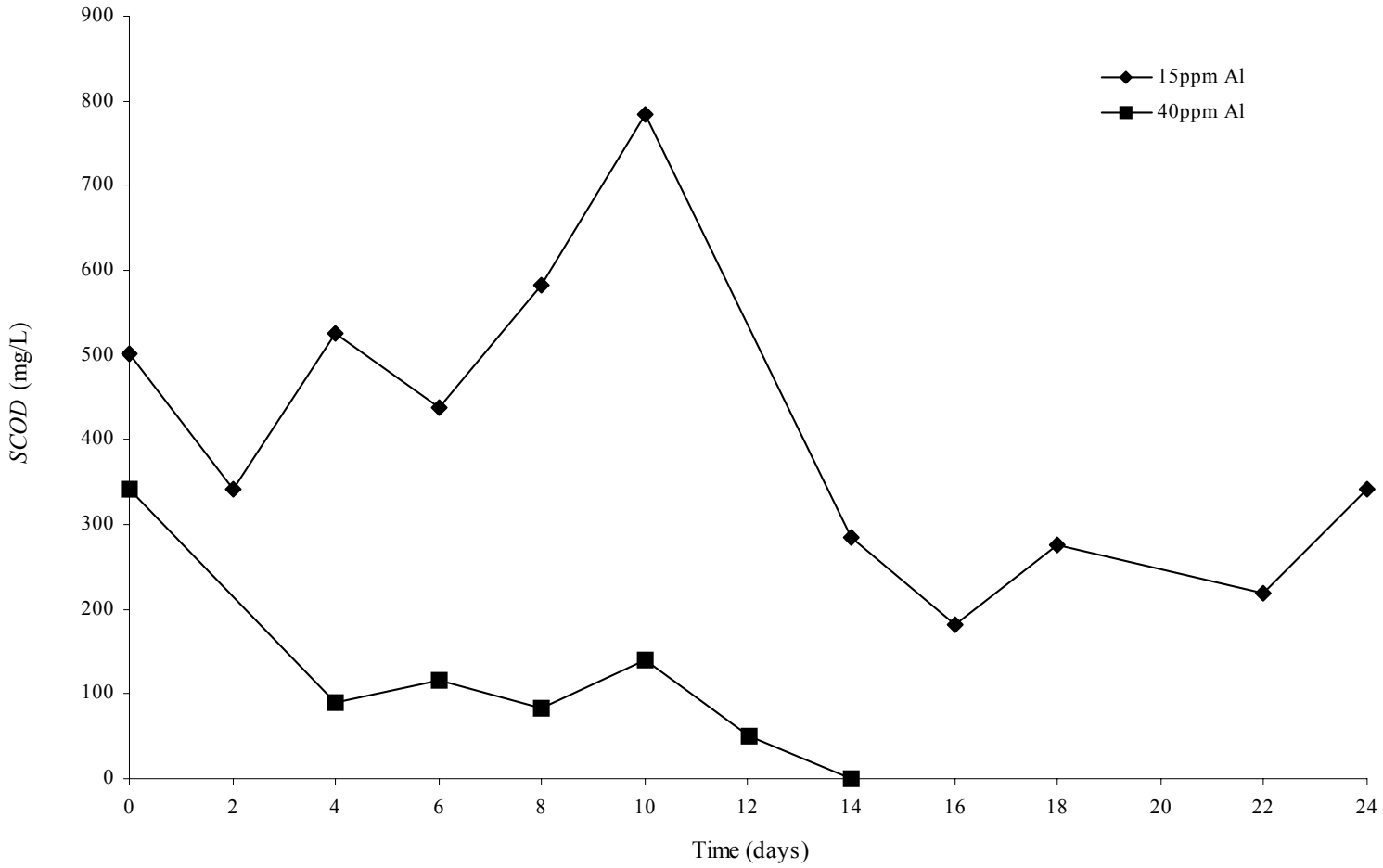

Figure 5.5. SCOD for MC CSTR run at 15 and 40 ppm of Al^{3+}.

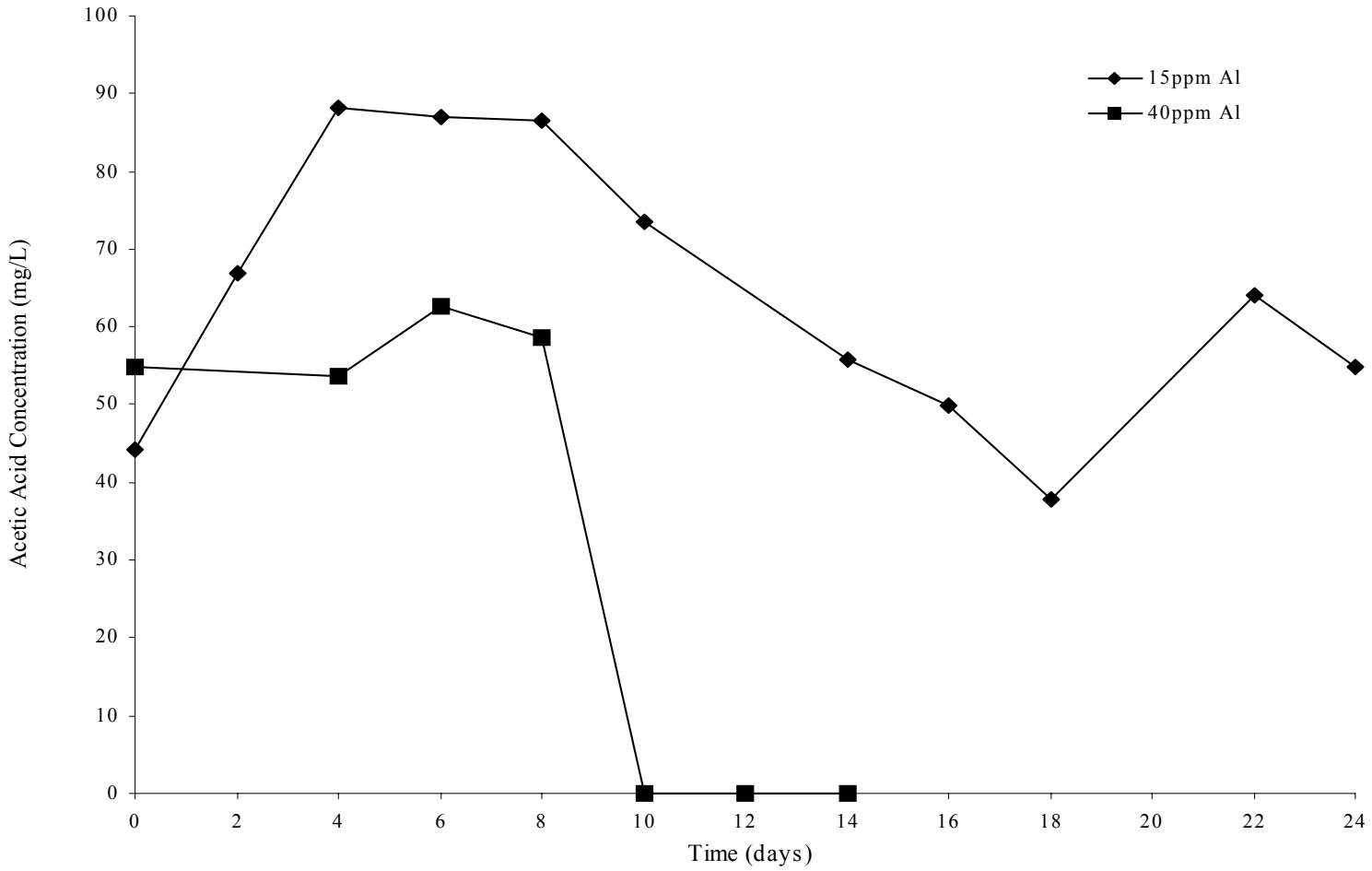

Figure 5.6. Acetic acid concentration for MC CSTR run at 15 and 40 ppm of Al^{3+}.

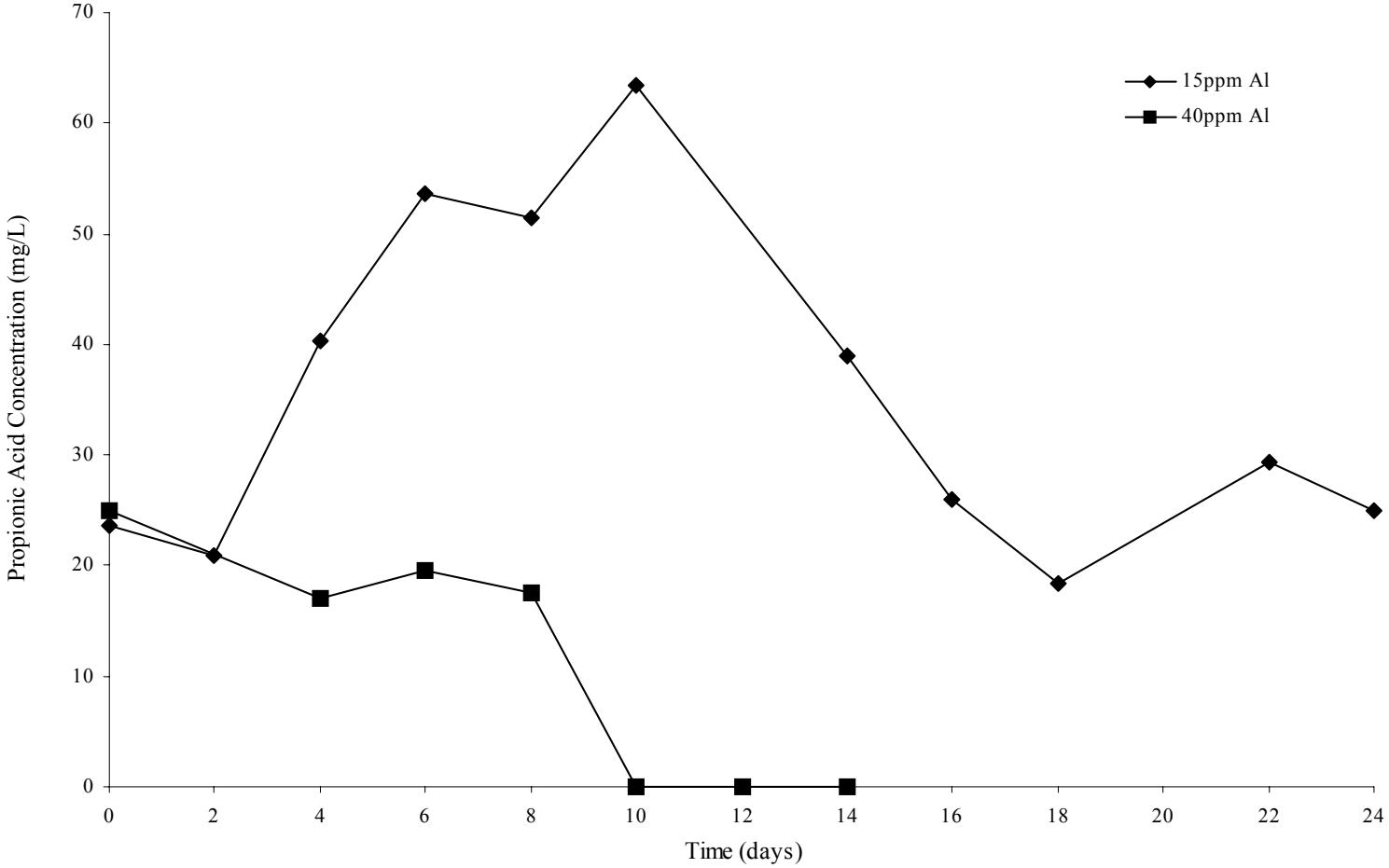

Figure 5.7. Propionic acid concentration for MC CSTR run at 15 and 40 ppm of Al^{3+}.

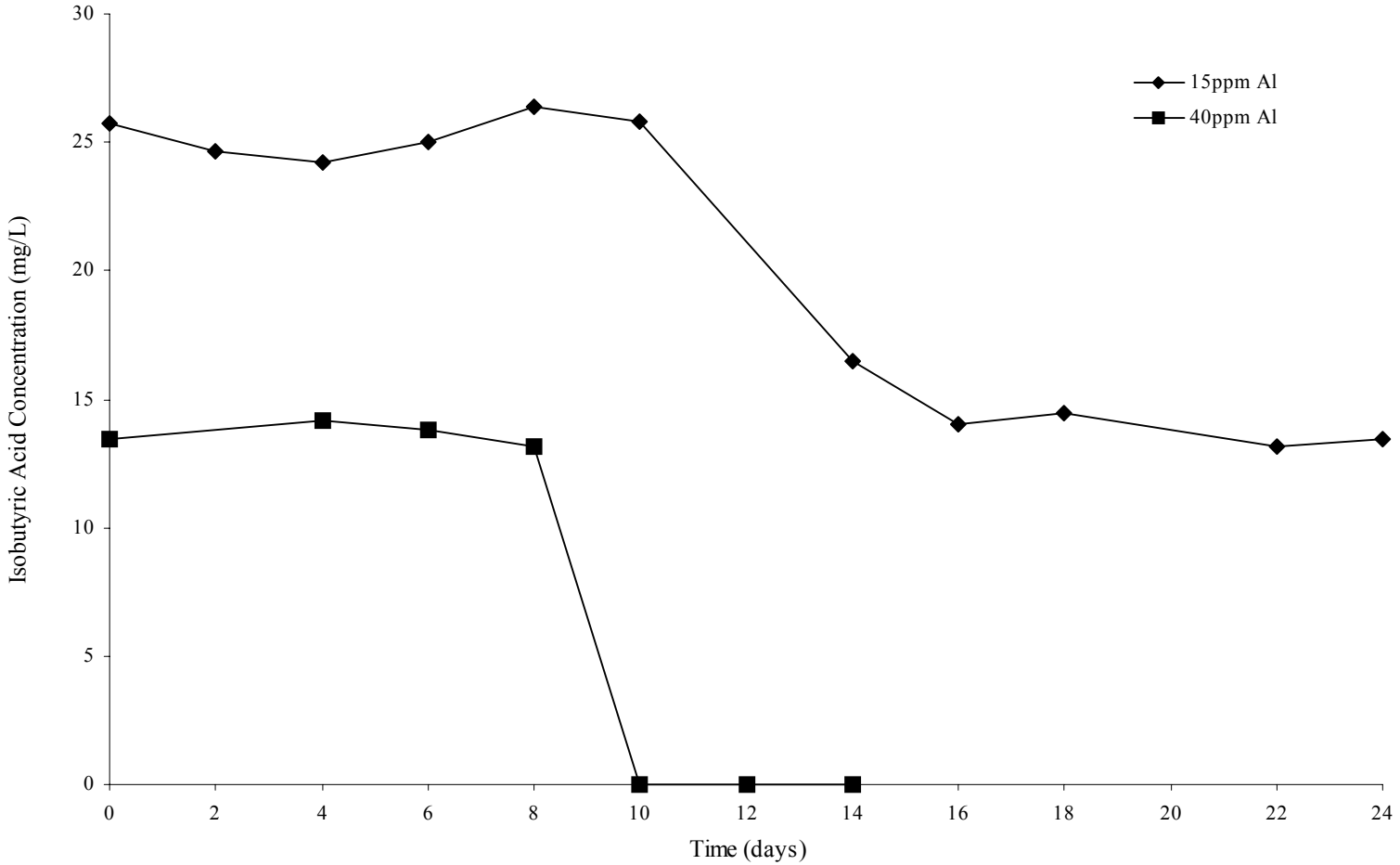

Figure 5.8. Isobutyric acid concentration for MC CSTR run at 15 and 40 ppm of Al^{3+}.

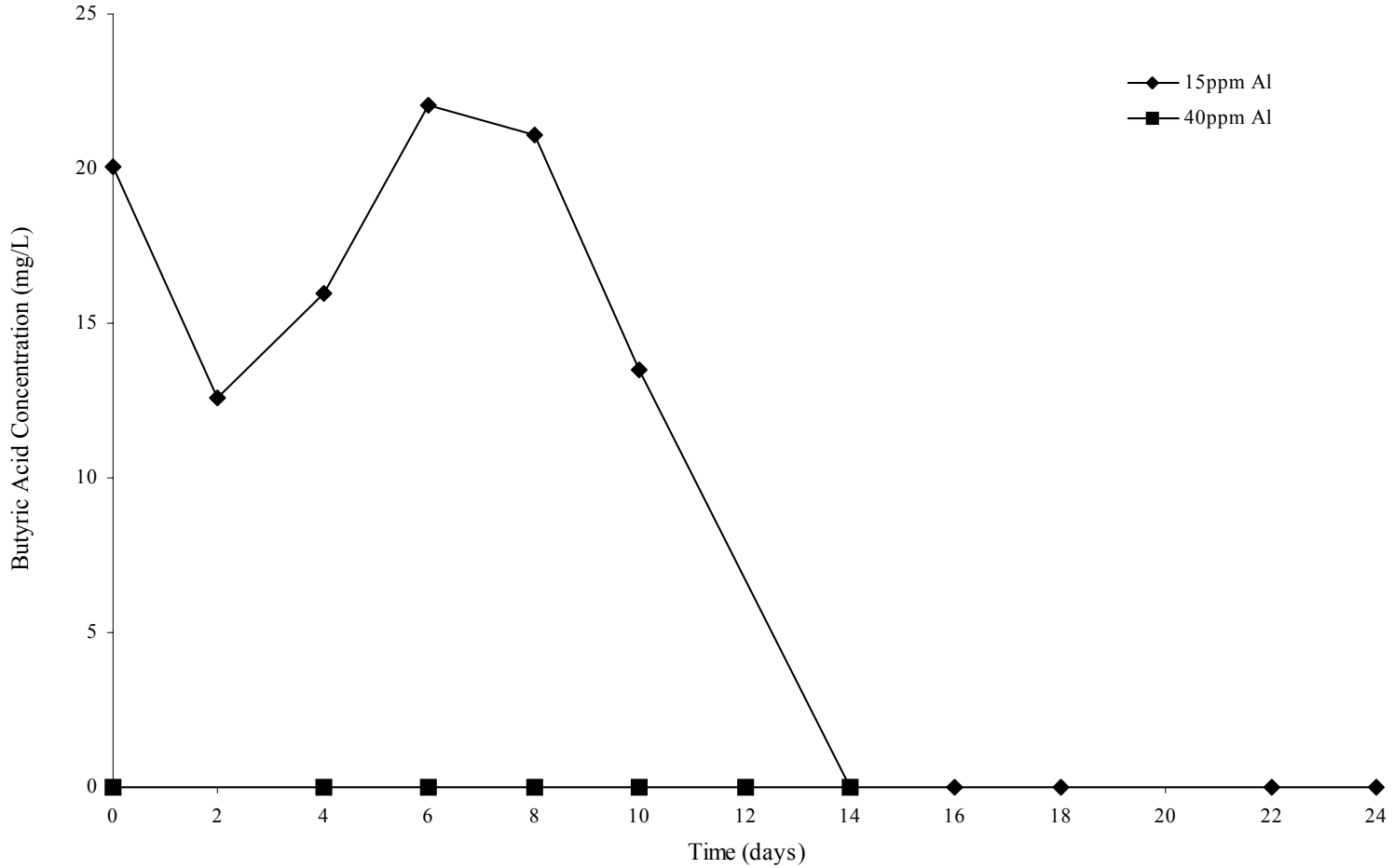

Figure 5.9. Butyric acid concentration for MC CSTR run at 15 and 40 ppm of Al^{3+}.

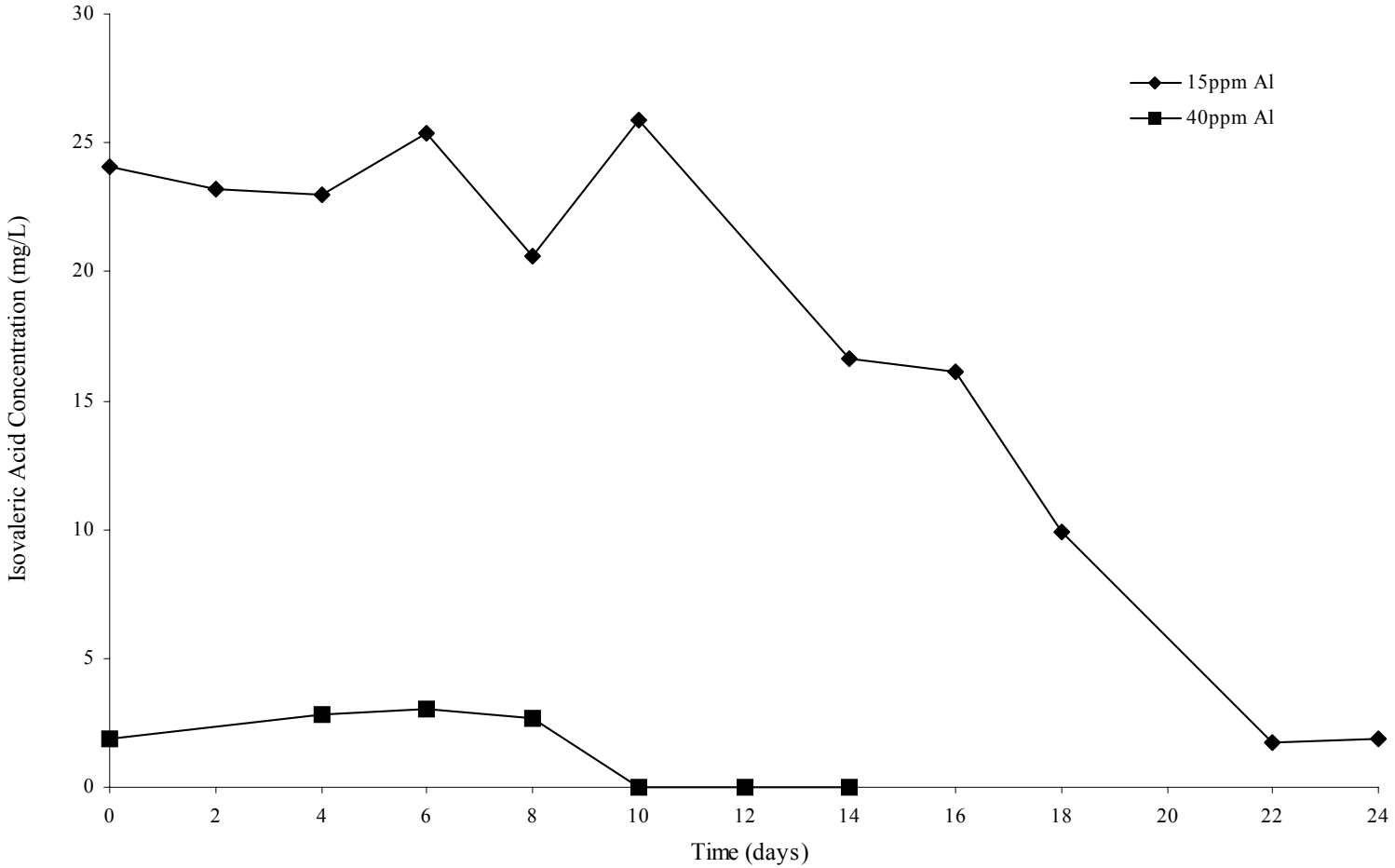

Figure 5.10. Isovaleric acid concentration for MC CSTR run at 15 and 40 ppm of Al^{3+}.

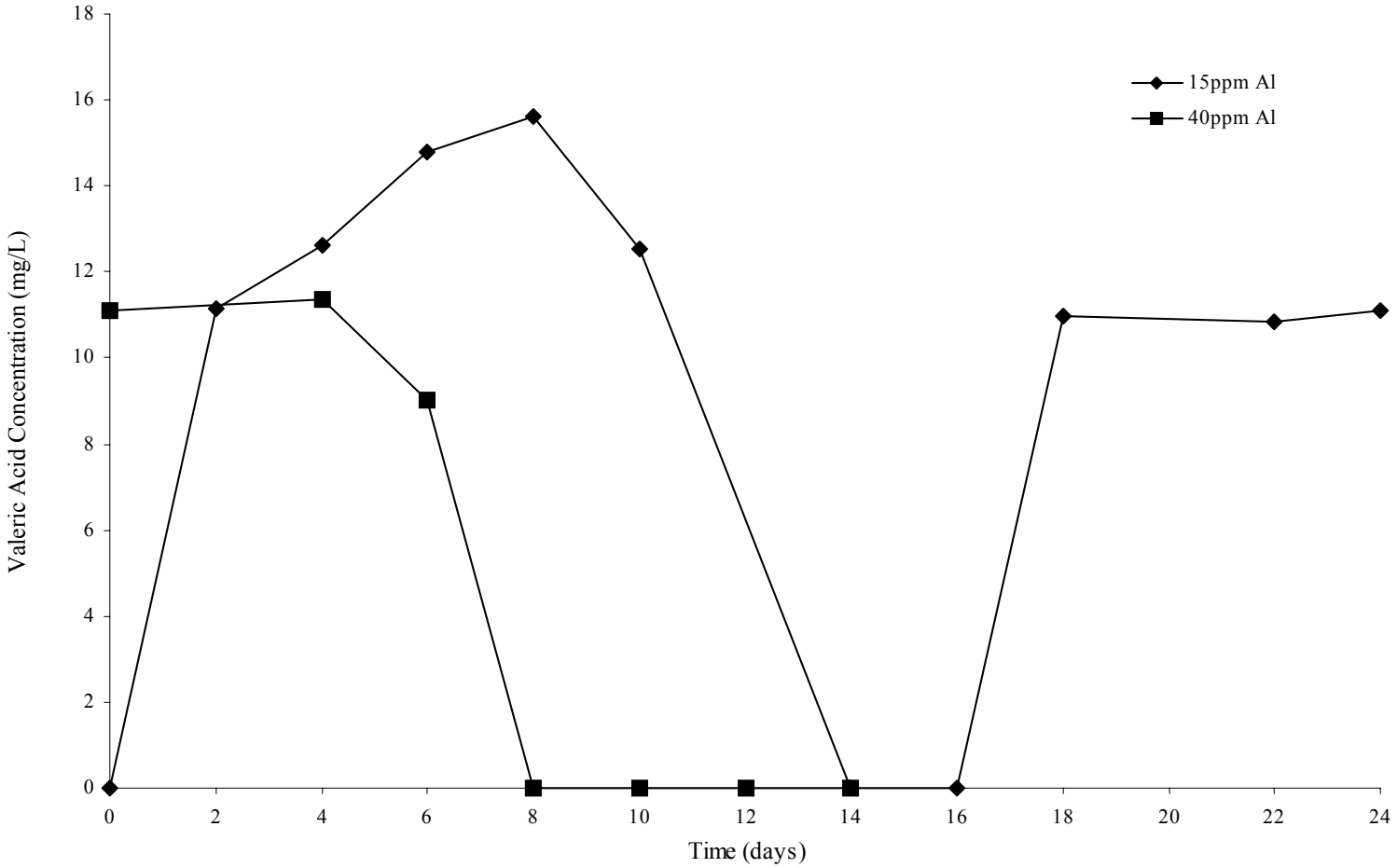

Figure 5.11. Valeric acid concentration for MC CSTR run at 15 and 40 ppm of Al^{3+}.

level of confidence, so the same level was adopted in this research. The *ANOVA* study for *SCOD* and acid concentrations for the group of data obtained from days 18 to 24 showed that the isovaleric acid concentration on day 18 was the only one significantly different from its concentrations on days 22 and 24. The same analysis for data points from days 22 to 24 showed that none of them were significantly different, so it is assumed that the steady state was reached on day 22. Table 5.2 shows the mean values for the steady state operation of a CSTR receiving 15 ppm of Al^{3+} in its influent. Since the steady state values for parameters at 15 ppm Al^{3+} are known, a comparison with those values for the reactor operating with 40 ppm Al^{3+} and no aluminum in the incoming influent will provide a better picture of the influence of aluminum on the anaerobic treatment of poultry slaughterhouse wastewater.

Table 5.2. Steady state variables for CSTR operation. MC wastewater at 15 ppm Al^{3+}.

SCOD (mg/L)	280.3
Acetic acid (mg/L)	59.5
Propionic acid (mg/L)	27.2
Isobutyric acid (mg/L)	13.3
Butyric acid (mg/L)	ND
Isovaleric acid (mg/L)	1.8
Valeric acid (mg/L)	11.0
TSS (mg/L)	506.3
VSS (mg/L)	393.8
pH	7.5

From Figures 5.6 to 5.11, it is evident that the CSTR operating at 40 ppm of Al^{3+} reached steady state in approximately 10 days, but for *SCOD* that was delayed until day 12. This visual assumption was also corroborated with the *ANOVA* test. The needed time for reaching steady state in this case was approximately half that needed for the reactor operating at 15 ppm Al^{3+}. This relatively short period of sludge adaptation for the reactor receiving influent with 40 ppm of aluminum could have two possible explanations. One is that aluminum was deficient for anaerobic microorganisms during the run with 15 ppm of aluminum, so an extra amount satisfies the requirement of aluminum for the microbes. The other is that aluminum interacts with some constituents in the reactor media that are harmful to the microorganisms, so the aluminum ions blocked or reduced these adverse effects. This will be discussed further in the next chapter. The steady state variables for the CSTR at 40 ppm of Al^{3+} are in Table 5.3.

Table 5.3. Steady state variables for CSTR operation. MC wastewater at 40 ppm Al^{3+}.

SCOD (mg/L)	24.69
Acetic acid (mg/L)	ND
Propionic acid (mg/L)	ND
Isobutyric acid (mg/L)	ND
Butyric acid (mg/L)	ND
Isovaleric acid (mg/L)	ND
Valeric acid (mg/L)	ND
TSS (mg/L)	528.8
VSS (mg/L)	397.5
pH	7.4

Typically, anaerobic degradation of wastewater generally yields CO_2, H_2, and CH_4. These gases are the result of the biodegradation of organic and inorganic matter contained in the wastewater. Table 2.1 showed some of the metabolic pathways that produce these gases. CO_2 is produced in the acidogenic and methanogenic steps from organic substances. H_2 is produced in almost any of the reactions listed in Table 2.1, but the larger contributor of H_2 is from the *LCFAs* due to their constituting a large portion of the organic matter in the slaughterhouse wastewater. On the other hand, CH_4 is only produced in the methanogenic step from organic compounds such as acetate and ethanol or inorganics such as H_2 and CO_2. Figure 5.12 shows the specific CH_4 production measured at 20°C and 1 atm for steady state conditions of the CSTR configuration. At 40 ppm of Al^{3+}, the system yielded about 50% more of methane than at 15 ppm of Al^{3+}, which is an indication that methanogenic activity was increased at higher aluminum concentration.

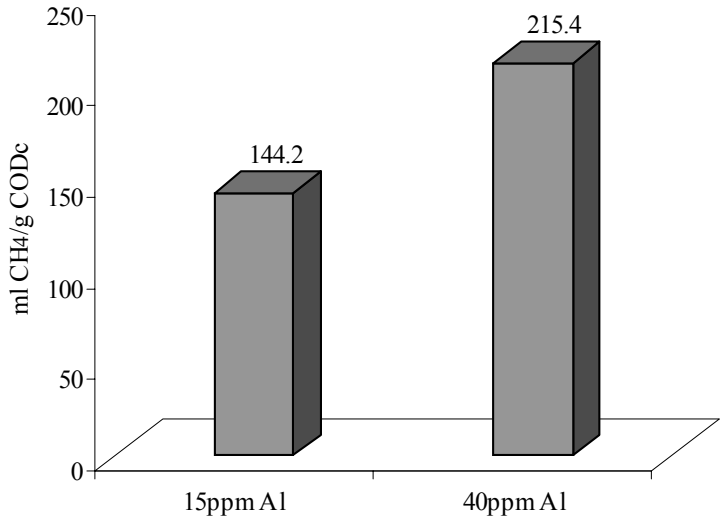

Figure 5.12. Specific methane production. MC run at 15 and 40 ppm Al^{3+}.

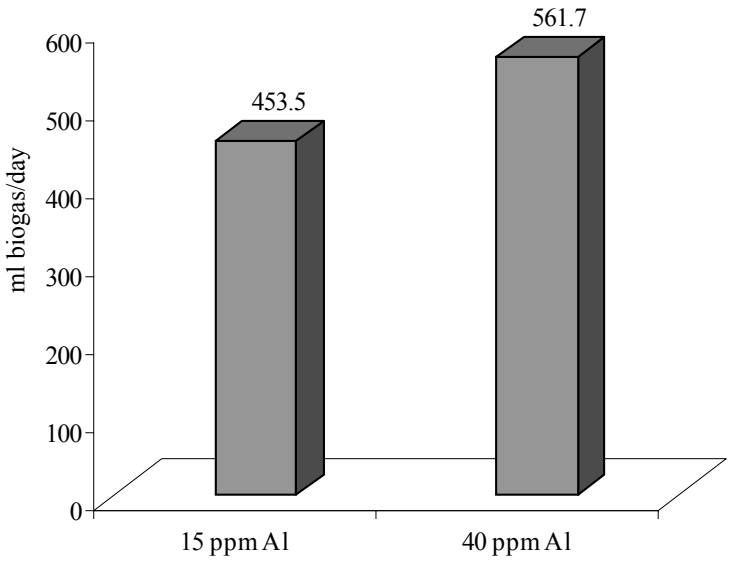

Figure 5.13. Daily biogas yield. MC run at 15 and 40 ppm Al^{3+}.

Figure 5.13 shows the quantity of biogas generated for the CSTR at the same conditions that are described in Figure 5.12. During the entire experimental run, H_2 was not detected in the biogas although the wastewater under study contained large amounts of *FOGs*. It is known that methanogenic microorganisms consume H_2 and CO_2 to produce CH_4, so it is possible that the intake rate of H_2 may be equal to the H_2 generation. In fact, the absence of H_2 in the biogas from the anaerobic degradation of *LCFA* was reported by Hanaki and his team (Hanaki et al., 1981), and their conclusions were extensively described in the background section. Therefore, it is very likely that this situation was present during this research. However, the absence of H_2 could also be associated with the low degradability of *LCFA* due to a strong bond with Al^{3+}, resulting in insufficient production of H_2. In fact, this decrease in *LCFA* biodegradability due to the cage effect of the aluminum ion was first mentioned by Gossett et al. (1978).

Although the anaerobic degradation of *LCFA* yields a considerable amount of H_2, this particular wastewater has high protein content, which is enough to produce H_2 during the acidogenic step.

Experimental Data for MC Wastewater with No Aluminum

Since the experimental data obtained during this particular run are compared to those obtained for 15 and 40 ppm of Al^{3+}, only final values will be shown. However, experimental data for the entire run are included in Appendix A. After a sludge-acclimation period that lasted 16 days in batch mode operation, the bioreactor was switched to CSTR. Twenty days after this point, this run was considered finished. As evident from Figures 5.14 to 5.16, there is a slight increase in parameters between 0 and 15 ppm Al^{3+}. However, at 40 ppm Al^{3+}, notable differences are observed. Furthermore, it is evident that the system operating at 40 ppm Al^{3+} did not show detectable levels of C_2 to C_5 monocarboxilic acids. The fact that odd carbon chain organic acids were not present in the reactor media is an indication of good performance of the system because it is well known that these organic acids will build up in the reactor when the conditions are adverse to the anaerobic degradation. Biogas generation and methane yield at 20°C and 1 atm. showed similar trends to the other variables (Figures 5.17 and 5.18). It is surprising how different the methanogenic activities were for 0 and 40 ppm Al^{3+} runs (the later one about 4 times larger). At this point, it was observed that aluminum improved the anaerobic degradation of MC slaughterhouse wastewater, but what is, or are, the mechanisms that produce these observations are a matter of study and that will be elucidated during the next chapter.

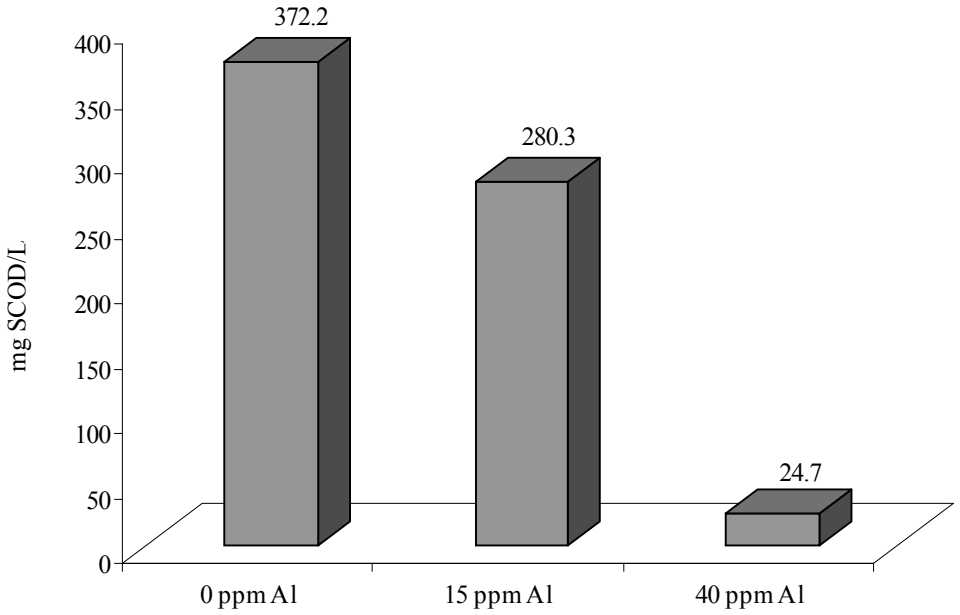

Figure 5.14. SCOD for MC CSTR run with 0, 15, and 40ppm Al^{3+}.

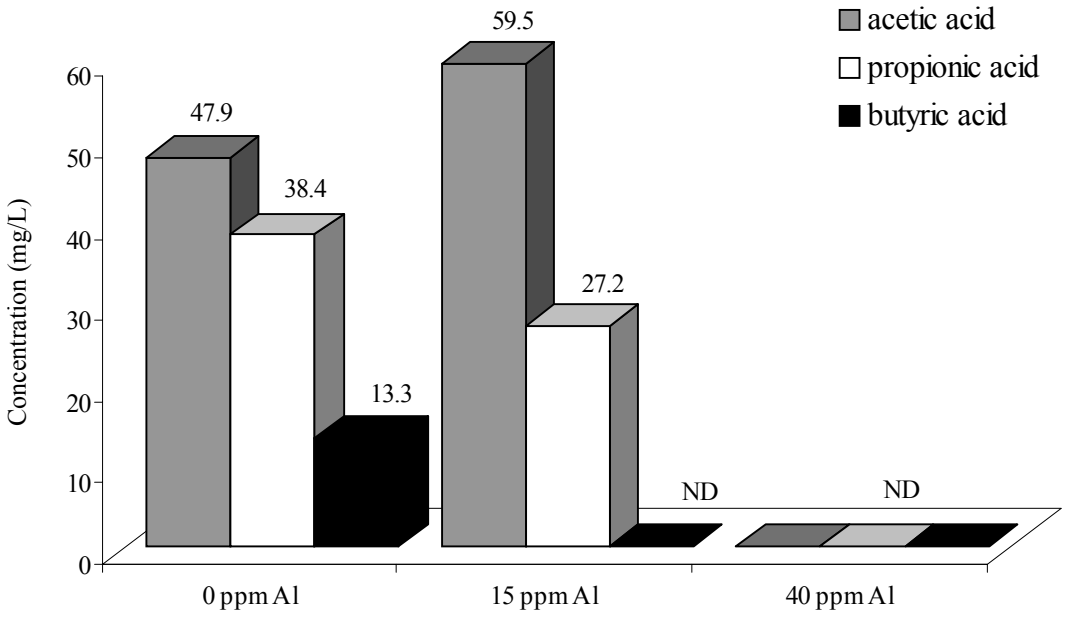

Figure 5.15. Acetic, propionic, and butyric acid concentrations for CSTR with 0, 15, and 40 ppm of Al^{3+}.

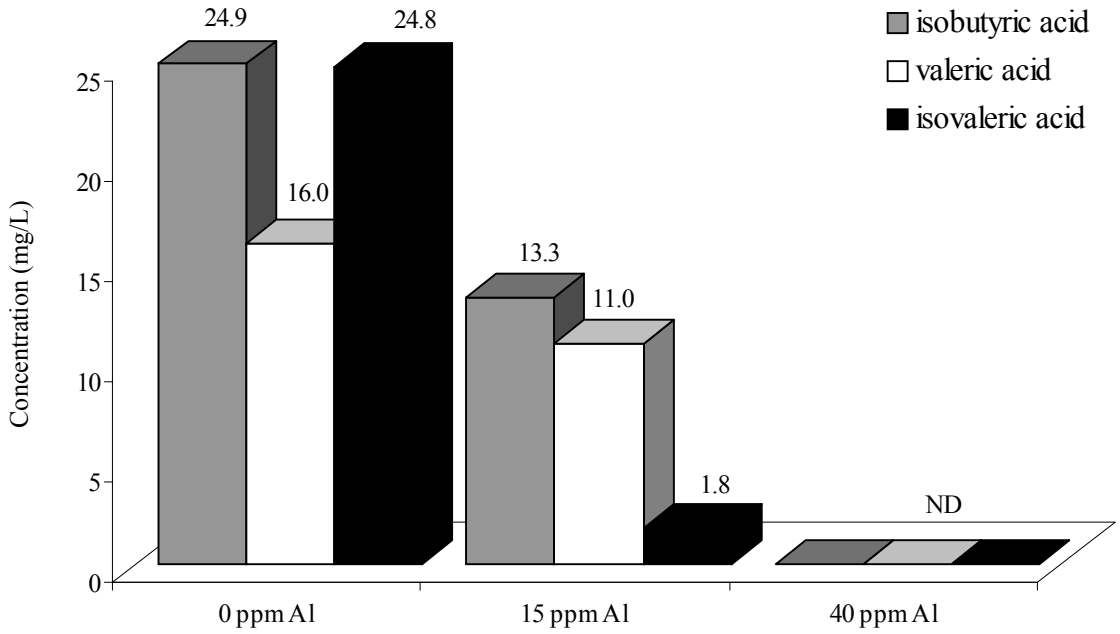

Figure 5.16. Isobutyric, valeric, and isovaleric acid concentrations for CSTR with 0, 15, and 40 ppm of Al^{3+}.

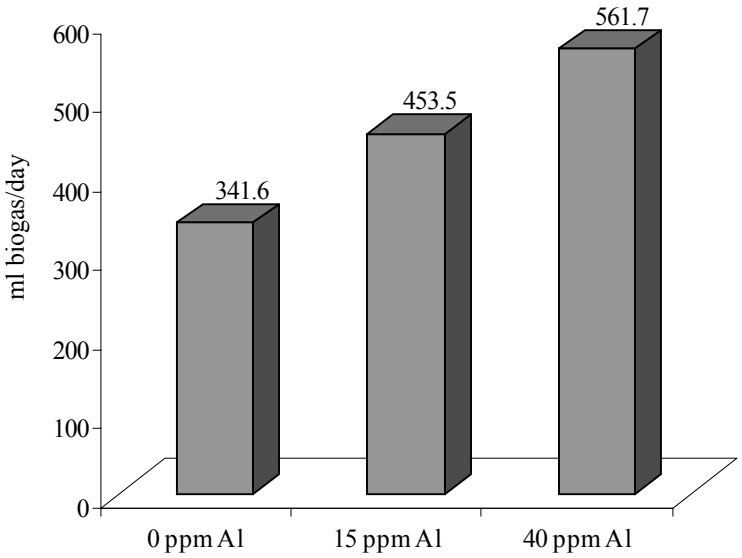

Figure 5.17. Daily biogas yield for MC CSTR run with 0, 15, and 40 ppm of Al^{3+}.

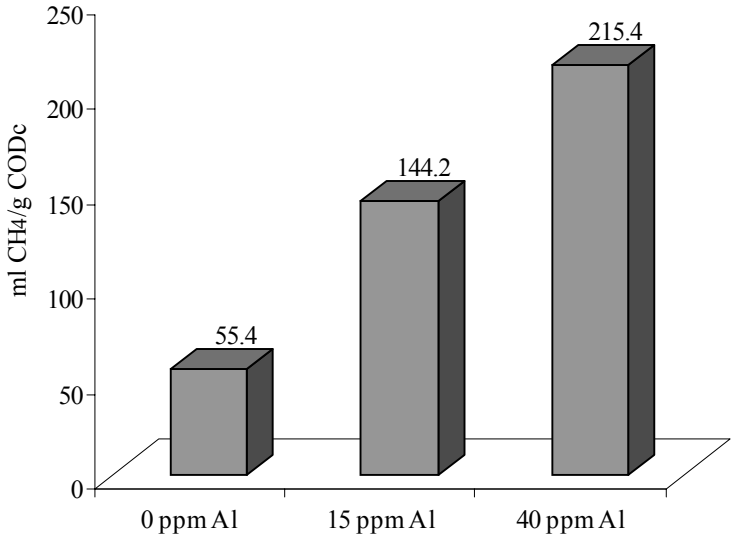

Figure 5.18. Specific methane production for MC CSTR run with 0, 15, and 40 ppm of Al^{3+}.

Experimental Data for FBF II Wastewater

After a 22 day sludge-acclimation period in a batch reactor, the system configuration was changed to CSTR. It took only 13 days for the reactor to reach no detectable levels on measured variables. This experimental observation was not expected since this wastewater performed almost the same as the one that contained 40 ppm Al^{3+}. Two remarkable differences in the wastewater composition between the previous runs and FBF II is that FBF II contained about 600 mg/L less oil & grease and extremely high concentrations of *TKN* and Ammonia–N. In order to provide clarity to this work, the final data point for the CSTR steady state operation will be reported. The entire experimental data set is provided in Appendix A.

Table 5.4. Steady State variables for CSTR operation. FBF II wastewater.

SCOD (mg/L)	ND
Acetic acid (mg/L)	ND
Propionic acid (mg/L)	ND
Isobutyric acid (mg/L)	ND
Butyric acid (mg/L)	ND
Isovaleric acid (mg/L)	ND
Valeric acid (mg/L)	ND
TSS (mg/L)	417.5
VSS (mg/L)	380
pH	7.6
ml CH_4 /g *CODc* [a]	89.1
ml biogas/day [a]	584.2

[a] measured at 20°C and 1 atm.

In Table 5.4, it can be observed that the biogas generation rate is similar to the run at 40 ppm Al^{3+}, but the specific methane yield is about 3 times less. This apparent anomaly may have been caused by the large amount of nitrogen. Atmospheric contamination was not evident since the presence of oxygen was not detected in the biogas. One possible explanation for the observation is based on a process called *anaerobic ammonium oxidation* (*ANAMMOX*) that yields N_2 gas from the ammonium acting as the electron donor compound and nitrite acting as the electron acceptor. Special conditions must exist for *ANAMMOX* to occur and some of them were met during this run, but this particular topic is far beyond the scope of this thesis, so it will not be covered. Information related to *ANAMMOX* can be found in Strous et al. (1998).

Experimental Data for FBF I Wastewater

After 35 days of operating the reactor in a batch mode for FBF I wastewater, this experimental run was terminated. This action was taken based on the fact that the biogas yield was not appreciable during the entire run. The final values for the parameters and the total accumulative biogas generation are shown in Table 5.5. Data for the entire run are in appendix A.

Table 5.5. Final values for FBF I run.

parameters	FBF I
SCOD (mg/L)	476.2
Acetic acid (mg/L)	42.7
Propionic acid (mg/L)	ND
Isobutyric acid (mg/L)	ND
Butyric acid (mg/L)	ND
Isovaleric acid (mg/L)	10.1
Valeric acid (mg/L)	ND
TSS (mg/L)	2030
VSS (mg/L)	895
pH	6.8
accum. ml biogas [a]	373

[a] 20°C and 1 atm.

As one can appreciate, some of the parameters presented ND level, and a relatively low concentration of acetic acid was also observed. Sixteen days after this run began, there was no production of biogas. However, the run was continued for another 19 days to observe any change. During that time, acetic acid showed a reduction in its

concentration, but still no signs of methane production were observed. The stoichiometric relation for acetate consumption to CH_4 formation established that, for each mole of acetate consumed, 1 mol of CH_4 is produced with a gas volume of 22.4 liters at 0˚C and 1 atm. Therefore, detectable biogas generation should be observed. The reason for this behavior is not really understood. However, FBF I wastewater contained about 500 mg/L more oil and grease than FBF II.

CHAPTER VI

DISCUSSION

Influence of Aluminum Ion on Anaerobic Degradation

The presence of aluminum ion has been reported to be detrimental to anaerobic digestion processes. Gossett et al. (1978) showed that anaerobic digestion of sludge produced from domestic wastewater by the addition of alum reduced the production of biogas and the % *COD* reduction. A few years later, Dentel and Gossett (1982) reported that alum decreased the generation of biogas during the anaerobic digestion of zein and palmitic acid sludge. Both works concluded that a cage effect of aluminum over degradable substances in the sludge was responsible for such observations. On the other hand, this research found that the presence of Al^{3+} in the reaction media was beneficial to the anaerobic degradation of poultry slaughterhouse wastewater. The fact that Gossett and Dentel's experimental research dealt with the anaerobic degradation of sludge obtained from the addition of alum to a solution of organic materials, and this research anaerobically degraded substances in the reactor media, affected or not by the presence of Al^{3+}, could be responsible for the opposing experimental observations rather than different influences of aluminum ion on anaerobic processes.

Gossett and Dentel employed in their experiments alum as a coagulant. For commercially available alum, SO_4^{2-} represents 14% of alum's molecular weight. Since

the concentration of sulfate in the sludge produced by alum was not reported either by Gossett et al. (1978) or by Dentel and Gossett (1982), the hypothesis that SO_4^{2-} was present in the sludge at sufficient concentrations to reduce the methane yield cannot be over looked. However, Dentel reported in the same work that no appreciable reduction was observed for methane production from glucose and butyric acid sludge. He attributed this observation to the low interaction of Al^{3+} with those two substances. Dentel also reported that $FeCl_3$ showed a similar tendency to that of alum, demonstrating that the cage effect was also produced with Fe^{3+}. Therefore, any interference of methane yield due to SO_4^{2-} seems to be negligible from the observations mentioned before.

Rudolfs et al. (1932) also studied the influence of chemical coagulation on anaerobic sludge digestion in which alum and sodium aluminate ($Na_2Al_2O_4$) were some of the coagulants employed. Rudolfs and his team reported that anaerobic degradation of chemically produced sludge was significantly better for sodium aluminate than for alum. Furthermore, the $Na_2Al_2O_4$ run yielded more biogas than the zero coagulant control sample. In other words, they showed that the anaerobic digestion of sludge was improved by the presence of Al^{3+}, but affected by the presence of an aluminum counter ion such as SO_4^{2-}.

With the information presented previously, one cannot generalize that Al^{3+} increases or decreases the performance of anaerobic processes. Perhaps its influence is associated with the process where the aluminum ion is being used rather than its effects over anaerobic degradation. However, during this research, an improvement was clearly

observed, so the mechanisms that may contribute to those experimental observations will be described.

Aluminum Ion Acting as Microbial Nutrient

It is possible to consider that the improvement of anaerobic degradation observed in this research was associated with Al^{3+} acting as a nutrient. For example, Williams et al. (1986) reported that poultry waste lacks the necessary amount of nickel for methanogenic processes. They observed that the addition of nickel to a final concentration of 10 μM in the poultry waste could increase the production of biogas up to 10%. Therefore, the same situation for Al^{3+} could have occurred during this research.

The general elemental composition of methanogenic microorganisms has already been determined and can be found, for example, in Speece (1996). From the list of these elements, the aluminum ion appears not to be present among them. This means that aluminum is not an element that plays a role in biological processes, or aluminum is present in methanogens at non-detectable levels, so it is not needed in a large amount to satisfy methanogen requirements. For either one or both situations, the hypothesis that aluminum was a nutrient for the poultry slaughterhouse wastewater is discarded as the main reason for the observed improvement. Moreover, improvements by the addition of Al^{3+} were observed at the ppm level, so a relatively large quantity of Al^{3+} in the reaction media was required in comparison with the amount of other metals that are present in the reactor media and listed in the general elemental composition of methanogenic microorganisms.

Interaction between Al^{3+} and Species in the Reactor Media

Organic compounds in the reaction media could be present as colloids, which can be either hydrophilic or hydrophobic, or present as dissolved species. In both cases, aluminum ion interacts with them by coagulation, adsorption, and/or precipitation. The precipitation occurs when the concentrations of two or more given ions dissolved in solution are larger than the maximum possible concentration that can be held in solution, so the extra amount of dissolved ions are removed by the formation of a solid phase, a salt. The precipitation is studied as the equilibrium between the dissolved and the solid phase, so the Gibbs Free Energy concept can be employed. Basically for two compounds in solution that form a precipitate, the following relation is applied.

$$C_{(S)} \rightleftharpoons a\,A^{+} + b\,B^{-}$$

$$\Delta G_r^0 = -R\,T\,ln\,K_{eq} \tag{6.1}$$

$$K_{eq} = \left[A^{+}\right]^a \left[B^{-}\right]^b \tag{6.2}$$

where K_{eq} is the known solubility constant, and ΔG_r^0 is the change of standard Gibbs free energy during the reaction.

Colloids dispersed in water consist of discrete particles held in suspension by their extremely small size (1 to 200 millimicrons), state of hydration, and surface electrical charges (Clark et al., 1971). Due to their small sizes, colloids pose a high surface area to mass ratio, so electrostatic repulsion and hydration become important. Coagulation of colloids is possible when those surface phenomena are disrupted. In this case, Van der Waals attractive forces and Brownian movement make these colloids aggregate, so they

become heavier and settle. However, coagulation of organic substances in suspension may be governed by processes that are different from counteracting surface forces. For example, Dentel (1984) showed that Al^{3+} can interact with certain active sites of organic colloids in order to promote their coagulation.

Adsorption is another way that aluminum flocks can interact with species in the reactor media. Adsorption refers to the formation of complexes on the surface of precipitates by ion exchange (Galarneau, 1995). Aluminum flock has the capacity to exchange weak surface ions such as (OH^-) for other negative ions that produce a strong bond with the surface. Hsu (1973) experimentally observed that the reduction of *COD* from a wastewater by aluminum hydroxide addition could not be represented by the Freundlich isotherm, which is a widely known mathematical model for adsorption. Therefore, he concluded that the reduction of *COD* was associated with coagulation rather than adsorption processes, so adsorption of substances over aluminum flock is not considered an important process for this research.

It was observed during this research that Al^{3+} substantially improved the anaerobic degradation of poultry slaughterhouse wastewater. The methane yield for MC runs with 0, 15, and 40 ppm of Al^{3+} was shown to be statistically different at the 95% level of confidence. Figure 5.18 shows the direct relationship between an increase in Al^{3+} concentration and an increase on the efficiency of conversion of *COD* into CH_4. It has already been discussed that Al^{3+} is not an important nutrient for these types of microorganism, so aluminum ion could be acting as a blocker ion of some substances to avoid a toxic action of them over methanogens by removing these inhibitory compounds

from the reactor media by coagulation and/or precipitation. In Chapter II, it was explained that *LCFAs* negatively affect methanogenic microorganisms, so it is possible that the aluminum ion blocked *LCFA* toxicity. For example, Roy et al. (1985) observed that the addition of calcium to an anaerobic reactor media reduced the toxicity of *LFCA* over methanogens. Moreover, Roy and his team experimentally obtained a mathematical expression that relates the amount of calcium needed to avoid methanogenic inhibition as a function of *LCFA* concentration based on the assumption that calcium precipitates *LCFA*. Therefore, it is not surprising that aluminum showed similar trends as calcium since it is generally known that the solubility of aluminum salts is smaller than that of the calcium salts.

It was pointed out previously that the FBF II run did perform in a similar manner to MC at 40 ppm of Al^{3+}. However for the FBF I run, the degradation process failed. It is observed in Table 5.1 that FBF I wastewater contained approximately 500 mg/L more of fat and grease than FBF II. It turns out that the difference in *FOG* between FBF I and FBF II contributed to such dissimilar behavior and this is supported by the fact that *LCFAs* have a negative influence on methanogenic microorganisms. Actually this is not a surprise since the failures of anaerobic units are well known when the conditions were adverse for methanogenic microorganisms.

The total aluminum concentration that can be theoretically dissolved in the presence of aluminum ion in water, and the concentration of soluble aluminum species measured in this research are shown in Figure 6.1. Details for the calculation of the aluminum theoretical line are covered in Appendix C. Experimental data are given in

Appendix A. In this research, the total aluminum concentration analyses were performed at the end of MC run at 40 ppm of Al^{3+} during eight consecutives days by lowering the pH of the reactor with concentrated hydrochloric acid in order to avoid any dilution. The axis, $\log(Al_T)$, stands for the logarithm (base 10) of the total aluminum dissolved concentration, $[Al_T]$, expressed in mg/L. It is observed in Figure 6.1 that experimental data lie under the solid line, which means that the aluminum ion interacted with species in the reactor media to form insoluble precipitates with smaller solubility constants than $Al(OH)_3(s)$. Even at a pH of 4.6, the aluminum dissolved in the reactor media is less than the theoretical amount indicating that Al^{3+} possesses strong bonds with those species that were removed from the reaction media. This clearly means that aluminum removed materials from the liquid media, and the fact that increasing the amount of Al^{3+} improved anaerobic degradation of poultry wastewater indicates that these removed materials are likely to be toxic to anaerobic microorganisms. The experimental data for pH 7.1 and 6.7 were not included in Figure 6.1 since they yield ND levels of aluminum.

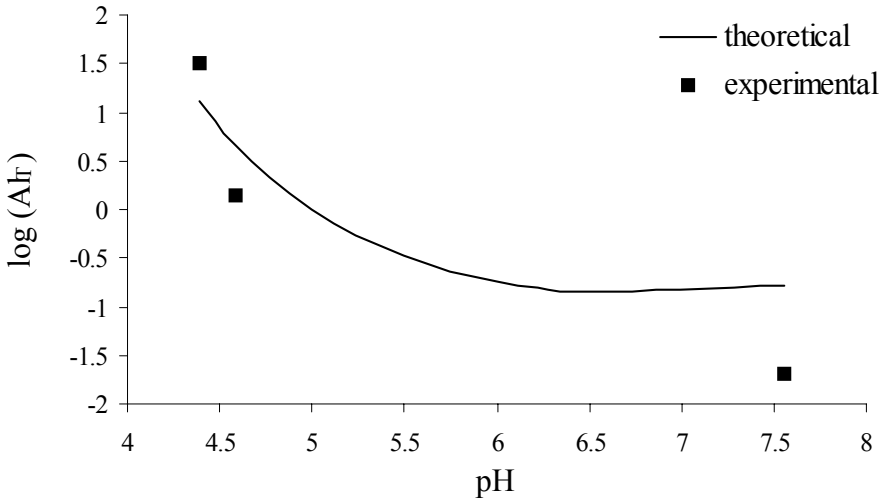

Figure 6.1. Total aluminum soluble in water as function of pH.

Degradation Rate Study

One of the objectives of this research was the estimation of Monod kinetic parameters for the degradation of poultry slaughterhouse wastewater to show any improvements of the degradation process due to the addition of Al^{3+} to the system. Since the system studied did not deal with a pure cell culture and substrate, estimation of Monod kinetic parameters presents a certain degree of difficulty. Furthermore, this difficulty is increased by the fact that poultry slaughterhouse wastewater contains large amounts of inert solid material. Estimation of Monod parameters by the proposed methodology in Chapter IV failed during the estimation of parameters *C* and *D* in equation 3.5. The use of equation 3.5 to estimate *C* and *D* from experimental data did not perform well when *SCOD* was employed as *S*. Actually, it yielded negative *C* and *D* values, which are meaningless. Moreover, the same outcome was obtained when acetic acid concentration was employed as *S*. Rittmann and McCarty (2001) discussed the fact that the estimation of biomass is not possible for a system with a large amount of inert solids. In fact, for a system with large amounts of inert material, the generation of biomass represents a small portion of *TSS* or *VSS*, so the error in estimating these two parameters could hide the growth of biomass. Therefore, it is possible that this situation was present during this research. Another drawback of this type of wastewater is that more than one substrate is available for microorganisms to degrade, so there is no way to define a priori the value of *S*. The following assumptions were considered appropriate for this system in order to avoid the limitations mentioned before during Monod parameter estimation.

- The degradation of acetic acid by methanogens will be studied since the *LCFAs* seem to be responsible for affecting the degradation rate of the system.
- *C* and *D* will be considered equal to kinetic parameters available in the literature for aceticlastic methanogens.
- *C* and *D* values will be not affected by the addition of Al^{3+} in the reactor media.

The chosen *C* and *D* values were taken from Pavlostathis and Giraldo-Gomez (1991) for aceticlastic methanogens in a mixed culture operating at 30 ºC, which are the conditions at which this experimental research was performed. These parameters are presented in the Table 6.1.

Table 6.1. Monod parameters for aceticlastic methanogenesis.

y (mgVSS/mg acetic ac.)	0.057
K (mg acetic/L)	334.6
μ_{max} (day^{-1})	0.275
b (day^{-1})	0.037
f_d	0.8 [a]

[a] Assumed f_d

The assumptions that *C* and *D* are known and not influenced by the addition of Al^{3+} only fixes the relation among the Monod kinetic parameters rather than their numerical values, so final estimated parameters from MC batch runs with 0 and 15 ppm of Al^{3+} should reveal any influence of Al^{3+} on the reaction media. The final estimated parameters for these 2 cases are shown in Table 6.2. As one can see, *y* and *K* are very similar in both

experimental runs. However, a large difference is observed for μ_{max}. Actually, this observation is not surprising since *LCFAs* reduce the utilization of acetate by methanogens. Specifically, this type of inhibition is called noncompetitive. References for noncompetitive inhibition can be found in Rittmann and McCarty (2001). The main idea is that the inhibitor substance, a *LCFA*, slows down the degradation rate of acetate by methanogens, so increasing the concentration of *LCFA* reduces the μ_{max}/y ratio for acetate degradation. This type of inhibition is affected only by the concentration of inhibitory substance and its effects are not reduced by increasing the concentration of substrate (Rittmann and McCarty, 2001).

Table 6.2. Estimated Monod parameters for anaerobic degradation of poultry slaughterhouse wastewater.

parameters	0 ppm Al^{3+} run	15 ppm Al^{3+} run
y (mgVSS/mg acetic ac.)	0.052	0.052
K (mg acetic/L)	1994.8	1867.3
μ_{max} (day^{-1})	0.208	2.52
b (day^{-1})	0.005	0.067

Even though the parameters in Table 6.2 minimized the error between experimental and simulated data, they cannot be taken as true parameters for the studied systems since C and D values were not obtained from biomass growth data. They are only an approximation, which can be used for an eventual conclusion.

It is observed from the experimental data that all runs on CSTR reactor operation mode accommodated, in a relatively short period of time, the switch from Batch reactor

operation mode. These can be assumed as an improvement of the general conditions for the anaerobic degradation of poultry wastewater. These experimental observations are in part supported by McCarty's proposal for treating wastewaters with toxic substances for anaerobic microorganisms (McCarty, 1964). McCarty proposed that, for these types of wastewaters, the CSTR configuration should perform better than the batch one since the CSTR has the capacity to dilute the toxic substance in the reactor media. However, Azbar et al. (2001) concluded that the CSTR configuration is the worst for series of experimental runs at the bench scale. Although this contradiction is from two very respectable works, this research observed that the CSTR configuration is the right option for the anaerobic treatment of poultry slaughterhouse wastewater since noncompetitive inhibition over aceticlastic methanogens by *LCFA* is reduced by the dilution effect that the CSTR possess.

CHAPTER VII

CONCLUSION

It was observed in this research that the addition of aluminum ion did improve the anaerobic degradation of poultry slaughterhouse wastewater. Methane yield, % *COD* reduction, and *VAs* concentrations showed a direct relation to Al^{3+} concentrations in the reactor media. The MC run with 40 ppm of Al^{3+} yielded the largest methane yield, which was 42 % smaller than the theoretical value of 375 ml CH_4/g. *CODc* at 20°C and 1atm. The absence of H_2 in the produced biogas is a clear indication that *LCFAs* did not inhibit H_2-consuming methanogens. Therefore, it is concluded that *LCFAs* affected the aceticlastic methanogenic microorganisms. However, their influence was reduced by the presence of Al^{3+} in the reactor media. Under zero detectable level of H_2 present during this research, *LCFAs* should not have any thermodynamic limitations for their degradation. Furthermore, there was not observed accumulation of *VSS* when the reactor switched from 15 to 40 ppm of Al^{3+} in the influent, so *LCFAs* removed by Al^{3+} were still degraded by acidogenic microorganisms. The influence of *LCFAs* on aceticlastic methanogenic microorganisms was also corroborated with the proposed approach for estimating Monod kinetic parameters. Due to the inhibitory effect of *LCFAs*, FBF and MC companies should treat anaerobically their wastewaters under a CSTR configuration. Although this research studied the influence of Al^{3+} in poultry slaughterhouse

wastewater, the concepts displayed throughout this thesis can be employed to any food process industry that deals with fat and grease in its wastewater.

In this study, a novel methodology for a complete estimation of Monod kinetic parameters and X_a^0 from batch reactor data was also developed and presented. This proposed methodology almost completely eliminates non-experimental bias over estimated Monod parameters due to microbial endogenous decay. Also, it provided estimates that were not influenced by a change in the X_a^0/X_{OB}^0 ratio in the simulated experimental data. Although the performance of the proposed methodology was demonstrated, it partially fails in this research, because the estimation of C and D were affected by the large amounts of inert material in the poultry wastewater. However, this proposed methodology provides Monod parameters that must satisfy certain experimental and mathematical restrictions, so it provides sense to the estimated parameters.

LITERATURE CITED

1. American Public Health Association (1985) "Standard Methods for the Examination of Water and Wastewater, 16th ed." *APHA Washington, DC*.

2. Azbar, N., Ursillo, P., and Speece, R.E. (2001) "Effect of Process Configuration and Substrate Complexity on the Performance of Anaerobic Processes". *Water Research*, 35, 817-829.

3. Batstone, D., Keller, J., Newell, B., and Newland, M. (1997) "Model Development and Full Scale Validation for Anaerobic Treatment of Protein and Fat Based Wastewater" *Water Science and Technology*, 36, 423-431.

4. Bull, M.A., Sterritt, R.M., and Lester, J.N. (1984) "An Evaluation of Single and Separated Phase Anaerobic Industrial Wastewater Treatment in fluidized Bed Reactor" *Biotechnology and Bioengineering,* 26, 1054-1065.

5. Burden, R.L. and Faires, J.D. (1989) "Numerical Analysis" *Boston: PWS-Kent*.

6. Choi, E. and Rim J.M. (1991) "Competition and Inhibition of Sulfate Reducers and Methane Producers in Anaerobic Treatment" *Water Science and Technology*, 23, 1259-1264.

7. Christensen, D. R. and McCarty P.L. (1975) "Muli-process Biological Treatment Model", *Journal Water Pollution Control Federation*, 47, 2652-2664.

8. Clark, J.W., Viessman W. Jr, and Hammer M.J. (1971) "Water Supply and Pollution Control" *International Textbook Company.* Scranton. United States of America.

9. Dentel, S.K., and Gossett J.M. (1982) "Effect of Chemical Coagulation on Anaerobic Digestion of Organic Materials" *Water Research*, 16, 707-718.

10. Dentel, S.K. (1984) "Coagulation of Organic Suspensions with Aluminum Salts" *Ph.D. Dissertation. Cornell University*.

11. Freund, R.J. and Wilson, J.W. (1997) "Statistical Methods" *London: Academic Press*.

12. Galarneau, E. (1995) "Mechanism of Phosphorus Removal from Wastewater by Aluminum" *M. T., McGill University*.

13. Ghosh, S., Conrad, J.R., and Klass, D.L. (1975) "Anaerobic Acidogenesis of Wastewater Sludge" *Journal Water Pollution Control Federation*, 47, 30-45.

14. Goovaerts, P., Semrau, J., and Lontoh, S. (2001) "Monte Carlo Analysis of Uncertainty Attached to Microbial Pollutant Degradation Rates" *Environmental Science and Technology*, 35, 3924-3930.

15. Gossett, J.M., McCarty, P.L., Wilson, J.C., and Evans, D.S. (1978) "Anaerobic Digestion of Sludge from Chemical Treatment" *Journal Water Pollution Control Federation*, 50, 533-542.

16. Grady, C.P., Smets, B.F., and Barbeau, D.S. (1996) "Variability in Kinetic Parameters Estimates: A Review of Possible Causes and a Proposed Terminology". *Water Research*, 30, 742-748.

17. Hanaki, K., Matsuo, T., and Nagase, M. (1981) "Mechanism of Inhibition Caused by Long-Chain Fatty Acids in Anaerobic Digestion Process" *Biotechnology and Bioengineering*, 23, 1591-1610.

18. Hsu, D.Y. (1973) "The Effects of Aluminum Hydroxide on the Conventional Wastewater Treatment Processes" *Ph.D. Dissertation, Northwestern University*.

19. Jeris, J.S. and McCarty P.L. (1965) "The Biochemistry of Methane Fermentation Using C^{14} Tacers" *Journal Water Pollution Control Federation*, 37, 178-192.

20. Kabara, J.J., Vrable, R., and Lie Ken Jie, M.S.F. (1977) "Antimicrobial Lipids: Natural and Synthetic Fatty Acids and Monoglycerides" *Lipids*, 12, 753-759.

21. Kesavan, P. and Law, V.J. (1998) "Parameter Estimation of Monod Kinetics without Biomass Data and Initial Substrate Concentration" *Chemical Engineering Communication*, 167, 107-132.

22. Koster, I.W. and Cramer A. (1987) "Inhibition of Methanogenesis from Acetate in Granular Sludge by Long-Chain Fatty Acids" *Applied and Environmental Microbiology*, 53, 403-409.

23. Kotrly, S. and Sucha, L. (1985) "Handbook of Chemical Equilibria in Analytical Chemistry" *Ellis Horwood Limited. West Sussex. England*.

24. Lalman, J.A. and Bagley, D.M. (2000) "Anaerobic Degradation and Inhibitory Effects of Linoleic Acid" *Water Research*, 34 (17), 4220-4228.

25. Lalman, J.A. and Bagley, D.M. (2001) "Anaerobic Degradation and Methanogenic Inhibitory Effects of Oleic and Stearic Acids" *Water Research*, 35(12), 2975-2983.

26. Lalman, J.A. and Bagley, D.M. (2002) "Effects of C18 Long Chain Fatty Acids on Glucose, Butyrate, and Hydrogen Degradation" *Water Research*, 36, 3307-3313.

27. Lawrence, A.W. and McCarty, P.L. (1970) "Unified Basis for Biological Treatment Design Operation" *Journal of the Sanitary Engineering Division*, 96, 757-778.

28. Marquardt, D.W. (1963) "An Algorithm for Least-Square Estimation of Nonlinear Parameters" *Journal of the Society for Industrial and Applied Mathematics*, 11, 431-441.

29. McCartney, D.M. and Oleszkiewicz, J.A. (1993) "Competition Between Methanogens and Sulfate Reducers: Effect of COD:Sulfate Ratio and Acclimation" *Water Environmental Research*, 65, 655-664.

30. McCarty, P.L. (1964) "Anaerobic Waste Treatment Fundamentals" *Public Works*, 95, 91-94.

31. Mississippi Department of Agriculture and Commerce. "U.S. Per Capital Consumption of Pork and Chicken, 1970-1999". www.nass.usda.gov/ms.

32. Monod, J. (1949) "The Growth of Bacterial Culture" *Annual Review of Microbiology*, 3, 371-394.

33. Nieman, C. (1954) "Influence of Trace Amounts of Fatty Acids on the Growth of Microorganism" *Bacteriological Reviews*, 18, 147-163.

34. Nihtilä, M. and Virkkunen, J. (1977) "Practical Identifiability of Growth and Substrate Consumption Models", *Biotechnology and Bioengineering*, 19, 1831-1850.

35. Okaygun, M.S. (1991) "Kinetic of Phenol Degradation". *Ph.D. Dissertation, Texas A&M University*.

36. Ong, S.L. (1983) "Least-square Estimation of Batch Culture Kinetic Parameters" *Biotechnology and Bioengineering*, 25, 2347-2358.

37. Orzechowski, G. (1994). "Modified Monod and Linear Substrate Utilization Rate Equations for Activated Sludge Biodegradation Processes". *M.S. Thesis*. *University of Ottawa*.

38. Pavlostathis, S.G. and Giraldo-Gomez, E. (1991) "Kinetics of Anaerobic Treatment: A Critical Review" *Critical Reviews in Environmental Control*, 21, 411-490.

39. Pholand, F.G. and Ghosh, S. (1971) "Developments in Anaerobic Stabilization of Organic Wastes- the Two-Phase Concept" *Environmental Letters*, 1, 255-266.

40. Ren, N., Wang, B., and Huang, J. (1997) "Ethanol-Type Fermentation from Carbohydrate in High Rate Acidogenic Reactor" *Biotechnology and Bioengineering*, 54 (5), 428-433.

41. Rittmann, B.E. and McCarty, PL. (2000) "Environmental Biotechnology: Principles and Applications" *New York: McGraw-Hill*.

42. Robinson, J.A. and Tiedje, J.M. (1983) "Nonlinear Estimation of Monod Growth Kinetic Parameters from a Single Substrate Depletion Curve" *Applied and Environmental Microbiology*, 45, 1453-1458.

43. Roy, F., Albagnac, G., and Samain, E. (1985) "Influence of Calcium Addition on Growth of Highly Purified Syntrophic Cultures Degrading Long-chain Fatty Acids" *Applied and Environmental Microbiology*, 49, 702-705.

44. Rudolfs, W., Baumgartmer, W.H., and Setter, L.R. (1932) "Effect of Coagulant on Sludge Digestion" *Sewage Works Journal*, 4, 628-637.

45. Salminen, E., Rintala, J., Lokshina, L.Y., and Vavilin, V.A. (2000) "Anaerobic Batch Degradation of Solid Poultry Slaughterhouse Waste" *Water Science and Technology*, 41, 33-41.

46. Smith, P.S. and McCarty, P.L. (1986) "Anaerobic Wastewater Treatment" *Environmental Science and Technology*, 20, 1200-1206.

47. Smith, P.S. and McCarty, P.L. (1989) "Energetic and Rate Effects on Methanogenesis of Ethanol and Propionate in Perturbed CSTRs" *Biotechnology and Bioengineering*, 34, 39-54.

48. Smith, L.H. and McCarty, P.L. (1998) "Spread Sheet Method for Evaluation of Biochemical Reaction Rate Coefficients and their Uncertainties by Weighted Nonlinear Least-square Analyses of the Integrated Monod Equation" *Applied and Environmental Microbiology*, 64, 2044-2050.

49. Speece, R.E. (1996) "Anaerobic Biotechnology" *Nashville, Tennessee: Archae Press*.

50. Strous, M., Heijnen, J.J., Kuenen, J.G., and Jetten, M.S.M. (1998) "The Sequencing Batch Reactor as a Powerful Tool for the Study of Slowly Growing Ammonium-oxidizing Microorganisms" *Applied Environmental Microbiology*, 50, 589-596.

51. Thauer, R.K., Jungermann, K., and Decker, K. (1977) "Energy Conservation in Chemotrophic Anaerobic Bacteria" *Bacteriological Reviews*, 41, 100-180.

52. The Clarion Ledger (2002) "Community spotlight: Scott County" *www.clarionledger.com/misshomes/community/scott*.

53. The committee on Data for Science and Technology. CODATA Key Values for Thermodynamics. www.codata.org/codata/databases/key1.html.

54. U.S. EPA (1998) "Microwave Assisted Acid Digestion of Sediments, Sludges, Soils, and Oils" *EPA 3051-A*.

55. Van Uden, N. (1967) "Transport-limited Growth in the Chemostat and Its Competitive Inhibition; A Theoretical Treatment" *Archiv f*ur *Mikrobiologie*, 58, 145-154.

56. Viswanathan, C.V., Meera, B.B., and Pillai, S.C.. (1962) "Fatty Matter in Aerobic and Anaerobic Sewage Sludge" *Journal Water Pollution Control Federation*, 34, 189-194.

57. Wang, Q., Kuninobu, M., Ogawa, H.I., and Kato, Y. (1999) "Degradation of Volatile Fatty Acids in Highly Efficient Anaerobic Digestion" *Biomass and Bioenergy*, 16, 407-416.

58. Weng, C.N. and Jeris, J.S. (1976) " Biochemical Mechanism in the Methane Fermentation of Glutamic and Oleic Acids" *Water Research*, 10, 9-18.

59. Williams, C.M., Shih, J.C.H., and Spears, J.W. (1986) "Effect of Nickel on Biological Methane Generation from a Laboratory Poultry Waste Digester" *Biotechnology and Bioengineering*, 28, 1608-1610.

60. Yu, H.Q., Fang, H.H.P, and Tay, J.H. (2001) "Enhanced Sludge Granulation in Upflow Anaerobic Sludge Blanket (UASB) Reactors by Aluminum Chloride" *Chemosphere*, 44, 31-36.

61. Zeikus, J.G. (1977) "The Biology of Methanogenic Bacteria" *Bacteriological Review*s, 41, 514-541.

62. Zoetemeyer, R.J., Van Den Heuvel, J.C., and Cohen, A. (1982) "pH Influence on Acidogenesis Dissimilation of Glucose in an Anaerobic Digestor" *Water Research*, 16, 303-311.

NOMENCLATURE

atm	Unit of pressure (atmosphere)
ATP	Adenosine 5-triphosphate
b	Endogenous decay coefficient ($time^{-1}$)
BOD	Biochemical oxygen demand
CBOD	Carbonaceous *BOD*
COD	Chemical oxygen demand
CODc	Chemical oxygen demand consumed
f_d	Bacterial degradable fraction
FADH	Flavine adenine dinucleotide
FOG	Fat, oil, and grease
K	Half saturation constant (mg substrate/liter)
LCFA	Long chain fatty acid
NADH	Nicotinamide adenine dinucleotide
S	Substrate concentration (mg/liter)
SCOD	Soluble chemical oxygen demand
t	Time
TOC	Total organic carbon

TSS	Total suspended solid concentration (mg of total solids/liter)
μ_{max}	Maximum specific growth rate ($time^{-1}$)
VA	Volatile monocarboxilic acid
VSS	Volatile suspended solid concentration (mg of volatile solid/liter)
X_a	Active matter concentration (mg active biomass/liter)
X_i	Inert matter concentration (mg inert biomass/liter)
X_{OB}	Observed matter concentration (mg observed biomass/liter)
y	yield (mg active biomass generated/mg substrate)

superscript

^{0}	initial concentration

APPENDIX A

RAW EXPERIMENTAL DATA

Table A.1. Experimental data for batch reactor run with no aluminum. FBF II wastewater [a].

Time	TSS	VSS	SCOD	acetic ac	propionic ac	isobutyric ac	butyric ac	isovaleric ac	valeric ac
0	707.3 [b]	704.6 [b]	1341.5	70.3 (2.6)	9.8 (0.9)	ND	3.8 (0.4)	1.1 (1.1)	ND
5	830.0 [b]	730.0 [b]	939.8	226.6 (13.8)	88.8 (3.3)	16.7 (1.0)	25.3 (1.1)	26.9 (0.8)	ND
10	950.0 (0)	720.0 (0)	934.9 (140.8)	1100.4 (56.9)	ND	57.0 (2.2)	63.5 (2.6)	77.9 (5.3)	ND
15	805.0 (7.1)	705.0 (35.4)	493.8 (0)	169.6 (9.3)	ND	66.9 (3.2)	75.0 (3.4)	92.4 (5.4)	ND
20	635.0 (7.1)	590.0 (42.4)	736.2 (0)	321.5 (6.1)	ND	53.7 (3.8)	51.5 (2.1)	67.0 (13.6)	ND
22	365.0 (35.4)	345.0 (35.4)	745.3 (124.2)	266.1 (10.7)	ND	21.0 (0.5)	ND	27.9 (2.6)	ND

[a] values are expressed as the mean and its standard deviation in parenthesis. Time in days, other parameters in mg/L.
[b] one experimental data point.
ND = not detectable.

Table A.2. Biogas generation for batch reactor run with no aluminum. FBF II wastewater.

time [a]	biogas [b]	time	biogas	time	biogas
0:00:00	0	270:42:00	2210	502:00:00	5350
75:54:00	115	273:04:00	2450	504:50:00	5400
81:26:00	195	292:31:00	2550	508:00:00	5450
119:41:00	250	310:34:00	2400	512:40:00	5500
126:00:00	300	315:02:00	2450	526:55:00	5875
146:05:00	425	321:00:00	2560	530:29:00	5900
151:05:00	500	333:20:00	2950	534:20:00	6000
151:05:00	600	338:00:00	3325	537:22:00	6325
165:30:00	1000	357:30:00	3500	549:38:00	6390
165:50:00	1050	365:52:00	3600	554:22:00	6450
187:36:00	1250	381:00:00	3760	554:50:00	6810
191:58:00	1345	386:45:00	3865	574:03:00	6900
194:52:00	1500	405:45:00	3925	576:46:00	7000
194:53:00	1600	411:30:00	4280	580:24:00	7135
217:48:00	1700	430:30:00	4305	599:36:00	7360
241:50:00	1790	461:10:00	4850	624:04:00	7500
261:19:00	2000	479:51:00	4900		
264:28:00	2050	486:50:00	5000		

[a] accumulative time in hours: minutes
[b] accumulative biogas in ml @ 20°C and 1atm.

Table A.3. Experimental data for CSTR run with no aluminum.
FBF II wastewater [a].

Time	TSS	VSS	SCOD	acetic ac	propionic ac	isobutyric ac	butyric ac	isovaleric ac	valeric ac
0	330 (84.6)	225.0 (35.4)	387.2 (145.8)	125.2 (3.7)	ND	18.9 (0.8)	2.0 (3.5)	22.1 (1.3)	ND
2	440 (127.3)	225.0 (35.4)	437.7 (145.8)	ND	ND	ND	ND	18.1 (2.2)	ND
5	415 (21.2)	395.0 (49.5)	ND	ND	ND	ND	ND	ND	ND
7	420 (0)	365.0 (21.2)	ND	ND	ND	ND	ND	ND	ND

[a] values are expressed as the mean and its standard deviation in parenthesis. Time in days, other parameters in mg/L.
ND = not detectable.

Table A.4. Biogas generation for CSTR run with no aluminum. FBF II wastewater.

time[a]	biogas [a]	time	biogas	time	biogas
0: 00:00	0	100:30:00	3835	166:59:00	8150
1:06:00	305	102:40:00	3950	168:43:00	8330
24:20:00	500	106:17:00	4000	171:12:00	8400
24:50:00	800	107:14:00	4335	173:47:00	8500
31:20:00	950	118:07:00	4500	176:52:00	8635
45:11:00	1320	120:15:00	4830	178:28:00	9000
52:16:00	1390	121:16:00	5000	178:44:00	9350
58:51:00	1500	123:16:00	5300	190:55:00	9625
68:46:00	1860	130:35:00	5500	191:59:00	9850
72:46:00	2000	130:58:00	5825	194:38:00	9950
75:16:00	2340	142:34:00	6000	199:11:00	9975
80:41:00	2500	142:38:00	6130	201:50:00	10000
94:41:00	3000	144:27:00	6330	202:47:00	10150
95:53:00	3295	146:33:00	6500	213:33:00	10375
98:47:00	3350	147:21:00	6780		
99:35:00	3450	151:18:00	7000		
99:46:00	3500	152:37:00	7310		

[a] accumulative time in hours:minutes
[b] accumulative biogas in ml @ 20°C and 1atm.

Table A.5. Experimental data for batch reactor run with no aluminum. MC wastewater [a].

Time	TSS	VSS	SCOD	acetic ac	propionic ac	isobutyric ac	butyric ac	isovaleric ac	valeric ac
0	850 (14.1)	665 (7.1)	778.1 (51.2)	265.9 (5.4)	ND	23.8 (0.7)	15.9 (0.3)	22.1 (1.7)	13.7 (0.8)
4	1140 (7.1)	805 (14.1)	987.4 (61.6)	294.4 (24.2)	85.6 (4.8)	25.5 (1.0)	29.2 (2.6)	27.4 (1.4)	15.3 (0.8)
9	1200.5 (98.3)	852.5 (10.6)	965.9 (59.8)	419.3 (9.3)	ND	26.6 (0.2)	25.7 (4.1)	30.2 (0.8)	16.9 (0.2)
14	1122.5 (74.2)	782.5 (53.0)	811.2 (48.5)	272.6 (17.3)	ND	26.2 (0.6)	25.2 (4.3)	28.5 (1.2)	15.6 (0.6)
16	1212.5 (17.7)	830 (42.4)	549.6 (61.4)	224.4 (4.0)	ND	28.1 (1.6)	22.1 (0.3)	29.4 (0.8)	16.7 (1.3)

[a] values are expressed as the mean and its standard deviation in parenthesis. Time in days, other parameters in mg/L.
ND = not detectable.

Table A.6. Experimental data for CSTR run with no aluminum. MC wastewater [a].

Time	TSS	VSS	SCOD	acetic ac	propionic ac	isobutyric ac	butyric ac	isovaleric ac	valeric ac
0	1212.5 (17.7)	830 (42.4)	549.6 (61.4)	224.4 (4)	ND	28.1 (1.6)	22.1 (0.3)	29.4 (0.8)	16.7 (1.3)
8	947.5 (24.7)	590 (28.3)	182.61 (0.6)	74.6 (0.7)	22.9 (0.5)	25.4 (0.2)	19.2 (0.4)	25.1 (0.7)	12.1 (0.2)
11	880 (0)	552.5 (3.5)	ND	81.6 (5.6)	42.0 (2.9)	25.0 (1.0)	12.1 (10.4)	26.4 (1.8)	11.0 [b]
14	942.5 (31.8)	572.5 (3.5)	904.4 (109.6)	61.6 (1.4)	48.0 (1.4)	24.3 (0.4)	16.0 (0.2)	23.4 (1.7)	13.0 (0.3)
17	925 (7.1)	565 (14.1)	930.2 [b]	59.0 (2.3)	58.5 (1.8)	26.5 (0.6)	16.0 (1.8)	28.3 (2.5)	14.0 (0.6)
20	882.5 (24.7)	610 (7.1)	372.21 (35.1)	47.9 (1.0)	38.4 (0.6)	24.9 (0.3)	13.3 [b]	24.8 (1.5)	16.0 (3.6)

[a] values are expressed as the mean and its standard deviation in parenthesis. Time in days, other parameters in mg/L.
[b] one experimental data point.
ND = not detectable.

Table A.7. Biogas generation for MC wastewater run with no aluminum.

Batch		CSTR			
time [a]	biogas [a]	time	biogas	time	biogas
0:00:00	0	0:00:00	0	323:25:00	1925
336:00:00	275	65:25:00	50	326:20:00	1960
342:30:00	325	107:25:00	350	335:25:00	2050
376:30:00	350	112:35:00	425	348:25:00	2225
386:00:00	400	119:35:00	475	353:10:00	2325
388:35:00	450	133:25:00	550	360:25:00	2400
		158:25:00	725	371:25:00	2450
		179:55:00	850	374:25:00	2500
		191:25:00	925	377:25:00	2550
		204:00:00	975	383:25:00	2700
		215:40:00	1050	398:15:00	2900
		229:55:00	1225	407:55:00	2950
		254:15:00	1375	422:25:00	3050
		262:25:00	1425	444:10:00	3400
		275:10:00	1475	449:05:00	3475
		287:25:00	1550	455:15:00	3550
		298:55:00	1725	468:25:00	3700

[a] accumulative time in hours:minutes
[b] accumulative biogas in ml @ 20°C and 1atm.

Table A.8. Experimental data for batch reactor run with 15 ppm aluminum. MC wastewater [a].

Time	TSS	VSS	SCOD	acetic ac	propionic ac	isobutyric ac	butyric ac	isovaleric ac	valeric ac
0	927.5 (24.7)	712.5 (3.5)	762.9 (76.0)	115.7 (5.5)	114.5 (5.4)	20.0 (0.8)	16.6 (0.5)	17.6 (2.2)	11.1 (0.2)
1	895 (106.1)	705 (63.6)	812.6 (87.4)	143.4 (8.2)	122.0 (2.7)	29.5 (10.3)	20.5 (2.3)	38.4 (21.2)	11.2 (0.1)
5	1060 (28.3)	805 (7.1)	796.0 (149.3)	352.6 (31.2)	18.2 [b]	24.5 (1.6)	17.1 (0.3)	20.6 (2.8)	15.8 (0.8)
6	975 (35.4)	812.5 (53.0)	950.0 (86.6)	374.9 (8.8)	17.5 (0.1)	26.1 (0.2)	19.8 (0.3)	23.7 (0.1)	15.1 (0.3)
12	1167.5 (10.6)	917.5 (31.8)	816.7 (28.9)	441.4 (3.0)	19.7 (0)	27.9 (0.2)	20.1 (0.1)	27.1 (0.1)	13.4 (0.2)
17	1052.5 (17.7)	865 (7.1)	772.0 (48.3)	317.2 (0.6)	21.7 (0.1)	28.4 (0)	23.9 (0.3)	28.0 (0.1)	13.0 (0.1)
19	1060 (7.1)	830 (28.3)	675.5 (48.3)	191.4 (1.9)	22.1 (0)	28.0 (0.1)	23.5 (0.1)	27.7 (0.2)	13.0 (0.1)
21	922.5 (17.7)	727.5 (38.9)	643.3 (55.7)	94.8 (16.2)	23.0 (0.7)	29.2 (1.9)	24.6 (2.4)	29.9 (3.8)	13.1 (0)
17	925 (7.1)	565 (14.1)	930.2 [b]	59.0 (2.3)	58.5 (1.8)	25.8 (0.6)	20 (1.2)	24.1 (0.4)	ND

[a] values are expressed as the mean and its standard deviation in parenthesis. Time in days, other paramters in mg/L.
[b] one experimental data point.
ND = not detectable.

Table A.9. Experimental data for CSTR run with 15 ppm aluminum. MC wastewater [a].

Time	TSS	VSS	SCOD	acetic ac	propionic ac	isobutyric ac	butyric ac	isovaleric ac	valeric ac
0	1062.5 (60.1)	785 (35.4)	502.0 (27.8)	44.1 (5.9)	23.6 (2.7)	25.8 (0.6)	20 (1.2)	24.1 (0.4)	ND
2	1067.5 (3.5)	775.0 (7.1)	341.4 (50.2)	66.9 (0.8)	21.0 (0.2)	24.7 (0.1)	12.6 (0)	23.2 (0.2)	11.2 (0.1)
4	950.0 (0)	710.0 (21.2)	526.1 (97.4)	88.2 (4.1)	40.4 (2.7)	24.2 (1.2)	16.0 (0.3)	23.0 (2.3)	12.6 [b]
6	822.5 (38.9)	645.0 (14.1)	437.8 (27.8)	86.9 (5.5)	53.6 (4.6)	25.0 (1.0)	22.1 (0.6)	25.4 (2.4)	14.8 (0.7)
8	802.5 (3.5)	630.0 (7.1)	582.3 (27.8)	86.4 (5.3)	51.4 (2.2)	26.4 (6.7)	21.1 (0.6)	20.6 (0.4)	15.6 (0.2)
10	645.0 (14.1)	545.0 (14.1)	783.1 (34.1)	73.6 (0.4)	63.4 (0)	25.8 (0)	13.5 (0.1)	25.9 (0.1)	12.5 (0.3)
14	605.0 (7.1)	470.0 (0)	284.4 (50.7)	55.8 (0.2)	39.0 (0.7)	16.5 (0.7)	ND	16.6 (1.2)	ND
16	580.0 (0)	440.0 (28.3)	182.8 (155.1)	49.9 (2.2)	25.9 (0.9)	14.0 (0)	ND	16.1 (0.6)	ND
18	590.0 (0)	432.5 (17.7)	276.3 (28.1)	37.9 (1)	18.4 (0)	14.4 (0.2)	ND	9.9 (0.3)	11.0 [b]
22	505.0 (28.3)	397.5 (31.8)	219.4 (73.1)	64.0 (0.2)	29.4 (0.1)	13.2 (0.1)	ND	1.7 (0.2)	10.9 (0.1)
24	507.5 (24.7)	390.0 (7.1)	341.3 (48.8)	54.9 (0.9)	25.0 (0.1)	13.5 (0.1)	ND	1.9 (0.1)	11.1 (0.1)

[a] values are expressed as the mean and its standard deviation in parenthesis. Time in days, other parameters in mg/L.
[b] one experimental data point.
ND = not detectable.

Table A.10. Biogas generation for run with 15 ppm aluminum. MC wastewater.

Batch run		CSTR run			
time [a]	biogas [b]	time	biogas	time	biogas
0:00:00	0	0:00:00	0	239:20:00	4050
422:50:00	210	34:15:00	50	261:50:00	4500
474:05:00	340	51:45:00	110	269:50:00	4580
517:00:00	450	70:45:00	320	286:05:00	4770
566:15:00	480	94:15:00	620	298:05:00	5180
		97:45:00	920	310:50:00	5470
		104:15:00	1040	321:55:00	5550
		118:30:00	1080	335:05:00	5640
		121:15:00	1120	343:15:00	5740
		129:00:00	1220	365:00:00	6180
		142:45:00	1370	368:45:00	6250
		147:15:00	1480	385:55:00	6390
		152:15:00	1600	407:20:00	6590
		166:15:00	2160	416:50:00	6760
		171:35:00	2240	432:50:00	7230
		175:25:00	2290	459:40:00	7450
		176:50:00	2320	484:15:00	7600
		190:35:00	2520	528:29:00	8300
		194:15:00	2570	537:20:00	8470
		202:39:00	3060	562:19:00	8940
		214:55:00	3310	575:00:00	9110
		218:05:00	3360	586:15:00	9320
		238:00:00	3770		

[a] accumulative time in hours:minutes
[b] accumulative biogas in ml @ 20°C and 1atm.

Table A.11 Experimental data for CSTR run with 40 ppm aluminum. MC wastewater [a].

Time	TSS	VSS	SCOD	acetic ac	propionic ac	isobutyric ac	butyric ac	isovaleric ac	valeric ac
0	507.5 (24.7)	390.0 (7.1)	341.3 (48.8)	54.9 (0.9)	25.0 (0.1)	13.5 (0.1)	ND	1.9 (0.1)	11.1 (0.1)
4	465 (28.3)	320 (0)	90.5 (37.7)	53.8 (0.5)	17.0 (0)	14.2 (0)	ND	2.9 (0.1)	11.4 (0.1)
6	462.5 (17.7)	357.5 (17.7)	115.2 (75.4)	62.7 (0.5)	19.6 (0.1)	13.8 (0.1)	ND	3.1 (0.2)	9.0 (5.0)
8	582.5 (24.7)	437.5 (31.8)	82.3 (102.8)	58.7 (1.2)	17.6 (0.2)	13.1 (0.1)	ND	2.6 (0)	ND
10	492.5 (24.7)	392.5 (10.6)	139.9 (28.5)	ND	ND	ND	ND	ND	ND
12	545 (14.1)	400 (0)	49.4 (0)	ND	ND	ND	ND	ND	ND
14	512.5 (10.6)	395 (7.1)	ND	ND	ND	ND	ND	ND	ND

[a] values are expressed as the mean and its standard deviation in parenthesis. Time in days, other parameters in mg/L.
ND = not detectable.

Table A.12. Biogas generation for run with 40 ppm aluminum. MC wastewater.

time [a]	biogas [b]
0:00:00	0
13:07:00	550
21:00:00	700
44:47:00	1000
61:00:00	1490
91:19:00	1810
110:30:00	2020
136:10:00	2670
156:14:00	2870
163:00:00	2970
180:30:00	3400
194:37:00	3670
211:00:00	3970
228:40:00	4480
252:50:00	4750
282:15:00	5170
306:00:00	5700
325:30:00	6010
330:24:00	6130

[a] accumulative time in hours:minutes
[b] accumulative biogas in ml @ 20°C and 1atm.

Table A.13. Experimental data for batch reactor run.
FBF I wastewater [a].

Time	TSS	VSS	SCOD	acetic ac	propionic ac	isobutyric ac	butyric ac	isovaleric ac	valeric ac
5	2445 [b]	1720 [b]	1071 [b]	306.3 [b]	31.7 [b]	17.3 [b]	8.2 [b]	33.8 [b]	ND [b]
10	2610 [b]	1535 [b]	843.4 [b]	185.2 (16.9)	32.8 (1.5)	18.2 (1.4)	6.9 (0.2)	37.0 (2.1)	ND
15	2880 [b]	1775 [b]	621.1 [b]	234.7 (65.1)	31.2 (8.4)	18.6 (4.9)	25.2 (6.4)	33.8 (9.5)	7.5 (1.4)
20	2520 [b]	1290 [b]	990.7 (21.3)	120.0 (31.8)	28.7 (8.1)	15.1 (4.8)	7.5 (2.7)	30.4 (9.8)	2.3 (3.2)
25	2705 [b]	1220 [b]	853.7 [b]	94.9 [b]	21.8 [b]	11.3 [b]	ND [b]	21.9 [b]	ND [b]
35	2030 [b]	895 [b]	476.2 [b]	42.7 (12.7)	ND	ND	ND	10.1 (2.6)	ND

[a] values are expressed as the mean and its standard deviation in parenthesis. Time in days, other parameters in mg/L.
[b] one experimental data point.
ND = not detectable.

Table A.14. Volumetric percentage for biogas constituents.
All experimental data runs [a].

FBF II wastewater. CSTR				MC wastewater. CSTR no Al^{3+}			
Sample time[b]	CH_4	N_2	CO_2	Sample time	CH_4	N_2	CO_2
0	36 [c]	59 [c]	5 [c]	14	12.6 [c]	61.0 [c]	26.4 [c]
7	39.3 (0.1)	55.3 (0.5)	5.3 (0.5)	17	20.2 (0.8)	79.8 (0.8)	ND
				20	26.5 (0.6)	73.5 (0.6)	ND

MC wastewater. Batch 15 ppm Al^{3+}				MC wastewater. CSTR 15 ppm Al^{3+}			
Sample time	CH_4	N_2	CO_2	Sample time	CH_4	N_2	CO_2
5	ND	ND	ND	2	13.7 (0.7)	83.0 (0.8)	3.4 (0.2)
6	ND	ND	ND	10	36.9 (2.0)	56.6 (2.3)	6.6 (0.3)
12	ND	99.5 (0.9)	0.5 (0.9)	24	55.6 (1.6)	36.3 (1.8)	8.1 (0.2)
17	0.6 (0.1)	99.4 (0.1)	ND				
19	3.0 (0.0)	97.0 (0.0)	ND				

MC wastewater. CSTR 40 ppm Al^{3+}			
Sample time	CH_4	N_2	CO_2
14	72.4 (1.5)	17.3 (1.7)	10.3 (0.2)

[a] values are expressed as the mean and its standard deviation in parenthesis.
[b] Sample time = time in days from time =0 for each run.
[c] one experimental data point.
ND = not detectable.

Table A.15. Aluminum experimental data for MC wastewater at 40 ppm Al^{3+} [a].

	pH					
aluminum conc. (mg/L)	7.6	7.2	7.1	6.7	4.6	4.4
Dissolved phase	0.04 (0.06)	___	ND	ND	1.5 [b]	32.6 (0.3)
Total [c]	35.3 (3.5)	14.3 (1.2)	21.3 (0.4)	27.5 (0.1)	___	0.29 (0.13)

[a] values are expressed as the mean and its standard deviation in parenthesis.
[b] one experimental data point.
[c] Total = (sludge + soluble) aluminum concentration.
ND = not detectable.

APPENDIX B

EFFECT OF HYDROGEN PARTIAL PRESSURE

When a given chemical equilibrium reaction is thermodynamically evaluated at a condition different from the standard, ΔG^{0}' value is affected by Equation 2.1 in order to contemplate the change of Gibbs free energy. Therefore, the influence for the change in P_{H_2} for the degradation of Propionate and Palmitate is mathematically represented by the following relations. The ΔG^{0}' values for these two reactions were obtained from Table 2.1.

Propionate acidogenesis

$$Pr^- + 3\ H_2O \rightleftharpoons Ac^- + HCO_3^- + H^+ + 3H_2$$

$$\Delta G' = 76.1\,KJ/mol + 2.303\,R\,T\,log[H_2]^3$$

Palmitate acidogenesis

$$Palmitate + 14\ H_2O \rightleftharpoons 8\ Ac^- + 7\ H^+ + 14H_2$$

$$\Delta G' = 345.6\,KJ/mol + 2.303\,R\,T\,log[H_2]^{14}$$

For both equilibrium reactions, one can appreciate why a change in P_{H_2} strongly influences Palmitate degradation, so it is important to provide good control over P_{H_2} for anaerobic degradation of wastewaters with high fat and grease content. Although the large influence of P_{H_2} on Palmitate degradation, these two equilibrium reactions progress to products when $P_{H_2} < 10^{-5}$ atm.

APPENDIX C

EQUILIBRIUM REACTIONS FOR AL^{3+} IN WATER

The presence of aluminum ion in water leads to a large number of reactions in which hydroxyl aluminum compounds and a precipitate of aluminum hydroxide are formed. Figure C.1 shows these reactions in water. It is observed that these reactions are strongly influenced by the pH in the reaction media.

$$Al^{3+} + OH^{-} \rightleftharpoons AlOH^{2+}$$

$$Al^{3+} + 2OH^{-} \rightleftharpoons Al(OH)_2^{+}$$

$$Al^{3+} + 3OH^{-} \rightleftharpoons Al(OH)_3^{0}$$

$$Al^{3+} + 4OH^{-} \rightleftharpoons Al(OH)_4^{-}$$

$$Al^{3+} + 3OH^{-} \rightleftharpoons Al(OH)_3(s)$$

Figure C.1. Equilibrium reactions for Al^{3+} in water.

The numerical values for the constants of these equilibrium reactions are shown in table C.1. These values were taken from Galarneau (1995), but they are well established and known. The tabulated constants in Table C.1 were obtained by considering that the activities of those compounds are equal to their molar concentration, and the activity of $Al(OH)_3(s) = 1$.

Table C.1 Equilibrium constants for aluminum species in water at 25°C.

$[Al(OH)^{2+}] = 10^{-4.97} [Al^{3+}]/[H^{+}]$
$[Al(OH)_2^{+}] = 10^{-9.31} [Al^{3+}]/[H^{+}]^2$
$[Al(OH)_3^{0}] = 10^{-15.01} [Al^{3+}]/[H^{+}]^3$
$[Al(OH)_4^{-}] = 10^{-23.01} [Al^{3+}]/[H^{+}]^4$
$[Al^{3+}] = 10^{9.66} [H^{+}]^3$
$[H^{+}]\ [OH^{-}] = 10^{-14}$

By definition, the total aluminum concentration soluble in the water, $[Al_T]$, is described by Equation C.1.

$$[Al_T] = [Al^{3+}] + [Al(OH)^{2+}] + [Al(OH)_2^{+}] + [Al(OH)_3^{0}] + [Al(OH)_4^{-}] \quad \text{(C.1)}$$

Or by further substitution, $[Al_T]$ can be made only a function of $[H^+]$:

$$[Al_T] = [Al^{3+}]\ \{1 + 10^{-4.97}/[H^+] + 10^{-9.31}/[H^+]^2 + 10^{-15.01}/[H^+]^3 + 10^{-23.01}/[H^+]^4\}$$

where

$$Al^{3+} = 10^{9.66}\ [H^+]^3$$

Figure C.2 provides a graphical representation of $[Al_T]$ from pH 0 to 14. It is observed that for a pH range between 6 to 8, the $[Al_T]$ is almost constant.

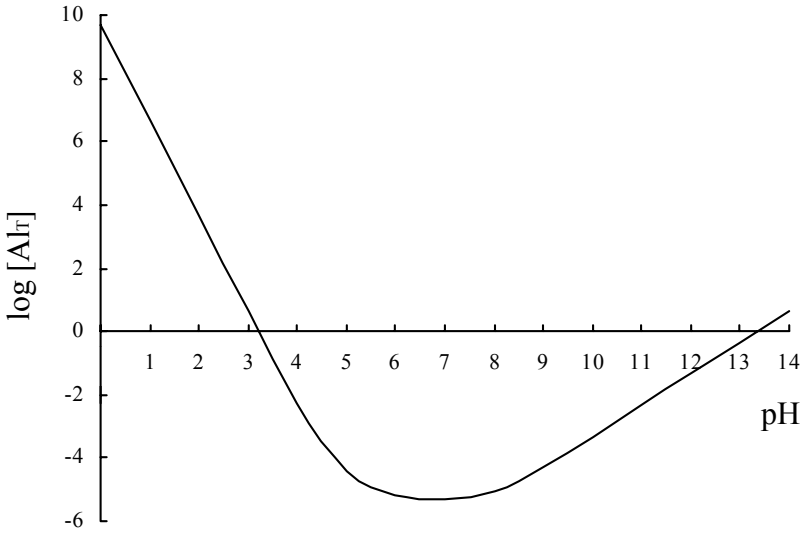

Figure C.2. $[Al_T]$ concentration as function of pH.

It was described in Chapter IV that the anaerobic degradation of poultry wastewater was carried out at 30 ºC. Therefore, in order to be consistent, equilibrium constants in Table C.1 should be affected by increment of 5 ºC. If Equation 6.1 is differentiate with respect to temperature, the well known van't Hoff equation is obtained, which is used for evaluating the change of equilibrium constant due to temperature.

$$\frac{d\,ln\,K}{dT} = \frac{\Delta H_r^0}{RT^2} \tag{C.2}$$

where:

K = solubility constant.

$\Delta H_r{}^0$ = change of standard enthalpy.

For integration purposes, $\Delta H_r{}^0$ can be considered not dependent on the temperature or a linear function of T. Kotrly and Sucha (1985) suggest that, for a aqueous solution, a $\Delta H_r{}^0$ with a value larger than 40 kJ/mol is almost independent of temperature. For example, the change of solubility constant for $Al(OH)_3(s)$ by the increment of temperature from 25 to 30°C is equal to:

$$Al(OH)_3(s) \rightleftharpoons Al^{3+} + 3OH^- \qquad \Delta H_r{}^0 = 47.6 \text{ KJ/mol}$$

Therefore, ΔH^0 is assumed no function of T

$$ln\,K_2 = ln\,K_1 + \frac{\Delta H_r^0}{R}\left(\frac{1}{T_1} - \frac{1}{T_2}\right)$$

and finally

$$Al(OH)_3(s) \rightleftharpoons Al^{3+} + 3OH^- \qquad K(30°C) = 10^{-33.19}$$

The change in solubility by increasing the temperature from 25 to 30°C is almost negligible for $Al(OH)_3(s)$. This is because aluminum salts possess very low solubility. Thermodynamic difficulties exist to determine the ΔH^0 for the other reactions described in Figure C.1, so in this research it is assumed that this increment of 5°C will not affect the $[Al_T]$ appreciably. Therefore, the constants in Table C.1 are considered to be the same for T = 30 ˚C.